

DEFINING THE MOLECULAR MECHANISMS THAT REGULATE SHIP1
ACTIVITY AND MEMBRANE LOCALIZATION IN IMMUNE CELLS

by

GRACE L. WADDELL

A DISSERTATION

Presented to the Department of Chemistry and Biochemistry
and the Division of Graduate Studies of the University of Oregon
in partial fulfillment of the requirements
for the degree of
Doctor of Philosophy

December 2022

DISSERTATION APPROVAL PAGE

Student: Grace L. Waddell

Title: Defining the Molecular Mechanisms that Regulate SHIP1 Activity and Membrane Localization in Immune Cells

This dissertation has been accepted and approved in partial fulfillment of the requirements for the Doctor of Philosophy degree in the Department of Chemistry and Biochemistry by:

Dr. Mike Harms	Chairperson
Dr. Scott D. Hansen	Advisor
Dr. Brad Nolen	Core Member
Dr. Karen Guillemin	Institutional Representative

and

Krista Chronister	Vice Provost for Graduate Studies
-------------------	-----------------------------------

Original approval signatures are on file with the University of Oregon Division of Graduate Studies

Degree awarded December 2022.

© 2022 Grace L. Waddell
This work is licensed under a Creative Commons
Attribution NonCommercial-NoDerivs (United States) License



DISSERTATION ABSTRACT

Grace L. Waddell

Doctor of Philosophy

Department of Chemistry and Biochemistry

December 2022

Title: Defining the Molecular Mechanisms that Regulate SHIP1 Activity and Membrane Localization in Immune Cells

Spatial heterogeneity in many membrane proximal signaling reactions emerges from biochemical reactions involving phosphatidylinositol phosphate (PIP) lipids, kinases, phosphatases, and Rho-family GTPases. Interconnected positive and negative feedback loops control the communication between these distinct families of signaling molecules to regulate cell polarization, cortical oscillations, and transient spikes in biochemical activities. Together, these networks of biochemical reactions provide the molecular basis for signal adaptation modules that control cell polarity and migration. Of particular importance to these cellular processes is the hematopoietic-cell-specific lipid phosphatase, SHIP1, which regulates the dephosphorylation of PI(3,4,5)P₃ lipids to generate PI(3,4)P₂. We find that in non-migratory PLB-985 cells, SHIP1 colocalizes to cortical oscillations with Cdc42 GTPase and FBP17. In the presence of chemoattractant, SHIP1 polarizes to leading-edge membranes of migrating cells. Molecular dissection of SHIP1 domain organization and activities identified a minimal C-terminal motif that is necessary and sufficient for targeting to SHIP1 to cortical oscillations. Using supported lipid bilayers to biochemically characterize SHIP1 revealed that the full-length protein is autoinhibited. SHIP1 autoinhibition is predominantly regulated by its N-terminal SH2 domain and can be relieved with the addition of immune receptor derived phosphotyrosine

peptides. Finally, single molecule dwell time measurements *in vitro* and *in vivo* revealed that interactions between SHIP1 and various lipid species are surprisingly weak and likely serve a secondary role following membrane recruitment mediated by SHIP1-protein interactions. This dissertation includes unpublished co-authored material.

CURRICULUM VITAE

NAME OF AUTHOR: Grace L. Waddell

GRADUATE AND UNDERGRADUATE SCHOOLS ATTENDED:

University of Oregon, Eugene OR
College of Charleston, Charleston SC

DEGREES AWARDED:

Doctor of Philosophy, Chemistry, 2022, University of Oregon
Bachelor of Science, Biochemistry, 2017, College of Charleston

PROFESSIONAL EXPERIENCE:

Graduate Research Assistant, Hansen Lab, University of Oregon, Eugene, OR,
2017-2022

Graduate Teaching Assistant, Department of Chemistry and Biochemistry,
University of Oregon, Eugene, OR, 2017-2018

Undergraduate Researcher, Fox lab, College of Charleston, Charleston, SC, 2014-
2017

GRANTS, AWARDS, AND HONORS:

UO Women in Graduate Science Leadership Award, 2022

Peter O'Day Fellowship, 2021

UO Institute of Molecular Biology Retreat Best Poster Award, 2021

NIH Molecular Biology & Biophysics Training Grant, 2018-2021

PUBLICATIONS:

Waddell GL, Drew E, Rupp H, and Hansen SD. (2022). Molecular basis for SHIP1 autoinhibition and membrane dependent activation. *Manuscript in Preparation*.

Waddell GL, Rupp H, and Hansen SD. (2022). Molecular Dissection of SHIP1 recruitment into the excitable signaling network in neutrophils. *Manuscript in Preparation*.

McKnight LE, Crandall JG, Bailey TB, Banks OGB, Orlandi KN, Truong VN, **Waddell GL**, Wiles ET, Donovan DA, Hansen SD, Selker EU, and McKnight JN. (2020). Rapid and Inexpensive Preparation of Genome-Wide Nucleosome Footprints from Model and Non-Model Organisms. *STAR Protocols*. 2(2):100486

Anderson JA, Loes AN, **Waddell GL**, and Harms MJ. (2019) Tracing the evolution of novel features of human Toll-like receptor 4. *Protein Science*. 28(7):1350-1358

Waddell GL, Gilmer CR, Taylor NG, Reveral JRS, Forconi M, and Fox JL. (2017). The eukaryotic enzyme Bds1 is an alkyl but not an aryl sulfohydrolase. *Biochemical and Biophysical Research Communications*. 491(2):382-387

ACKNOWLEDGMENTS

I first thank my advisor, Scott Hansen, for his mentorship, patience, and willingness to take me on as his first graduate student. You taught me so much more than I thought I could possibly learn in the span of 5 years, and I'm extremely grateful. I would also like to thank Scott's family, Ann and Rose, for always being so welcoming and hosting so many lab gatherings.

I wish to thank all the current and past members of the Hansen lab, and I would especially like to thank Benjamin Duewell. I am so thankful you joined the lab, and you have since become one of my best friends. I have deeply enjoyed all of our lively discussions about science, books, movies, and philosophy. Henry - you joined the lab at a time when I really needed someone like you. Thank you for your support both in and outside the lab. Emma - thank you for sharing a similar level of excitement about SHIP1; I know the projects are in good hands.

I would like to thank the Department of Chemistry and Biochemistry for accepting me, the NIH and NSF for supporting my research, and my thesis committee – Professors Mike Harms, Brad Nolen, and Karen Guillemin – for your insightful feedback, words of encouragement, and excitement about the research I presented.

To my family, I could not have done this without your unconditional love and endless support. Mom and Dad, thank you for always believing in me. I'm extremely lucky to have you both. To my grandmother, Sharon Dixon, thank you for always being so loving and understanding. To my siblings – Hannah, Andrew, and Luke – thank you for always being a source of comfort and support. Thank you, Susan, Mark, Olivia, and Jade, for being my second home and taking care of me during hard times. I love you all.

I am also deeply grateful for the support of my friends, both old and new. Nora, thank you for finally convincing me to read the Wheel of Time series and being there for me throughout all these years. To the rest of the Chucktown crew – Savannah, Rebecca, Chad, and Steven – thank you for staying close despite the physical distance. To the squad – Turner, Michael, Rachael, Zack, Rebecca, Steph, and Taylor – thank you for filling the last five years with lots of laughs and fun memories.

Most importantly, thank you to my partner, Dr. Turner Newton. Thank you for being my rock, the best cat dad to Kitty, and for always picking me up (literally and figuratively). Without your constant love, patience, and support this surely would have been an impossible journey. I'm excited for our next chapter and everything the future will bring. ♥

I dedicate this work to my family, whose love and support made this possible.

TABLE OF CONTENTS

Chapter	Page
I. INTRODUCTION	1
II. MECHANISMS CONTROLLING MEMBRANE RECRUITMENT AND ACTIVATION OF AUTOINHIBITED SHIP1	13
Introduction.....	13
Results.....	18
SHIP1 transiently interacts with phospholipids with low specificity	18
SHIP1(PH-PPtase-C2) transiently localizes to the plasma membrane	21
The central domain of SHIP1 catalyzes PI(3,4,5)P3 dephosphorylation with simple unimolecular kinetics	24
Full-length SHIP1 is autoinhibited by the N-terminal SH2 domain.....	27
Membrane recruitment and activation of SHIP1 by a phosphotyrosine peptide.....	29
Discussion.....	32
Materials and Methods.....	38
Bridge to Chapter III.....	51
III. MOLECULAR DISSECTION OF SHIP1 RECRUITMENT INTO THE EXCITABLE SIGNALING NETWORK IN HUMAN NEUTROPHILS	52
Introduction.....	52
Results.....	56
SHIP1 exhibits local excitability and polarizes to the leading edge in neutrophils.....	56
Role of PIP lipids in regulating SHIP1 membrane localization in neutrophils.....	58
Molecular dissection of SHIP1 membrane localization.....	59
SHIP1 and FBP17 colocalize and display synchronized oscillations in PLB-985 cells.....	63
Cdc42 functions upstream of SHIP1 and FBP17.....	64

Discussion	66
Materials and Methods.....	69
IV. CONCLUDING REMARKS.....	74
APPENDICES	78
A. SUPPLEMENTARY INFORMATION FOR CHAPTER III	78
REFERENCES CITED.....	80

LIST OF FIGURES

Figure	Page
1. Figure 1.1: PIP lipids and their subcellular localization	2
2. Figure 1.2: Lipid kinases and phosphatases regulate the abundance and spatial distribution of PIP lipids	3
3. Figure 1.3: PI3K pathway	5
4. Figure 1.4: SHIP1 domain structure and proposed molecular interactions	9
5. Figure 2.1: SHIP1 displays weak lipid binding specificity in vitro	20
6. Figure 2.2: SHIP1(PH-PP-C2) transiently associates with the plasma membrane in live cells	23
7. Figure 2.3: SHIP1 catalyzes the dephosphorylation of PI(3,4,5)P3 with simple unimolecular kinetics that can be enhanced with PS.....	26
8. Figure 2.4: Full-length SHIP1 is autoinhibited by the N-terminal SH2 domain.....	28
9. Figure 2.5: Phosphotyrosine peptides regulate membrane recruitment and activation of SHIP1	30
10. Figure 3.1: SHIP1 localizes to both actin-based membrane protrusions and cortical oscillations in differentiated neutrophil-like cells.....	58
11. Figure 3.2: Dynamics of SHIP1 product in stimulated neutrophil-like cells..	59
12. Figure 3.3: Molecular dissection of SHIP1 membrane localization	61
13. Figure 3.4: SHIP2 localizes to cortical oscillations in differentiated neutrophil-like cells.....	62
14. Figure 3.5: SHIP1 and FBP17 colocalize to leading-edge membranes and cortical oscillations.....	63
15. Figure 3.6: Cdc42 inhibition disrupts SHIP1 and FBP17 cortical oscillations.....	65
16. Supplemental Figure 1: Cortical oscillations are specific to differentiated PLB-985 cells.....	78

17. **Supplemental Figure 2: SHIP1 localizes to puncta on neutrophil membranes.** 79

CHAPTER I

INTRODUCTION

PIP lipids, One of the Most Universal Signaling Entities in Eukaryotic Cells

Phosphatidylinositol phosphate (PIP) lipids comprise of less than 1% of total cellular lipids, yet they play essential roles regulating fundamental cellular processes, including membrane trafficking, cytoskeletal organization, cell growth, survival, differentiation, tissue organization, cell division, and cell migration (Balla 2013). As expected from such vital signaling molecules, mutations in PIP lipid metabolic genes can be linked to serious human diseases, including cancer (Fruman et al. 2017).

There are seven different PIP lipid species generated through reversible phosphorylation at the 3', 4', and 5' positions of their inositol rings (**Figure 1.1**). These lipids are enriched in different subcellular compartments and function by selectively recruiting proteins to intracellular membranes and locally controlling their activity (**Figure 1.1**) (Kutateladze 2010). The concentration and spatiotemporal distributions of PIP lipids are dynamically altered during cell signaling. Some PIP lipids, such as PI(4)P and PI(4,5)P₂, are constitutively present at the inner leaflet of the plasma membrane, while PI(3,4,5)P₃ is nearly undetectable until G-protein coupled receptors (GPCRs) or receptor tyrosine kinases (RTKs) are activated. Tightly controlling the localization and turnover of these lipids are different classes of PIP specific lipid kinases and phosphatases (**Figure 1.2**). PIP5K, for example, phosphorylates PI(4)P to generate

PI(4,5)P₂, which is maintained at a homeostatic level of 2-5% of the total plasma membrane composition (Nasuhoglu et al. 2002; Wenk et al. 2003).

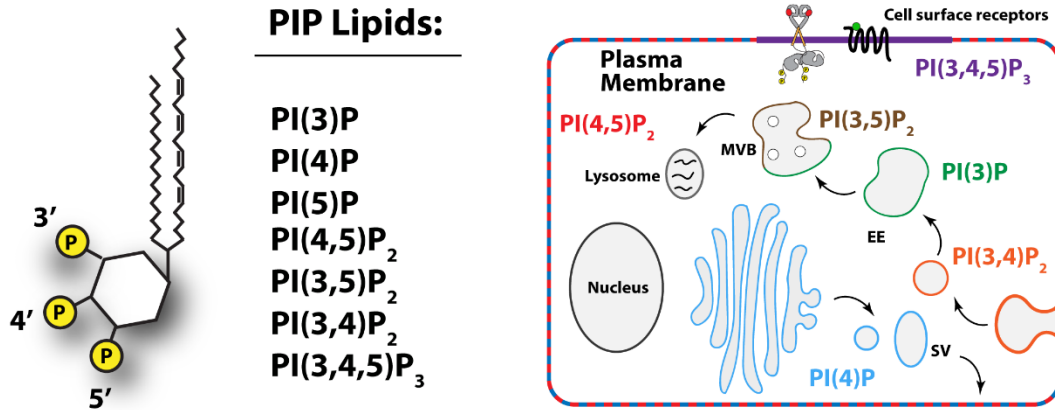


Figure 1.1: PIP lipids and their subcellular localization. There are seven PIP lipid species that differ by the placement and number of phosphate groups on the inositol headgroup. PIP lipids serve as markers of different intracellular compartments and serve as docking sites for various protein effectors. The intracellular localization of PI(5)P is not shown because it is not a predominant PIP lipid. MVB, multivesicular bodies; EE, early endosome.

The pleckstrin homology (PH) domain was the first protein domain identified to interact with PIP lipids (Harlan et al. 1994). Since this discovery, the list of PIP lipid binding domains has been expanded to include other domains such as C2 (conserved region-2 of protein kinase C), FYVE (Fab1, YOTB, Vac1 and EEA1), PX (Phox homology), and more (Kutateladze 2010). These domains exhibit a wide range of affinities and specificities and play a critical role in recruiting host proteins to distinct intracellular membranes. Given the vast array of PIP effectors, it's unsurprising that these ubiquitous regulators can be linked to nearly every aspect of a cell's life and death.

Understanding how the activities of PIP lipid kinases and phosphatases are balanced is critical for understanding how cells regulate PIP lipid signaling and cope with the devastating cellular consequences associated with misregulation in PIP lipid metabolism.

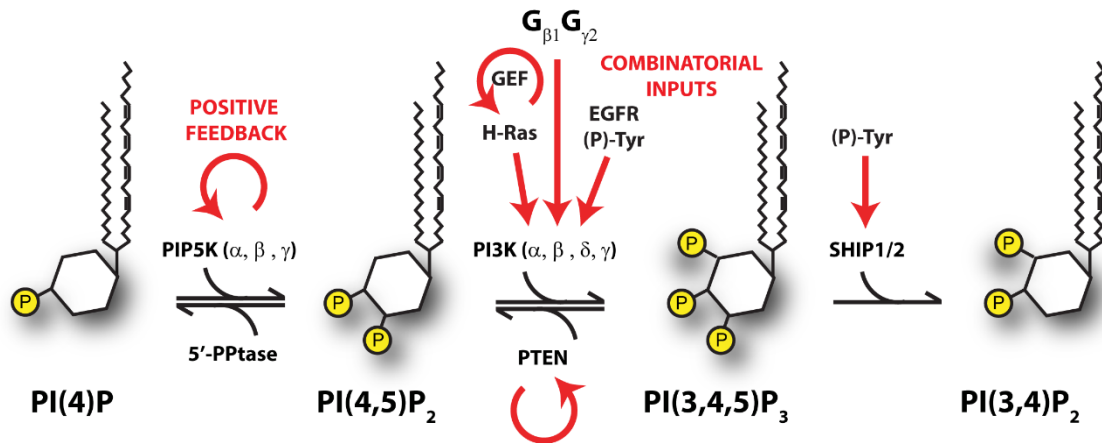


Figure 1.2: Lipid kinases and phosphatases regulate the abundance and spatial distribution of PIP lipids. Simplified PIP lipid phosphorylation and dephosphorylation pathways. Many PIP lipid kinases and phosphatases are subject to tight regulation. For example, PI3K requires interactions with numerous other proteins for full activation.

The PI(3,4,5)P₃ signaling pathway

The mechanism of cell polarization is fundamentally important for diverse cellular processes including tissue organization, asymmetric cell division, activation of the immune response, and cell migration (Drubin and Nelson 1996). Underlying the establishment and maintenance of numerous cell polarity pathways is the asymmetric localization of PI(3,4,5)P₃ lipids, which are synthesized at the plasma membrane by class I phosphoinositide-3-kinases (PI3Ks) (Servant 2000; Luo and Mondal 2015). In the absence of receptor activation, class I PI3Ks are considered to be cytosolic autoinhibited

heterodimeric complexes consisting of a catalytic subunit bound to an inhibitory regulatory subunit (Vadas et al. 2011). Upon receptor activation, PI3K is membrane recruited and activated to phosphorylate the omnipresent PI(4,5)P₂ and generate PI(3,4,5)P₃ (**Figure 1.3**) (Cantley 2002).

PI(3,4,5)P₃ is widely considered a lipid second messenger because it is highly effective at relaying signals from cell surface receptor to various intracellular protein effectors (Newton, Bootman, and Scott 2016). To exert its function, PI(3,4,5)P₃ selectively recruits a myriad of PH domain containing signaling proteins (i.e. Akt/PKB, PDK1, BTK, GEFs) to the plasma membrane (**Figure 1.3**) (Kutateladze 2010). The membrane translocation of these proteins is critical for cellular processes such as cell growth, survival, proliferation, migration, and immune cell activation. Many of these processes are misregulated by an overabundance of PI(3,4,5)P₃ lipids, which is a hallmark of tumorigenesis. There is also a strong correlation between elevated PI3K signaling and numerous human cancers (Fruman et al. 2017). For cellular homeostasis, PI(3,4,5)P₃ levels are tightly regulated via dephosphorylation mediated by the 5' inositol phosphatases, SHIP1 and SHIP2, and the 3' inositol phosphatase, PTEN (Backers et al. 2003; Maehama, Taylor, and Dixon 2001; Majerus and York 2009). Of these, SHIP1 is uniquely expressed in immune and hematopoietic cells, which makes SHIP1 an excellent drug target for PI3K-related inflammatory diseases and hematopoietic malignancies (Qiurong Liu et al. 1998; Pauls and Marshall 2017).

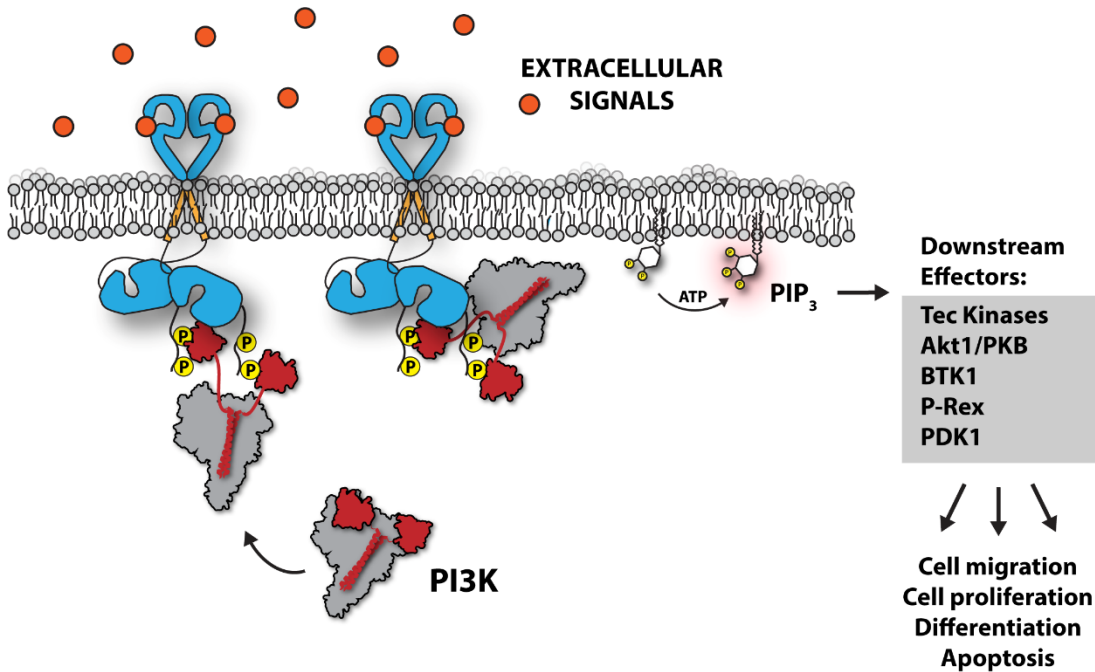


Figure 1.3: PI3K pathway. PI3K is an autoinhibited heterodimer that is recruited and activated at the membrane during receptor signaling events. Depicted is an activated Receptor Tyrosine Kinase membrane recruiting and activating PI3K. Once active, PI3K generates PI(3,4,5)P₃, which recruits a myriad of downstream effectors that are implicated in critical cellular pathways.

Mechanisms controlling PI(3,4,5)P₃ signaling during neutrophil migration

The innate immune system relies on neutrophils to recognize and destroy invading pathogens, such as viruses, bacteria, and even cancer cells. This requires neutrophils to properly sense chemicals released by pathogens, orient, polarize, and directionally migrate (chemotaxis). Critical for this cellular response and the proper organization of cytoskeletal activity is the localized accumulation of PI(3,4,5)P₃ lipids at leading edge membranes.

During chemotaxis, phosphoinositide 3-kinase (PI3K) rapidly produces PI(3,4,5)P₃ resulting in polarized F-actin polymerization and pseudopod extension in the direction of the chemoattractant gradient (Servant 2000; Yoo et al. 2010; Pollard and Borisy 2003). Directed cell migration relies on tight spatial and temporal regulation of PI(3,4,5)P₃ levels (L. Stephens, Ellson, and Hawkins 2002). Through the activity of two negative regulators: the 3' lipid phosphatase PTEN and the 5' lipid phosphatase SHIP1, cells limit the concentration of PI(3,4,5)P₃ at the plasma membrane (Weiner 2002; Luo and Mondal 2015) (**Figure 1.2**).

PTEN localizes to the rear of a migrating *Dictyostelium*, where it converts PI(3,4,5)P₃ to PI(4,5)P₂. *Dictyostelium* cells lacking PTEN are unable to polarize and directionally migrate (Iijima and Devreotes 2002). However, depletion of PTEN in neutrophils has only a small impact on directionality and overall chemotaxis was unaffected (Nishio et al. 2007; Mondal et al. 2012). In zebrafish, SHIP1-deficient neutrophils have enhanced migration and increased recruitment to wound site, suggesting that SHIP1 limits neutrophil motility *in vivo* (Lam et al. 2012). Depletion of SHIP1 in murine neutrophils resulted in PI(3,4,5)P₃ accumulation, elevated Akt activation, and enhanced cell adhesion that impaired cell polarity and migration (Nishio et al. 2007; Mondal et al. 2012). Studies using neutrophil cell lysate show that 5'-phosphatases contribute a large amount (>90%) of the PI(3,4,5)P₃ phosphatase activity (L. R. Stephens, Hughes, and Irvine 1991). Thus, although PTEN is the dominant phosphatase limiting PI(3,4,5)P₃ at the plasma membrane during *Dictyostelium* cell migration, SHIP1 seems to play this role in neutrophils. In chapter III, we investigate SHIP1 regulatory mechanisms in human neutrophils.

SHIP1 is a hematopoietic cell specific inositol phosphatase

SHIP1 was originally discovered in 1994 as a 145-kDa protein that associates with Shc and Grb2 downstream of B cell receptor and cytokine receptor activation (Lioubin and Rohrschneider' 1994). It has since been characterized as a hematopoietic-cell-specific lipid phosphatase that functions downstream of PI3K by dephosphorylating PI(3,4,5)P₃ lipids to generate PI(3,4)P₂ (Damen et al. 1996; Geier et al. 1997; Qiu et al. 1998) (**Figure 2**). SHIP1 is a large multidomain protein that contains several features identified to contribute to its various cellular functions: an N-terminal Src Homology 2 (SH2) domain, pleckstrin-homology related (PH-R) domain, phosphatase domain, C2 domain, and numerous C-terminal proline-rich and NPXY motifs (**Figure 1.4**) (Rohrschneider et al. 2000; Pauls and Marshall 2017). Considering SHIP1's domain organization, its many cellular functions are likely context dependent and regulated by specific protein and lipid binding interactions.

The SH2 domain of SHIP1 has been reported to interact with numerous immune cell receptors, including the FcγRIIB and the B-cell receptor (BCR), by binding either phosphorylated immunoreceptor tyrosine-based activation motifs (ITAM) or immunoreceptor tyrosine-based inhibition motifs (ITIM) (Pauls et al. 2016). SHIP1's interaction with FcγRIIB has been shown to be critically important for the negative regulation BCR-dependent B cell activation (Isnardi et al. 2006). Interactions mediated by SHIP1's SH2 domain are thought to be critical for its membrane recruitment mechanism, but SHIP1 has also been reported to interact with several membrane associated adaptor molecules via its C-terminus. SHIP1 can bind Src homology 3 (SH3) domain-containing proteins such as growth factor receptor-bound protein 2 (Grb2) and

the formin-binding protein 1 (FBNP1 or FBP17) via its C-terminal proline-rich regions (Manno et al. 2016; D. Xiong et al. 2016). Phosphorylation of SHIP1's C-terminal NPXY motifs facilitates interactions with Shc, Dok1, Dok3, and Nck via their phosphotyrosine binding (PTB) or SH2 domains (Kavanaugh et al. 1996; Lamkin et al. 1997; Sattler et al. 2001; Manno et al. 2016; Pauls, Hou, and Marshall 2020).

There is also the hypothesis that SHIP1's membrane localization is regulated by the two proposed lipid binding domains that flank the phosphatase domain. The pleckstrin-homology related (PH-R) domain was reported to interact with the substrate of SHIP1, PI(3,4,5)P₃, while the C2 domain reportedly binds the product of SHIP1, PI(3,4)P₂ (Ming-Lum et al. 2012; Ong et al. 2007; Nelson et al. 2021). The PH-R domain has been shown to be important for SHIP1's localization to the phagocytic cup during FcγR-mediated phagocytosis in macrophages (Ming-Lum et al. 2012), and the C2 domain is an allosteric activation site that can enhance SHIP1's activity via direct binding of PI(3,4)P₂ (Ong et al. 2007). Ser440 in the phosphatase domain is another allosteric site that can be phosphorylated by cyclic AMP-dependent protein kinase (PKA) to increase SHIP1 activity (J. Zhang, Ravichandran, and Garrison 2010). Mechanisms regulating SHIP1 activity and membrane localization are further discussed in chapter II.

In general, SHIP1 is believed to be a negative regulator of immune cell signaling by antagonizing PI3K activity. Consistent with this view, many studies demonstrate that knocking out SHIP1 results in the accumulation of PI(3,4,5)P₃ and increased phosphorylation of Akt (Aman et al. 1998; Q. Liu et al. 1999). However, some SHIP1 functions may not be mediated by degradation of PI(3,4,5)P₃. There is some evidence that SHIP1 could also play critical non-enzymatic functions by regulating the localization of

key factors for immune cell signaling and other polarity pathways. This was illustrated by SHIP1's suppression of NOD2-induced NFκB activation in monocytes by blocking the interaction between XIAP and RIP2, and by SHIP1's binding inhibiting the promigratory function of Dok1 (Condé et al. 2012; Sattler et al. 2001). It was also reported that a non-catalytic region of SHIP1's C-terminus was essential for its ability to inhibit signaling in B cells (Aman et al. 2000).

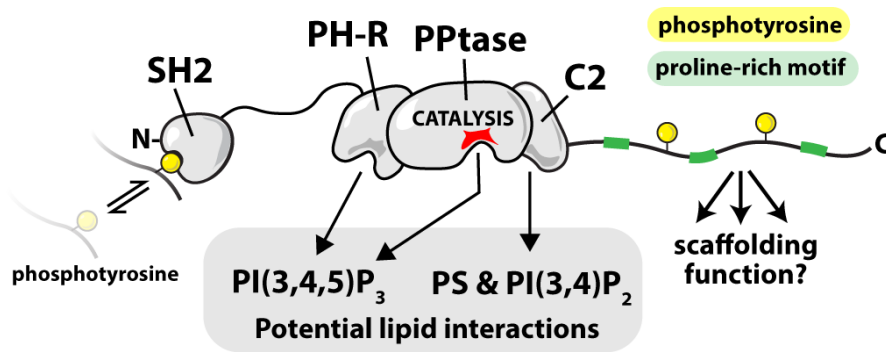


Figure 1.4: SHIP1 domain structure and proposed molecular interactions. SHIP1 has an N-terminal Src Homology 2 (SH2) domain, pleckstrin-homology related (PH-R) domain, phosphatase domain, C2 domain, and numerous C-terminal proline-rich and NPXY motifs.

SHIP1 and disease

PI3K activation and PI(3,4,5)P₃ production is quickly followed by its degradation into PI(3,4)P₂ via SHIP1 (Goulden et al. 2019; D. Xiong et al. 2016). Consistent with its biochemical function, SHIP1 deficiency can result in prolonged PI(3,4,5)P₃ signaling, which affects hematopoietic cell function and tissue homeostasis. Mice deficient in SHIP1 develop progressive myeloid hyperplasia, splenomegaly, myeloid infiltration of

vital organs, and a premature death associated a massive infiltration of the lung airspaces with distended lipid-laden macrophages (Qiurong Liu et al. 1999; Helgason et al. 1998). As a result of elevated PI(3,4,5)P₃ levels, neutrophils and mast cells isolated from SHIP1 $-/-$ mice displayed prolonged Akt activation and resistance to induced apoptosis (Qiurong Liu et al. 1999). Also reported in SHIP1 knockout mice is a deficiency in platelet aggregation (Séverin et al. 2007) and severe osteoporosis with enlarged and hypernucleated osteoclasts that are indistinguishable from those of patients with Paget disease (Sunao et al. 2002).

Aberrant expression or activity of SHIP1 is implicated to have roles in several different diseases, such as diabetic kidney disease (F. Li et al. 2017), Alzheimer's disease (McKeever et al. 2017), Crohn's disease (Ngoh et al. 2016), and cancer (Brooks et al. 2010; Chen et al. 2015; Nalaskowski et al. 2018; Fu et al. 2019). SHIP1 has roles in the development of hematopoietic tumors (Brooks et al. 2010; Chen et al. 2015), and compared to WT SHIP1, an acute myeloid leukemia derived SHIP1 mutant resulted in an increased proliferation rate of a leukemic cell line (Nalaskowski et al. 2018). Lastly, SHIP1 expression is reduced in solid tumors, such as non-small cell lung cancer, and overexpression of SHIP1 decreases cell proliferation, migration, invasion and tumorigenicity via the PI3K/AKT pathway (Fu et al. 2019). Understanding key functional details regarding how SHIP1 is regulated, activated, and recruited to the membrane could open doors for researchers to develop therapeutics that uniquely target SHIP1 and modulate immune cell functions in order to combat the myriad of hematopoietic malignancies caused by misregulation of SHIP1 or the PI3K/Akt pathway.

Multidisciplinary approaches for understanding SHIP1 regulatory mechanisms

Many questions remain regarding SHIP membrane recruitment and activation mechanisms. SHIP1 is a multidomain protein that has numerous protein interaction motifs and two proposed lipid binding domains (Pauls and Marshall 2017). Due to a lack of biochemical studies, SHIP1 lipid specificity and membrane recruitment mechanisms are unclear. There is also some ambiguous evidence that SHIP1 may be autoinhibited (J. Zhang, Ravichandran, and Garrison 2010).

Here, I describe biochemistry, biophysics, and cell biology techniques that were used to increase our understanding of SHIP1 membrane recruitment and activation mechanisms. In chapter II, I determined if SHIP1 is recruited to intracellular membranes largely by lipids or proteins using single molecule Total Internal Reflection Fluorescence (TIRF) microscopy to measure the membrane binding dynamics of SHIP1 on supported lipid bilayers and in live cells. This work showed that SHIP1 displays extremely transient interactions with lipids, which shifts the current model in the field and suggests that SHIP1 is directed to intracellular membranes via protein interactions. I also showed that full-length SHIP1 is autoinhibited and performed a molecular dissection (i.e. what domains are responsible) to understand the intramolecular mechanisms regulating SHIP1 activity. This work determined that SHIP1 activity is predominantly inhibited by its N-terminal SH2 domain. Interactions with receptor derived phosphopeptides can relieve autoinhibition and recruit SHIP1 to supported membranes. In chapter III, I visualized mNG tagged SHIP1 in resting and migrating neutrophils, which revealed that SHIP1 localizes to cortical oscillations and leading-edge membranes in a C-terminal dependent manner.

Overall, this work provides a deeper understanding of SHIP1's membrane recruitment and activation mechanisms. It also highlights the benefits of combining cell biology and biochemical approaches. From each approach, we learned unique molecular details that we would not have otherwise realized. This is a great example of how multidisciplinary research offers unique perspectives and can converge research findings more rapidly to address complex problems.

CHAPTER II

MECHANISMS CONTROLLING MEMBRANE RECRUITMENT AND ACTIVATION OF AUTOINHIBITED SHIP1

This chapter includes unpublished and co-authored material. Experiments were performed by me, Henry Rupp, Emma Drew, and Scott Hansen. This chapter was written by me with editorial assistance from Scott D. Hansen.

INTRODUCTION

Phosphatidylinositol phosphate (PIP) lipids play a crucial function in eukaryotic cell biology by regulating the recruitment and activation of numerous signaling proteins across intracellular membranes (Di Paolo and De Camilli 2006). In many cases, PIP lipids are transiently created by lipid kinases and phosphatases, which are activated during various cell signaling pathways (Burke 2018). Understanding how PIP lipid modifying enzymes are regulated is critical for determining how cells control the strength and duration and PIP lipid signaling in cell biology. Misregulation of PIP lipid homeostasis has been shown to profoundly affect cell growth and proliferation, which is linked to poor prognosis in numerous human diseases (Balla 2013).

The Src homology 2 containing inositol 5-phosphatase 1 (SHIP1) is a hematopoietic cell specific lipid phosphatase that regulates phosphatidylinositol phosphate (PIP) lipid synthesis at the plasma membrane (Pauls and Marshall 2017). SHIP1 specifically dephosphorylates phosphatidylinositol-(3,4,5)-phosphate (PI(3,4,5)P₃)

to generate phosphatidylinositol-(3,4)-phosphate (PI(3,4)P₂). PI(3,4,5)P₃ is a second messenger lipid that selectively recruits a myriad of signaling proteins (i.e. Akt, BTK, P-Rex1) to the plasma membrane that are critical for cell growth, survival, and development (Newton, Bootman, and Scott 2016; Fruman et al. 2017; Q. Liu et al. 1999). Because PI(3,4,5)P₃ lipids regulate critical cellular processes, these lipids need to be spatially and temporally regulated to maintain cellular homeostasis. Cells lacking SHIP1 display defects in cell adhesion and migration as a consequence of elevated PI(3,4,5)P₃ levels (Nishio et al. 2007; Mondal et al. 2012).

In order to access its lipid substrate, SHIP1 needs to localize to the plasma membrane. Antibody induced activation of the immunoglobulin E receptor (FcεRI) in mast cells revealed that SHIP1 undergoes dynamic cycles of plasma membrane recruitment and dissociation which leads to the emergent property of cortical oscillations (D. Xiong et al. 2016). It was also shown that stimulating the B cell- and FcγRIIB-receptors enhances SHIP1 plasma membrane localization compared to unstimulated cells (Pauls and Marshall 2017; Manno et al. 2016). Although SHIP1 is recruited to the plasma membrane upon activation of several types of immune cell receptors, the mechanism controlling membrane recruitment and activation is unclear. For example, it's unclear whether SHIP1 is recruited to the plasma membrane through direct interactions with PI(3,4,5)P₃ lipids or indirectly by proteins that bind to PI(3,4,5)P₃. Understanding how each domain of SHIP1 contributes to membrane localization and lipid phosphatase activity will close the gap in knowledge concerning whether SHIP1 directly interacts with activated receptors, newly synthesized PIP lipids, or proteins that bridge those interactions.

SHIP1 contains two proposed lipid binding domains that flank the central phosphatase domain and have been proposed to regulate membrane localization and catalytic activity (**Figure 1A**). The pleckstrin-homology related (PH-R) domain was shown to interact with the substrate of SHIP1, PI(3,4,5)P₃, while the C2 domain reportedly binds to the product of SHIP1, PI(3,4)P₂ (Ming-Lum et al. 2012; Ong et al. 2007; Nelson et al. 2021). Mutations in the PH-R domain disrupted localization to the phagocytic cup during FcγR-mediated phagocytosis in macrophages but did not affect SHIP1 catalysis. This suggests that SHIP1 localization to PI(3,4,5)P₃ containing membranes is independent of its catalytic domain (Ming-Lum et al. 2012). Biochemical analysis of the SHIP1 paralog, SHIP2, revealed a structural interface between the phosphatase and C2 domain capable of interdomain communication and allosteric regulation (Le Coq et al. 2017). The C2 domain of SHIP2 reportedly interacts with phosphatidylserine (PS) (Le Coq et al. 2017), while the SHIP1 C2 domain reportedly binds to PI(3,4)P₂ (Ong et al. 2007). Based on the high degree of primary sequence homology between these paralogs, it's unclear whether SHIP1 and SHIP2 bind to distinct phospholipids. Together, these reported lipid interactions suggest a possible mechanism for positive feedback and allosteric activation of SHIP1.

Complicating our understanding of mechanisms that regulate SHIP1 activity, previous biochemical characterization of SHIP1 suggests that the C-terminal domain attenuates 5-phosphatase activity. In particular, a C-terminal truncation was previously shown to increase SHIP1 activity approximately 8-fold compared to full-length (FL) SHIP1 (J. Zhang, Ravichandran, and Garrison 2010). Consistent with this result, C-terminal truncation mutants of SHIP2 were also more active than the full-length

phosphatase (Prasad, Werner, and Decker 2009). A potential mechanism for autoinhibition could be mediated through intramolecular interactions between the N-terminal SH2 domain and C-terminal phosphotyrosine(s). Supporting this model, a peptide derived from the C-terminal region of SHIP1 containing phosphorylated tyrosine residue Y1022 immunoprecipitated purified SH2 domains of SHIP1 (Mukherjee et al. 2012). Similar to Src-family tyrosine kinases (Sicheri, Moarefi, and Kuriyan 1997; Xu, Harrison, and Eck 1997), it's possible that the N-terminal SH2 domain of SHIP1 forms an auto-inhibitory interaction with a C-terminal phosphorylated residue (e.g. Y1022). Although Y1022 was shown to be phosphorylated by Src family kinases (Pauls et al. 2016), it remains unclear whether this specific post-translational modification is responsible for SHIP1 autoinhibition or if it regulates interactions with peripheral membrane binding proteins. Despite evidence supporting SHIP1 autoinhibition, the mechanism that regulates the formation and relief of intramolecular interactions remains unknown. Understanding the mechanism of autoinhibition could help elucidate how SHIP1 is recruited to the membrane and the functional consequences of SHIP1 mutants lacking autoinhibitory contacts.

To date, no biochemical studies have directly visualized the interaction between purified SHIP1 and proposed lipid binding partners. Previous experiments relied on surface plasma resonance (SPR) (Nelson et al. 2021) and protein lipid overlay (PLO) assays (Ong et al. 2007, Ming-Lum et al. 2012) to measure SHIP1 lipid interactions. Cell biology studies have also shown that genetic or chemical perturbations targeting phospholipid production can modulate SHIP1 membrane localization (D. Xiong et al. 2016). Given the combination of protein and lipid interactions that potentially regulate

SHIP1, it remains unclear whether SHIP1's membrane localization is controlled directly or indirectly by phospholipids. To directly visualize interactions between SHIP1 and different lipid species, we established a single molecule Total Internal Reflection Fluorescence (smTIRF) microscopy assay in combination with supported lipid bilayers (SLBs). Through the direct visualization of the proposed SHIP1 lipid binding domains we found that SHIP1 lacks strong lipid binding specificity compared to several well-established PIP lipid binding proteins that display a range of affinities (i.e. $K_D = 0.01 - 10 \mu\text{M}$) (Yeung et al. 2008; Baumann et al. 2011; Goulden et al. 2019; Corbin, Dirkx, and Falke 2004; He et al. 2008). In both our *in vitro* and *in vivo* studies, we find that central lipid phosphatase domain flanked by the two proposed lipid binding domains interacts very weakly with membranes *in vitro* and *in vivo*. Compared to previous reports, we observe a significantly lower affinity or complete absence of interactions between SHIP1 and lipids. Biochemical reconstitution of SHIP1 phosphatase activity also revealed that the full-length enzyme is autoinhibited compared to the central PH-PP-C2 domains. Characterization of SHIP1 truncation mutants revealed that both the N-terminal SH2 domain and the disordered C-terminal tail inhibit SHIP1 phosphatase activity. In the presence of an immune receptor derived phosphopeptide – in solution or membrane tethered – SHIP1 lipid phosphatase activity can be stimulated. Overall, our results reveal that interactions between SHIP1 and various lipid species are surprisingly weak and likely serve a secondary role following membrane recruitment mediated by SHIP1-protein interactions.

RESULTS

SHIP1 transiently interacts with phospholipids with low specificity

Flanking the central phosphatase domain, SHIP1 has two proposed lipid binding domains (i.e. “PH-R” and “C2”, **Figure 2.1A**). The pleckstrin-homology related domain (herein referred to as “PH”) was previously shown to interact with the substrate of SHIP1, PI(3,4,5)P₃ (Ming-Lum et al. 2012), while the C2 domain reportedly binds to the product of SHIP1, PI(3,4)P₂ (Ong et al. 2007). These lipid interactions are hypothesized to function in concert to regulate SHIP1 membrane docking and lipid phosphatase activity. A major limitation in our understanding of these lipid interactions is that previous experiments utilized binding assays that did not directly visualize dynamic membrane association, bilayer diffusion, and dissociation of SHIP1. Observing this behavior is an essential criterion for validating that proposed lipid bindings domains can autonomously and reversibly interact with a lipid membrane.

To assess the role that lipids serve in controlling SHIP1 membrane localization, we established a method to directly visualize the dynamic and reversible membrane binding interactions using supported lipid bilayers (SLBs) visualized by Total Internal Reflection Fluorescence (TIRF) microscopy (**Figure 2.1B**). We purified and fluorescently labeled a collection of lipid binding domains derived from Lact-C2, PLC δ , TAPP1, and Grp1. These lipid binding domains have well established interactions with phosphatidylserine (PS), PI(4,5)P₂, PI(3,4)P₂, and PI(3,4,5)P₃ respectively (Yeung et al. 2008; Baumann et al. 2011; Goulden et al. 2019; Corbin, Dirkx, and Falke 2004; He et al. 2008). Each protein has a K_D in the range of 0.01 – 10 μ M, providing a panel of positive controls. When we measure the localization of these lipid binding domains on SLBs

using a solution concentration of 20 nM for each individual protein, we observed robust membrane recruitment based on the high membrane fluorescence intensity compared to the background TIRF-M signal (**Figure 2.1C**). To compare the relative strengths of these lipid-protein interactions, we measured the dwell time of single spatially resolved membrane binding events (**Figure 2.1C**). Consistent with previous K_D measurements based on solution binding assays, we calculated a range of dwell times between 0.1 – 5 seconds for these lipid binding proteins (**Figure 2.1E**).

In order to measure single molecule interactions between SHIP1 and various phospholipids, we recombinantly expressed and purified a mNeonGreen (mNG) tagged SHIP1 truncation containing the central phosphatase domain flanked by two lipid binding domains (i.e. mNG-PH-PP-C2). Compared to the membrane localization seen for the control lipid binding domains described above, we observed little to no membrane association of mNG-SHIP1(PH-PP-C2) in the presence of either PS, PI(4,5)P₂, PI(3,4)P₂, and PI(3,4,5)P₃ alone (**Figure 2.1D**). Although a small fraction of molecules bound to the supported lipid bilayer, the lack of diffusivity indicated that this small number of binding events represent non-specific interactions with defects in the supported membrane (**Figure 2.1F**). Despite increasing the frame rate of image acquisition to ~80 frames per seconds, we were unable to observe any single molecule membrane binding events, suggesting that SHIP1 does not interact with lipids under these conditions.

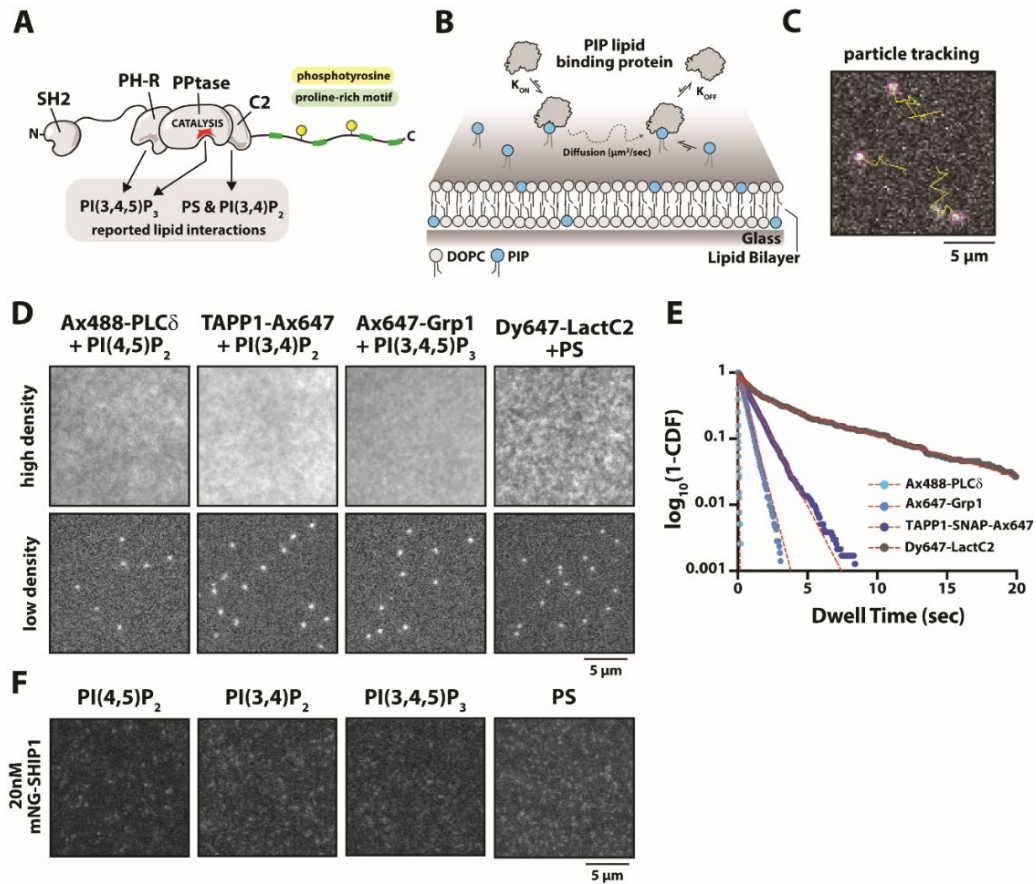


Figure 2.1: SHIP1 displays weak lipid binding specificity in vitro. A) Cartoon diagram showing the reported lipid binding domains of SHIP1, which include the phosphatase domain and flanking PH-R and C2 domains. B) Experimental setup for directly visualizing protein-lipid interactions on supported lipid bilayers using smTIRF-M. C) Representative image showing single particle detection (purple circle) and trajectories (yellow line) of 3 Ax647-Grp1 membrane bound molecules. Image collected in the presence of 1 pM Ax647-Grp1. Membrane composition: 2% PI(3,4,5)P₃ and 98% DOPC. D) Representative TIRF-M images showing bulk membrane recruitment in the presence of either 20 nM (“high density”) or (“low density”) Ax488-PLC δ (250 pM), TAPP1-SNAP-Ax647 (1 pM), Ax647-Grp1 (1 pM), or Dy647-Lact-C2 (2 pM) on SLBs containing DOPC lipids plus either 2% PI(4,5)P₂, 2% PI(3,4)P₂, 2% PI(3,4,5)P₃, or 20% DOPS lipids, respectively. E) Single molecule dwell time distributions of various PIP lipid binding domains plotted as dwell time versus log₁₀(1-cumulative distribution frequency). Curves are fit with a single or double exponential decay curve yielding the following dwell times: Ax488-PLC δ ($\tau_1 = 24 \pm 2$ ms) TAPP1-SNAP-Ax647 ($\tau_1 = 1.02 \pm 0.053$ s), Ax647-Grp1 ($\tau_1 = 0.544 \pm 0.007$ s), or Dy647-Lact-C2 ($\tau_1 = 0.765 \pm 0.191$ s, $\tau_2 = 6.58 \pm 0.539$ s, $\alpha = 0.5 \pm 0.04$). F) mNG-SHIP1(PH-PP-C2) does not robustly associated with SLBs containing PIP or PS lipids. Representative images showing bulk membrane recruitment in the presence of 20 nM mNG-SHIP1(PH-PP-C2) on SLBs containing DOPC lipids plus either 2% PI(4,5)P₂, 2% PI(3,4)P₂, 2% PI(3,4,5)P₃, or 20% DOPS, respectively. Note that image intensities were scaled in a similar manner to the top row of images shown in (C).

SHIP1(PH-PPtase-C2) transiently localizes to the plasma membrane

Our *in vitro* characterization of SHIP1 on supported membranes using smTIRF lacks some of the complexity that exists on the cellular plasma membrane. To determine whether the membrane binding behavior of SHIP1(PH-PP-C2) is significantly different *in vitro* and *in vivo*, we established conditions to visualize the single molecule plasma membrane localization of SHIP1 in HEK293 cells. The rationale for using this non-immune cell type is that SHIP1's interactions with lipids should be conserved across cell type. In addition, the lack of immune cell specific proteins that potentially interact with SHIP1, reduces the complexity of the observed membrane binding behavior of SHIP1 in HEK293 cells.

For these experiments, we tagged SHIP1 and several known lipid binding domains with photoconvertible mEos (**Figure 2.2A**). Genes encoding these proteins were transiently expressed in HEK293 cells, resulting in a uniform localization pattern across the plasma membrane that lacked single molecule resolution. In order to resolve single membrane binding events, we photoconverted a fraction of the mEos tagged proteins to the more photostable red fluorescent state using a pulse of 405 nm light (**Figure 2.2B**). Plots of single molecule molecular brightness distributions and photobleaching analysis indicate that the populations of molecules we tracked by smTIRF were labeled with a single fluorescent protein (**Figure 2.2C-2.2D**).

Next, we visualized single molecule membrane binding events for mEos tagged SHIP1(PH-PP-C2) and several well characterized membrane binding proteins. Dwell time analysis of established lipid binding domains revealed interaction lifetimes in the range of 0.1-5 seconds (**Figure 2E**). Conversely, mEos-SHIP1(PH-PP-C2) expressed in

HEK293 cells exhibited plasma membrane interactions that were very transient in nature ($\tau_1 = 0.037$ seconds) and nearly identical to our *in vitro* measurements on SLB containing 20% PS lipids (**Figure 2.3I**).

Analysis of mEos-SHIP1(PH-PP-C2) plasma membrane binding in human neutrophil-like cells (i.e. PLB-985), yielded similar dwell time kinetics, consistent with the membrane dwell time of mEos-SHIP1(PH-PP-C2) being dependent on transient lipid interactions, rather than cell-type specific proteins interactions.

To determine whether the membrane binding avidity of mEos-SHIP1(PH-PP-C2) can be modulated by changes in substrate availability at the plasma membrane, we stimulated PLB-985 neutrophil-like cells with the chemoattractant, N-formyl-methionine-leucine-phenylalanine (fMLF). Activation of the formyl peptide receptor with fMLF results in a transient spike in PI(3,4,5)P₃ and PI(3,4)P₂ production, which we visualized using a GFP-TAPP1 biosensor (**Figure 2.2F**) and mScarlet-Akt1 biosensor (data not shown). We observed no change in the bulk plasma membrane localization or single molecule dwell times of mEos-SHIP1(PH-PP-C2) following PLB-985 cell activation with 10 nM fMLF (**Figure 2.2G-2.2I**), further supporting an absence of high affinity interactions PI(3,4,5)P₃ and PI(3,4)P₂ lipids.

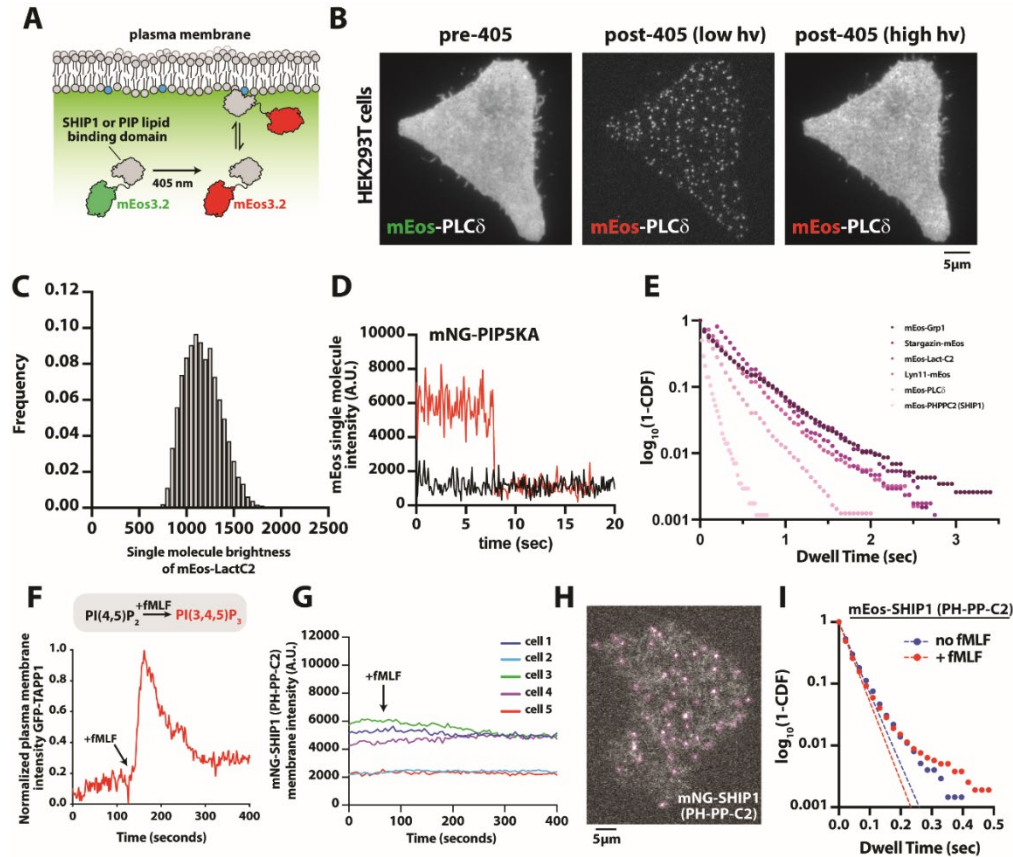


Figure 2.2: SHIP1(PH-PP-C2) transiently associates with the plasma membrane in live cells. A) Cartoon diagramming UV-dependent photoconversion and plasma membrane binding of a mEos tagged cytoplasmic protein in cells. B) Representative images showing localization of mEos3.2-PLC δ before and after photoconversion with 405 nm UV light (“low” and “high” laser power). Localization of mEos3.2-PLC δ was visualized using TIRF-M. C) Molecular brightness distribution of single plasma membrane localized mEos3.2-Lact-C2 molecules based on brightness of single kinases first attaching to the supported membrane. D) Stepwise photo-bleaching of a single membrane bound mNG-PIP5KA dimer compared to the background fluorescence of the cell. E) Single molecule dwell distributions of mEos3.2 tagged SHIP1(PH-PP-C2), Lact-C2, TAPP1, PLC δ , and Grp1. Curves were fit with a single or double exponential decay curve to calculate dwell times. F) Plot showing the translocation of GFP-TAPP1 to the plasma membrane following stimulation of PLB-985 cells with 10 nM fMLF. G) Bulk membrane localization of mEos3.2-SHIP1(PH-PP-C2) in PLB-985 cells does not change in response to stimulation with 10 nM fMLF (arrow). Traces represent the single cell plasma membrane intensity of mEos3.2-SHIP1(PH-PP-C2) measured by TIRF-M. H) Representative image showing single particle detection of mNG-SHIP1 in live PLB-985 cells. I) Single molecule dwell time distributions of photoconverted mEos3.2-SHIP1(PH-PP-C2) in PLB-985 cells \pm 10 nM fMLF plotted as dwell time versus $\log_{10}(1\text{-cumulative distribution frequency})$. Curves are fit with a single exponential decay curves and both curves yield the following dwell time, $\tau_1 = 0.037$ seconds.

The central domain of SHIP1 catalyzes PI(3,4,5)P₃ dephosphorylation with simple unimolecular kinetics

Based on reported lipid interactions, researchers have hypothesized that SHIP1 catalyzes the dephosphorylation of PI(3,4,5)P₃ with a positive feedback loop based on interactions with both substrate and product (Ming-Lum et al. 2012; Ong et al. 2007; Nelson et al. 2021). To measure potentially nonlinear reaction kinetics, we developed an *in vitro* activity assay to simultaneously visualize SHIP1 membrane binding and lipid phosphatase activity using TIRF microscopy.

For these experiments, we initially used fluorescently labeled TAPP1 PH domain to monitor PI(3,4)P₂ production by SHIP1. However, we found that the interaction between PI(3,4)P₂ and fluorescently labeled TAPP1 was too strong for our kinetic assays. TAPP1 displayed sustained membrane recruitment dynamics, which made quantification of reaction completion times ambiguous. For this reason, we used the Alexa647-Grp1 PH domain to monitor PI(3,4,5)P₃ dephosphorylation by SHIP1 (**Figure 2.3A**). We found that the Grp1 sensor rapidly dissociated from supported membranes, following SHIP1 mediated dephosphorylation of PI(3,4,5)P₃.

To display kinetic traces in terms of product formation, we converted the Grp1 membrane dissociation curves to represent the time dependent change in PI(3,4)P₂ levels (**Figure 2.3B**). Independent of how data was plotted, kinetic traces were hyperbolic shaped (**Figure 2.3B**). Consistent with SHIP1 catalyzing reactions with unimolecular kinetics, we observed no reciprocal regulation linking PI(3,4)P₂ production to membrane recruitment and activation of SHIP1 (**Figure 2.3C**). If there was any reciprocal regulation resulting from lipid interactions, albeit weak interactions, SHIP1 membrane recruitment

would be sigmoidal in character. However, membrane fluorescent intensity of mNG-SHIP1(PH-PP-C2) remained constant throughout the course of the reaction (**Figure 2.3C**). This was consistent with the very transient interactions we observed between mNG-SHIP1(PH-PP-C2) and PIP lipids by smTIRF (**Figure 2.1E**).

Phosphatidylserine (PS) lipids have been reported to bind to the C2 domain of SHIP2 and allosterically regulate its phosphatase activity (Le Coq et al. 2017). Consistent with this model, we measured enhanced SHIP1 phosphatase activity over a range of PS lipid densities (**Figure 2.3D-2.3E**). However, the increase in activity was not correlated with a dramatic change in membrane localization (**Figure 2.3F**) and single molecule dwell time analysis of mNG-SHIP1(PH-PP-C2) revealed very transient membrane binding dynamics on membranes with high percentages of PS (**Figure 2.3G**). PS dependent enhancements in activity without any associated enhancements in localization is consistent with a mechanism of allosteric regulation. Next, we aimed to determine if PS lipids could similarly increase phosphatase activity of full-length SHIP1 (1-1188aa) (FL SHIP1). We found that PS lipids enhanced the activity of FL SHIP1, but was still less active compared to SHIP1(PH-PP-C2) (**Figure 2.3H**). This suggests that FL SHIP1 is autoinhibited, even in the presence of PS lipids.

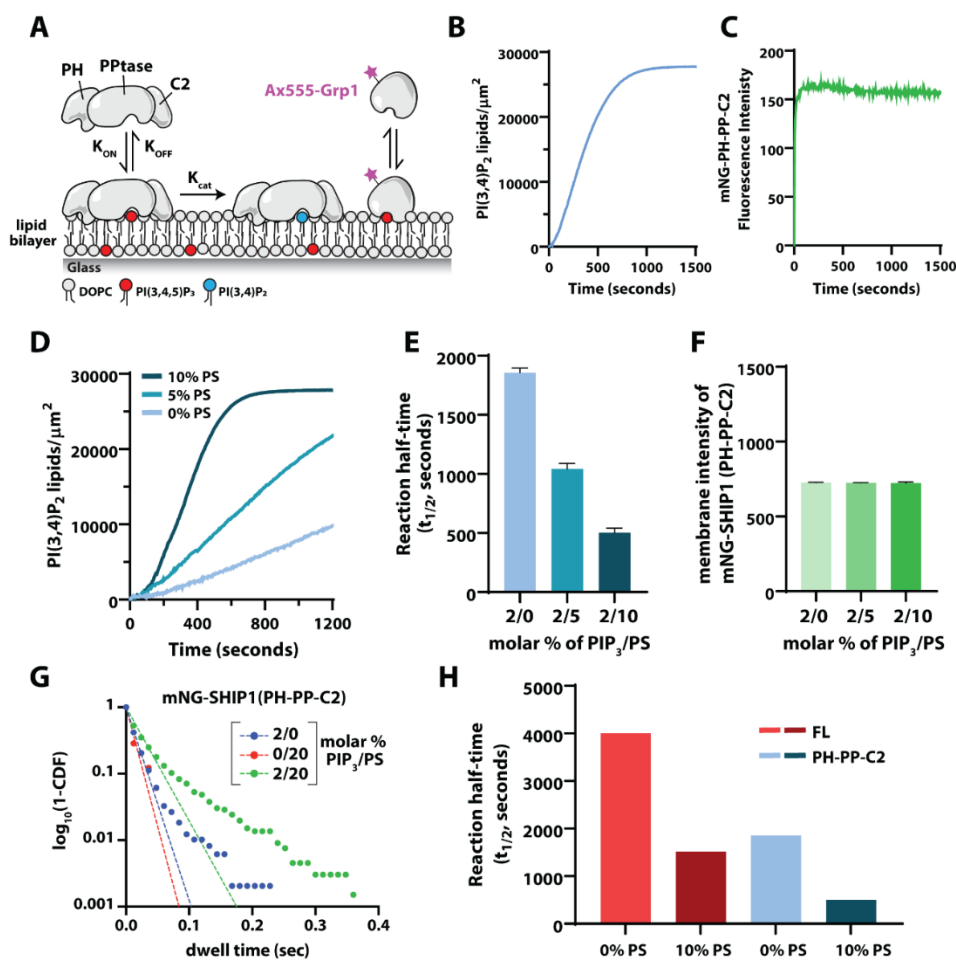


Figure 2.3: SHIP1 catalyzes the dephosphorylation of PI(3,4,5)P3 with simple unimolecular kinetics that can be enhanced with PS. A) Experimental design for measuring SHIP1 lipid phosphatase activity in vitro on supported lipid bilayers using TIRF-M. B) Kinetics of 20nM SHIP1(PH-PP-C2). PI(3,4,5)P3 dephosphorylation measured using 20 nM Ax647-Grp1. C) Bulk membrane localization of 20nM mNG-SHIP1 during catalysis shown in (B). D) PS lipids enhance SHIP1 phosphatase activity. Representative kinetics traces of 4 nM mNG-SHIP1 (PH-PPtase-C2 domain) in the absence and presence of PS lipids. Production of PI(3,4)P2 was monitored by the presence of 20 nM Ax647-Grp1. Initial membrane composition: 98-88% DOPC, 0-10% PS lipids, and 2% PI(3,4,5)P3. E) Quantification of reaction half time in (D). Bars equal mean values [N = 2 reactions per concentration, error = SD]. F) Quantification of mNG-SHIP1(PH-PPtase-C2) localization on SLBs containing 2% PI(3,4,5)P3 and 0, 5, 10% PS lipids [N = 10 fluorescent intensity measurements per sample from 1 experiment, error = SD]. G) Single molecule dwell time distributions of mNG-SHIP1(PH-PPtase-C2) measured in the presence of PS, PI(3,4,5)P3, and PS/PI(3,4,5)P3. H) Reaction half times comparing 4nM Full-length SHIP1 activity to 4nM SHIP1(PH-PPtase-C2). Activities were measured on SLBs containing 2% PI(3,4,5)P3 or 2% PI(3,4,5)P3 + 10% PS. Full-length SHIP1 is stimulated by PS lipids, but exhibits lower activity compared to SHIP1(PH-PPtase-C2).

Full-length SHIP1 is autoinhibited by the N-terminal SH2 domain

It was previously demonstrated that truncating the C-terminus of SHIP1 enhances phosphatase activity of FL SHIP1, suggesting the C-terminus negatively regulates phosphatase activity (J. Zhang, Ravichandran, and Garrison 2010). By contrast, studies using SHIP2 immunoprecipitated from cell lysate found that the N-terminal SH2 domain in conjunction with the C-terminus inhibits SHIP2 activity (Prasad, Werner, and Decker 2009). To investigate potential mechanisms of SHIP1 autoinhibition, we purified full-length (FL) recombinant SHIP1, an N-terminal truncation mutant (Δ SH2), and a C-terminal truncation mutant (Δ CT) using baculovirus expression in insect cells (**Figure 2.4A**). Using our TIRF phosphatase assay, we measured the phosphatase activity of FL SHIP1 and different truncation mutants. These experiments revealed that FL SHIP1 has reduced activity compared to SHIP1 (PH-PP-C2) construct (**Figure 2.4B**). Although it was previously demonstrated that truncating the C-terminus of SHIP1 increased activity 9-fold (J. Zhang, Ravichandran, and Garrison 2010), removal of this region only increased SHIP1 activity 1.8 fold compared to the FL protein (**Figure 2.4B-2.4D**). The C-terminus of SHIP1 has two NPxY motifs that can be phosphorylated. However, this increase in activity is not a result of lost post translational modification because dephosphorylating C-terminal tyrosine residues with the promiscuous tyrosine phosphatase, YopH, has no effect on SHIP1 phosphatase activity (data not shown).

Biochemical characterization of the SHIP2 isoform found that the N-terminal SH2 domain in conjunction with the C-terminus inhibits SHIP2 activity (Prasad, Werner, and Decker 2009). In our experiments, removal of the N-terminal SH2 domain of SHIP1

yielded an activity curve nearly identical to our PH-PP-C2 truncation mutant, suggesting that SHIP1 autoinhibition is largely dependent on the SH2 domain (Figure 2.4B-2.4D).

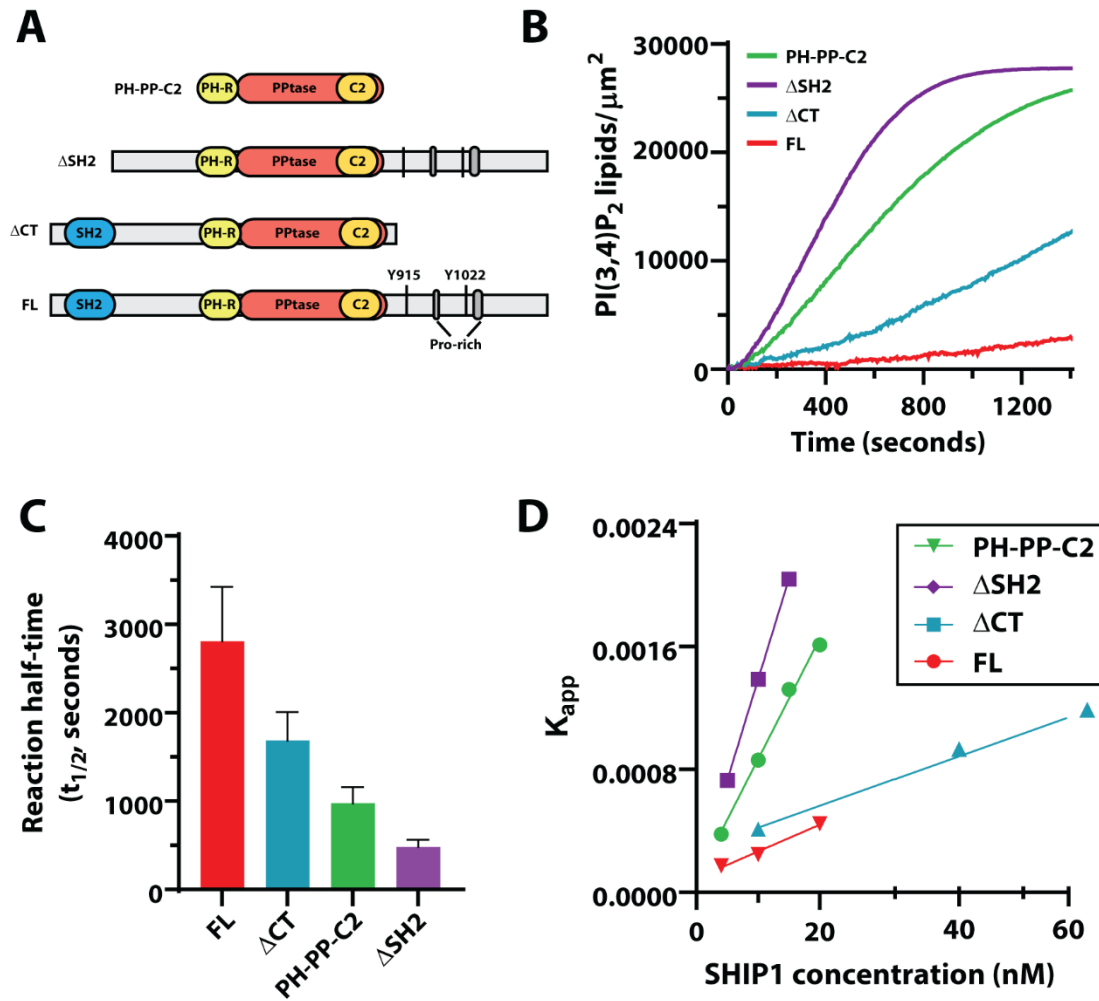


Figure 2.4: Full-length SHIP1 is autoinhibited by the N-terminal SH2 domain. A) Domain organization of full-length (FL) SHIP1 and truncation mutants used in supported lipid bilayer TIRF-M assays. B) Kinetic traces showing the dephosphorylation of PI(3,4,5)P₃ in the presence 10 nM mNG tagged FL SHIP1, SHIP1(PH-PPtase-C2), SHIP1(Δ SH2), and SHIP1(Δ CT). C) Quantification of reaction half times measured in the presence of 10 nM SHIP1, FL and truncation mutants. Bars equal mean values [N = 4-5 technical replicates, error = SD]. D) Plot shows the relationship between SHIP1 concentration and phosphatase activity. comparing FL SHIP1, SHIP1(PH-PPtase-C2), SHIP1 (Δ SH2), and SHIP1 (Δ C-terminus). (B-F) Initial membrane composition: 96% DOPC, 2% PI(3,4,5)P₃, 2% MCC-PE (quenched/non-reactive).

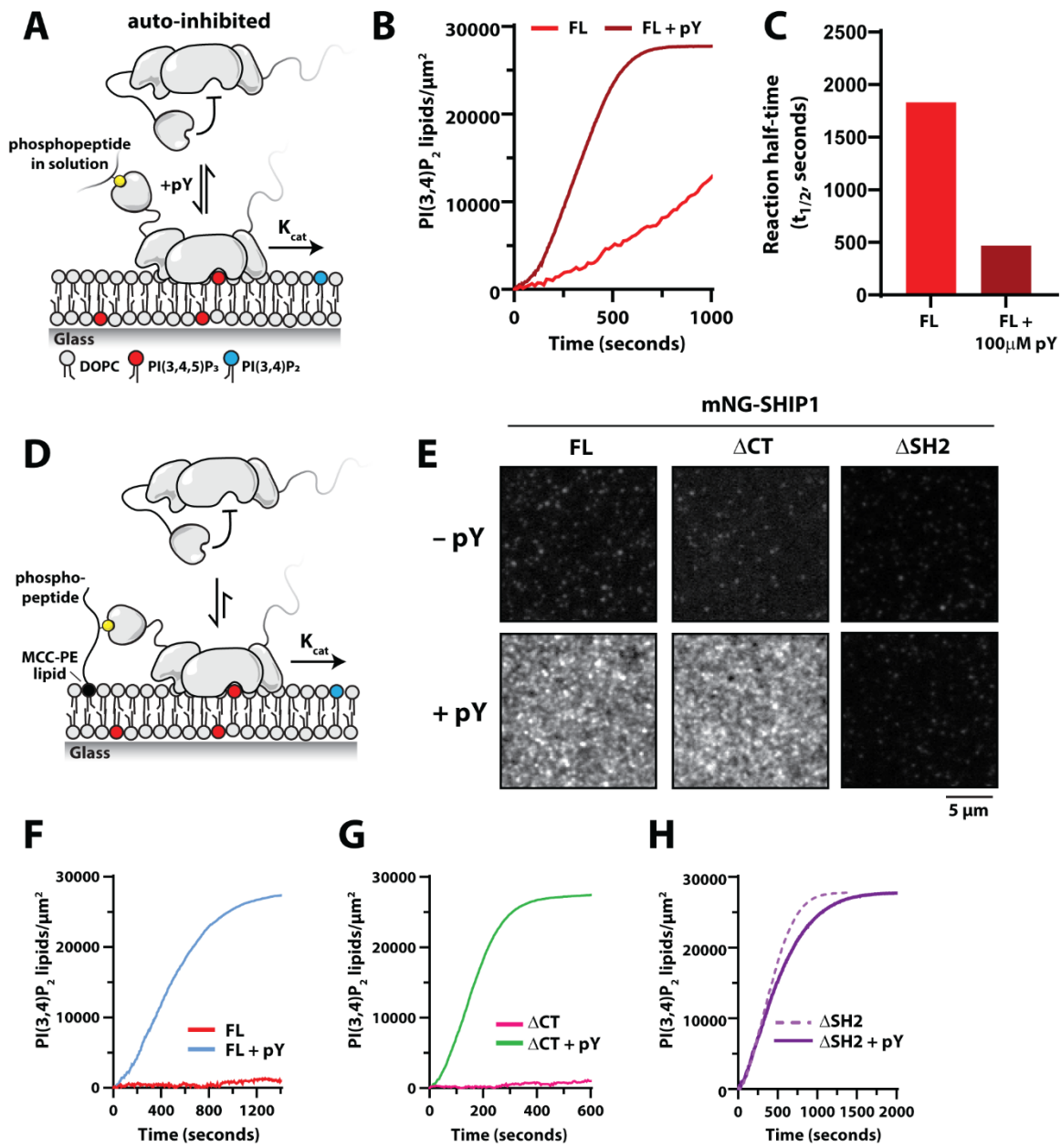
Membrane recruitment and activation of SHIP1 by a phosphotyrosine peptide

In cell signaling, Src-Homology 2 (SH2) domains play a critical role regulating interactions with immune receptors that contain tyrosine phosphorylated motifs (pY) (Pawson 2004; Pauls et al. 2016). Because truncating the SH2 domain of SHIP1 relieved autoinhibition, we hypothesized that phosphopeptide interactions with the SH2 domain could activate SHIP1 (**Figure 2.5A**). To decipher this mechanism, we derived a peptide from the immunoreceptor tyrosine inhibitory motif (ITIM) of the Fc γ RIIB receptor containing a single phosphotyrosine residue (pY-ITIM). SHIP1 is reported to be critical for the inhibitory function of Fc γ RIIB (Isnardi et al. 2006), and this peptide was previously shown to interact with the SH2 domain of SHIP1 in a pulldown assay (Mukherjee et al. 2012). In solution, the pY-ITIM peptide enhanced the activity of FL SHIP1 (**Figure 2.5B-2.5C**).

In vivo, SHIP1 is recruited to the plasma membrane by pY-ITIM following receptor activation in immune cells (Pauls et al. 2016). To determine how membrane anchored pY-ITIM regulates SHIP1 membrane recruitment and activation, we covalently attached the pY-ITIM peptide to a cysteine reactive maleimide lipid that was incorporated into a supported membrane containing PI(3,4,5)P₃ lipids (**Figure 2.5D**). We found that pY-ITIM covalently coupled to lipids rapidly activated SHIP1 compared to experiments performed with the pY-ITIM peptide in solution (**Figure 2.5F**). This further increase is likely a result of SHIP1 being recruited to the membrane and localized closer to its lipid substrate (**Figure 2.5E**). We also measured rapid activation of the partially autoinhibited C-terminal truncation mutant (Δ CT) (**Figure 2.5G**) and localization to SLBs (**Figure 2.5E**). We didn't see any pY dependent localization of the N-terminal

truncation mutant (Δ SH2) (**Figure 2.5H**), supported by the absence of pY binding (**Figure 2.5E**). Together, these results further support an autoinhibitory mechanism that's mediated by the N-terminal SH2 domain and demonstrates that receptor binding can both activate and membrane recruit SHIP1.

Figure 2.5: Phosphotyrosine peptides regulate membrane recruitment and activation of SHIP1. (Next Page) A) Experimental design for measuring SHIP1 phosphatase activity in the presence phosphotyrosine peptides derived from ITIM motif of the Fc γ RIIB receptor (pY-ITIM) in solution. B) 100 μ M pY-ITIM in solution stimulates the phosphatase activity of 20nM full-length SHIP. Initial membrane composition: 96% DOPC, 2% PI(3,4,5)P3, 2% MCC-PE (quenched/non-reactive). C) Quantification of reaction half times in (B). D) Experimental design for measuring SHIP1 phosphatase activity in the presence of membrane tethered pY-ITIM peptides. E) Representative TIRF-M images showing localization of 5nM mNG-SHIP1(FL, 1-1188aa), mNG-SHIP1(Δ CT), and mNG-SHIP1(Δ SH2) in the presence of pY-ITIM conjugated to the membrane. F) Membrane conjugated pY-ITIM peptide stimulates 0.1 nM SHIP1 (FL) phosphatase activity. G) Membrane conjugated pY-ITIM peptide stimulates 0.1 nM SHIP1 (Δ CT) phosphatase activity. H) Membrane conjugated pY-ITIM peptide does not stimulates 5 nM SHIP1 (Δ SH2) phosphatase activity. (F-H) Plots show representative kinetics traces. Production of PI(3,4)P2 was monitored by the presence of 20 nM Ax647-Grp1. (E-H) Initial membrane composition: 96% DOPC, 2% PI(3,4,5)P3, 2% MCC-PE-(pY conjugated).



DISCUSSION

SHIP1 lipid binding specificity

SHIP1 is a multidomain protein with two proposed lipid binding domains considered important for membrane localization and activity (Ming-Lum et al. 2012; Ong et al. 2007) (**Figure 1**). Due to a lack of structural data and mutational analysis of these domains, it has been difficult to define the molecular basis of SHIP1's lipid binding specificity. To gain insight about the nature of SHIP1 lipid binding specificity, we directly visualized membrane association and dissociation dynamics of fluorescently labeled SHIP1 of supported lipid bilayers using single molecule TIRF-M. Despite reports of PIP lipid interactions being mediated by both the pleckstrin-homology related (PH-R) (Ming-Lum et al. 2012) or C2 domains (Ong et al. 2007), our *in vitro* single molecule dwell time analysis indicates that SHIP1 does not strongly associate with PI(4,5)P₂, PI(3,4)P₂, PI(3,4,5)P₃, or PS lipids that are incorporated into supported membranes. Based on the reported affinity that SHIP1 has for PI(3,4)P₂ ($K_D = 6$ nM) and PI(3,4,5)P₃ ($K_D = 1$ nM) (Nelson et al. 2021), we expected to observe single molecule dwell times greater than 10 seconds. This estimate is based on the assumption that SHIP1 membrane association is diffusion limited (i.e. $K_{ON} = 10 \mu\text{M}^{-1}\text{sec}^{-1}$). Instead, we could only observe transient SHIP1 membrane interactions, which required reducing the buffer ionic strength or measuring single molecule dwell times in the presence of both PS and PI(3,4,5)P₃ lipids. Based on the proposed reciprocal regulation between SHIP1 and PIP lipids interactions, we also expected SHIP1 localization to be cooperative in nature and for activity traces to display positive feedback based on product recognition. Instead, SHIP1 catalyzed PI(3,4,5)P₃ dephosphorylation with unimolecular kinetics and displayed no

enhanced membrane recruitment over the course of any phosphatase catalyzed reaction. Overall, the lipid binding interactions we observed for SHIP1 were extremely transient in nature and inconsistent with the specificity and nanomolar affinities previously measured using surface plasma resonance (SPR), protein lipid overlay (PLO) assays, and nuclear magnetic resonance (NMR) spectroscopy (Ming-Lum et al. 2012; Ong et al. 2007; Nelson et al. 2021).

SHIP1 activation by phosphatidylserine (PS)

The C2 domain of the SHIP1 paralog, SHIP2, reportedly interacts with phosphatidylserine (PS) and allosterically enhances phosphatase activity (Le Coq et al. 2017). Despite including up to 20% PS lipids in our TIRF-M supported membrane experiments, we did not observe an enhancement in the bulk membrane recruitment of mNG-SHIP1(PH-PP-C2). PS lipids did, however, strongly stimulate the lipid phosphatase activity of mNG-SHIP1(PH-PP-C2), consistent with the reported mechanism of allosteric regulation for SHIP2 (Le Coq et al. 2017). Similarly, we observed a PS dependent increase in full-length SHIP1 activation. However, the overall activity was substantially lower compared to the SHIP1(PH-PP-C2) protein lacking autoinhibition. This suggests that full-length SHIP1 is autoinhibited by a mechanism that is partially resistant to PS-mediated activation. Considering that the plasma membrane contains 10-20% PS (Vance and Steenbergen 2005), full-length SHIP1 would be less susceptible to spuriously activation, which would prevent the disruption of cellular PI(3,4,5)P₃ and PI(3,4)P₂ lipid homeostasis. Based on our single molecule dwell time analysis of mNG-SHIP1(PH-PP-C2), the presence of both PS and PI(3,4,5)P₃ lipids synergistically enhanced membrane binding. However, the modest 2-fold increase in dwell time we

observe does not explain the 10-fold increase in activity caused by PS lipids. Perhaps a transient interaction between the C2 domain and PS lipids helps orient the phosphatase domain on the membrane in a manner that makes SHIP1 more catalytically efficient. Looking at sequence homology between SHIP1 and SHIP2, we find that the phosphatase domains share 65% identity, while the C2 domains share 43% homology. Although PS-dependent allosteric activation of SHIP1 is potentially mediated by the phosphatase and C2 domain interface, like has been described for SHIP2 (Le Coq et al. 2017), the molecular basis remains unclear.

Mechanism of SHIP1 autoinhibition

We performed a mutational analysis of full-length SHIP1 to determine which domains suppress lipid phosphatase activity. We found that deletion of the disordered C-terminus partially activates SHIP1, while deletion of the N-terminal SH2 domain fully activates the enzyme. Because the C-terminus of SHIP1 (892-1188aa) is predicted to be disordered, it remains unclear whether this region forms intramolecular contacts with a specific folded domain of SHIP1. Alternatively, the extended disordered C-terminal domain of SHIP1 could sterically hinder substrate binding. This type of mechanism was reported for the guanine nucleotide exchange factor (GEF) Son of Sevenless (SOS), which also contains an extended disordered C-terminal domain and multiple layers of autoinhibition (Lee et al. 2017). Based on biochemical assays for measuring activation of the small GTPase, H-Ras, researchers previously reported that the presence of the unstructured poly-proline motif attenuated SOS GEF activity by lowering the association rate constant of SOS (Lee et al. 2017). To date, no specific intramolecular interactions

have been identified to regulate SOS1's C-terminus dependent autoinhibition of GEF activity.

Since the N- and C-terminus both contribute to autoinhibition, we initially hypothesized that SHIP1 was regulated by intramolecular interactions between the SH2 domain and tyrosine phosphorylated residues located in the C-terminus. By this mechanism, SHIP1 could adopt an autoinhibited conformation similar to a Src-family non-receptor tyrosine kinase (Xu, Harrison, and Eck 1997; Sicheri, Moarefi, and Kuriyan 1997). Suggestive of this model, the SH2 domain of SHIP1 was previously shown to interact with an isolated peptide containing phosphorylated Y1022 derived from SHIP1 (Mukherjee et al. 2012). However, since these interactions were reconstituted using minimal fragments, it's unclear whether the SH2 domain and the phospho-Y1022 peptide can form intramolecular contact in the context of length of SHIP1. Ultimately, determining the exact intramolecular interactions that regulate SHIP1 autoinhibition will require combining structural biochemistry and mutational analysis.

In our investigations of SHIP1 autoinhibition, we found that incubating SHIP1 with the promiscuous tyrosine phosphatase, YopH (Z. Y. Zhang et al. 1992), did not relieve autoinhibition. This supports a model in which SHIP1 autoinhibition under our experimental conditions is not mediated by intramolecular interactions with phosphorylated tyrosine residues. However, in the context of immune cell signaling, post-translational modifications of the C-terminal NPxY motifs could cause SHIP1 to adopt an auto-inhibited conformation that is mediated by intramolecular head-to-tail interactions or intermolecular daisy-chain structures.

In considering potential mechanisms for SHIP1 autoinhibition, we can draw parallels to the structural understanding of autoinhibited class 1A phosphatidylinositol 3-kinase (PI3K) (Vadas et al. 2011). The regulatory subunit of PI3K contains two SH2 domains that each form intermolecular contacts with the catalytic subunit of PI3K. These interactions occur independently of a tyrosine phosphopeptide interaction. Similar to SHIP1, the SH2 domains of class I PI3Ks bind phosphorylated receptors, which releases autoinhibition to activate PI3K (Vadas et al. 2011). Like PI3K, mutating residue R30A in SHIP1's SH2 domain abolishes pY binding without disrupting autoinhibition. This suggests that SHIP1 autoinhibition is mediated by the SH2 domain, but these interactions are distal to the pY binding pocket.

Mechanisms controlling SHIP1 membrane localization in cells

The production of PI(3,4,5)P₃ lipids during immune cell signaling has been shown to enhance plasma membrane localization of full-length SHIP1 (Ming-Lum et al. 2012). However, it has been unclear whether this response is regulated by a direct SHIP1-PI(3,4,5)P₃ interaction or indirectly mediated by peripheral membrane binding proteins that bind to PI(3,4,5)P₃ lipids. Single molecule visualization of SHIP1 in cells using photoconvertible Eos3.2 revealed that a small fraction of mEos-SHIP1(PH-PP-C2) molecules transiently localize to the plasma membrane. The membrane binding dynamics of mEos-SHIP1(PH-PP-C2) measured in cells were similarly transient to those measured on SLBs containing 2% PI(3,4,5)P₃ and 20% DOPS. Consistent with membrane localization of purified mNG-SHIP1(PH-PP-C2) being insensitive to changes in PIP lipids composition *in vitro*, acute changes in PI(3,4,5)P₃ levels did not modulate the bulk or single molecule membrane binding dynamics of SHIP1 in immune cells. Overall, the

apparent lack of high affinity PS or PIP lipid interactions described here, suggests that SHIP1 membrane localization in cells is dominated by interactions with peripheral membrane proteins.

SHIP1 contains a variety of protein interaction domains and motifs that can potentially modulate its membrane localization and phosphatase activity in living cells. In the context of B-cell receptor signaling, SHIP1 is recruited by the ITIM motif of the inhibitory Fc γ RIIB receptor to down regulate this signaling process (Isnardi et al. 2006). SHIP1's interaction with the Fc γ RIIB receptor is dependent on its SH2 domain and tyrosine phosphorylation of the ITIM motif (Pauls et al. 2016). Our *in vitro* reconstitution demonstrates for the first time that membrane tethered phosphotyrosine peptides (i.e. pY-ITIM) robustly recruit and activate SHIP1 on PI(3,4,5)P₃ containing membranes. The data presented here also supports a model in which SHIP1 activity is largely regulated by its N-terminal SH2 domain. Although the C-terminus of SHIP1 has numerous protein interaction motifs that can potentially direct SHIP1 to critical locations at the plasma membrane, the molecular basis of those interactions are still being determined. By filling the gap in knowledge concerning how SHIP1 activity and membrane localization is regulated, in the future, we can better understand how cells control the strength and duration of PI(3,4,5)P₃ signaling events. Lastly, given that SHIP1 is implicated in several diseases, including cancer (F. Li et al. 2017) (McKeever et al. 2017)(Ngoh et al. 2016)(Brooks et al. 2010; Chen et al. 2015; Nalaskowski et al. 2018; Fu et al. 2019), the described regulatory mechanisms will undoubtedly be of pharmacological interest.

MATERIALS AND METHODS

Molecular Biology.

Genes coding for human phosphatidylinositol 4,5-bisphosphate phosphodiesterase delta-1 PH domain (PLC δ , Acc# P51178.2) was synthesized by GeneArt (Invitrogen) as a codon optimized open reading frame. Genes coding for human tandem pleckstrin homology-domain-containing protein-1 PH domain was cloned out of mKate2-P2A-APEX2-TAPP1-PH, a gift from Rob Parton (TAPP1, Addgene plasmid # 67662). Genes coding for human Src-homology-2-domain-containing inositol 5-phosphatase 1 (SHIP1 or INPP5D) was purchased as a cDNA clone from Dharmacon. Gene fragments were subcloned into bacterial and baculovirus protein expression vectors containing coding sequences with different solubility and affinity tags. SHIP1 was cloned into a modified FAST Bac1 vector using Gibson Assembly. The complete open reading frame of all vectors used in this study were sequenced by Genewiz to ensure the plasmids lacked deleterious mutations. Each protein expression construct was screened for optimal yield and solubility in either bacteria (BL21 DE3 Star, Rosetta, etc) or *Spodoptera frugiperda* (Sf9) insect cells.

Purification of BACMID DNA.

To create BACMID DNA, FASTBac1 plasmids were transformed into DH10 Bac cells and plated on agar containing 50 $\mu\text{g}/\text{mL}$ kanamycin, 10 $\mu\text{g}/\text{mL}$ tetracycline, 7 $\mu\text{g}/\text{mL}$ gentamycin, 40 $\mu\text{g}/\text{mL}$ X-GAL, and 40 $\mu\text{g}/\text{mL}$ IPTG. After 2-3 days of growth at 37°C, positive clones were isolated based on blue-white colony selection. Single white colonies were picked and re-struck on a BACMID agar plate for a secondary selection.

BACMIDs were purified from 3 mL bacterial cultures grown overnight in TPM. Bacteria are centrifuged and resuspended in 300 μ L of buffer containing 50 mM Tris [pH 8.0], 10 mM EDTA, 100 μ g/mL RNase A (Qiagen PI buffer). Bacteria were then lysed by adding 300 μ L of buffer containing 200 mM NaOH, 1% SDS (Qiagen P2 buffer). Neutralize lysis buffer by adding 300 μ L of 4.2 M Guanidine HCl, 0.9 M KOAc [pH 4.8] (Qiagen N3 buffer). Centrifuge sample at 23°C for 10 minutes at 14,000 x g. Remove supernatant and combine with 700 μ L 100% isopropanol. Centrifuge sample at 23°C for 10 minutes at 14,000 x g. Remove supernatant and add 200 μ L of 70% ethanol. Centrifuge sample at 23°C for 10 minutes at 14,000 x g. Remove supernatant and add 50 μ L of 70% ethanol. Centrifuge sample at 23°C for 10 minutes at 14,000 x g. Remove supernatant and dry DNA pellet slightly in biosafety hood. Solubilize DNA with 40 μ L of sterile water. Resuspend DNA pellet by tapping side of micro-centrifuge tube 15-20 times. Quantify concentration of DNA using NanoDrop (typically 200-300 ng/ μ L). Immediately used BACMID DNA for transfection of Sf9 cells. Remaining BACMID DNA can be stored in -20°C freezer.

Baculovirus production.

Baculoviruses was generated by transfecting 1×10^6 *Spodoptera frugiperda* (Sf9) insect cells plated for 24 hours in a Corning 6-well plastic dish (Cat# 07-200-80) containing 2 mL of ESF 921 Serum-Free Insect Cell Culture media (Expression Systems, Cat# 96-001, Davis, CA.). All media contains 1x concentration of Antibiotic-Antimycotic (Gibco/Invitrogen, Cat#15240-062). For transfection, 5-7 μ g BACMID DNA was incubated with 4 μ L Fugene (Thermo Fisher, Cat# 10362100) in 200 μ L of ESF 921

media for 30 minutes at 23⁰C. BACMID DNA and Fugene were added dropwise to 6-well dish. Media change before and after addition of transfection reagent is unnecessary. After 4-5 days of transfection, viral supernatant (termed 'P0') is harvested, centrifuged, and used to infect 7 x 10⁶ *Sf9* cells plated for 24 hours in 10 cm tissue culture grade petri dish containing 10 mL of ESF 921 media and 10% Fetal Bovine serum (Seradigm, Cat# 1500-500, Lot# 176B14). After 4 days, viral supernatant (termed 'P1') is harvested and centrifuged to remove cell debris. Typical P1 viral titer yield is 10-12 mL. The P1 viral titer is expanded in 100 mL *Sf9* cell culture grown to a density of 1.25-1.5 x 10⁶ cells/mL in a sterile 250 mL polycarbonate Erlenmeyer flask with vented cap (Corning, #431144). We typically transduce 100 mL *Sf9* culture with a concentration of 1% vol/vol of P1 viral titer. Remaining P1 virus is frozen as 1.5 mL aliquots that are stored in the -80⁰C freezer. The 10% Fetal Bovine serum serves as a cryo-protectant. After 4 days, viral supernatant (termed 'P2') is harvested, centrifuged, and 0.22 µm filtered in 150 mL filter-top bottle (Corning, polyethersulfone (PES), Cat#431153). The P2 viral supernatant is used for protein expression in either *Sf9* or High 5 cells grown in ESF 921 Serum-Free insect cell culture media. The MOI for optimal protein expression is determined empirically to minimize cell death and maximize protein yield (typically 1.5-2% vol/vol final concentration of P2 virus).

SHIP1 and SHIP1 mutants (FL, ΔCT, ΔSH2).

The coding sequence of full-length human SHIP1 (1-1188aa) was cloned into a modified FastBac1 vector containing an N-terminal his6-TEV-mNG fusion. High five insect cells were infected with baculovirus using an optimized multiplicity of infection

(MOI), typically 1.5–2% vol/vol, which we empirically determined based on small-scale test expressions (25-50 mL culture). Infected cells were typically grown for 48 hours at 27°C in ESF 921 Serum-Free Insect Cell Culture medium (Expression Systems, Cat# 96-001-01). Cells were harvested by centrifugation, transferred to 50 mL tubes by washing with 1x PBS [pH 7.2], pelleted and resuspended in 10 mL of 1x PBS [pH 7.2], 10% Glycerol, and 2x protease inhibitor cocktail (1 Sigma protease inhibitor tablet per 50 mL of buffer) and then stored in the -80°C freezer.

For purification, frozen cell pellets were thawed in an ambient water bath and lysed into buffer containing 30 mM Tris [pH 8.0], 10 mM imidazole, 400 mM NaCl, 1 mM PMSF, 2 mM BME, Sigma protease inhibitor cocktail EDTA free per 100 mL lysis buffer, and 100 µg/mL DNase using a dounce homogenizer. Lysate was then centrifuged at 37,000 rpm (140,000xg) for 60 minutes in a Beckman Ti70 rotor at 4°C. High speed supernatant (HSS) was then batch bound to 5 mL of Ni-NTA Agarose (Qiagen, Cat# 30230) resin at 4°C for 2 hours stirring in a beaker. The resin and HSS was collected in 50 mL tubes, centrifuged, and washed with buffer containing 20 mM Tris [pH 8.0], 30 mM imidazole, 300-400 mM NaCl, 5% Glycerol, and 2 mM BME before being transferred to gravity flow column. NiNTA resin with bound his6-TEV-mNG-SHIP1 was then washed with an additional 100 mL of 20 mM Tris [pH 8.0], 30 mM imidazole, 300-400 mM NaCl, 5% Glycerol, and 2 mM BME buffer and then eluted into buffer containing 300 mM imidazole. Peak fractions were pooled and desalted using a G25 Sephadex desalting column (GE Healthcare/Cytiva) equilibrated in 20 mM Tris [pH 8.0], 100 mM NaCl, and 1mM TCEP buffer. Any precipitation was removed via 0.22 µm syringe filtration. Clarified SHIP1 fractions were then bound to a MonoQ anion

exchange column (GE Healthcare/Cytiva) equilibrated in 20 mM Tris [pH 8.0], 100 mM NaCl, and 1 mM TCEP buffer. Proteins were resolved over a 10-100% linear gradient (0.1-1 M NaCl, 30 minutes, 1.5 mL/min flow rate). His6-TEV-mNG-SHIP1 elutes in the presence of 200-400 mM NaCl. Peak fractions containing SHIP1 were pooled, incubated with 400 μ L of 243 μ M his6-TEV protease (S291V) with poly-R tail for ~12-16 hours at 4⁰C, concentrated in a 30 kDa MWCO Amicon concentrator (Sigma Millipore), and then loaded onto a 24 mL Superdex 200 10/300 GL (GE Healthcare, Cat# 17-5174-01) size exclusion column equilibrated in 20 mM Tris pH [8] (20mM HEPES pH [7.5] for FL SHIP1), 150 mM NaCl, 10% glycerol, 1 mM TCEP, and 0.5% CHAPS buffer. Peak fractions were concentrated in a 30 kDa MWCO Vivaspin 6 centrifuge tube and flash frozen at a final concentration of 1-30 μ M using liquid nitrogen. Purification schemes for Δ SH2, Δ CT, and FL SHIP1 were nearly identical. Δ SH2 SHIP1 was incubated with 400 μ L of 243 μ M his6-TEV protease (S291V) with poly-R tail for ~12-16 hours at 4⁰C before Desalting, MonoQ, and S200 chromatography steps.

SHIP1 mutant (mNG-PH-PP-C2).

BL21 (DE3) Star bacteria were transformed with his10-TEV-mNG-GGGGG-SHIP1 (mNG-PH-PP-C2, 191-878aa) and plated on LB agar containing 50 μ g/ml kanamycin. The following day, 50mL of TPM media (20g tryptone, 15g yeast extract, 8g NaCl, 2g Na₂HPO₄, and 1g KH₂PO₄ per liter) containing 50 μ g/ml kanamycin was inoculated with one bacterial colony from the agar plate. This culture was grown for 12-16 hours at 27⁰C to an OD600 = 2–3, before being diluted to an OD600 = 0.05–0.1 in 2 liters of TPM media. These cultures were grown at 37⁰C to an OD600 = 0.6-0.8, shifted

to 30°C for 1 hour, and then bacteria were induced with 50 µM IPTG to express SHIP1 mutants. After 6-8 hours of expression at 30°C, bacterial cultures were harvested by centrifugation, transferred to 50 mL tubes by washing with 1x PBS [pH 7.2], pelleted, and then stored in the -80°C freezer.

For purification, frozen cell pellets were thawed in an ambient water bath and lysed into buffer containing 50 mM Na₂HPO₄ [pH 8.0], 400 mM NaCl, 1 mM PMSF, 0.4 mM BME, and 100 µg/mL DNase by micro-tip sonication (12-24 x 5 second pulses, 40% amplitude). Lysate was then centrifuged at 15,000 rpm (35,000xg) for 60 minutes in a Beckman JA-20 rotor at 4°C. During lysate centrifugation, a 5mL HiTrap chelating column (Cat#) was charged with 50 mL of 100mM CoCl₂, generously washed with water (phosphate buffer will precipitate unchelated CoCl₂ if not thoroughly removed) and equilibrated with lysis buffer lacking PMSF and DNase (>0.4mM BME will destroy charged HiTrap column and turn column brown or black). High speed supernatant (HSS) was then circulated over charged 5mL HiTrap column for 2 hours. Captured protein was washed with 100mL of 50 mM Na₂HPO₄ [pH 8.0], 400 mM NaCl, 10mM imidazole, and 0.4 mM BME and then eluted into buffer containing 500 mM imidazole. Peak fractions containing SHIP1 were pooled with 400 µL of 243 µM his6-TEV protease (S291V) with poly-R tail and dialyzed in 4L of 25 mM Na₂HPO₄ [pH 8.0], 400 mM NaCl, and 0.4 mM BME buffer at 4°C for ~12-16 hours to remove imidazole. The next day, the charged HiTrap column was equilibrated with dialysis buffer and dialyzed protein was recirculated for 2 hours at 4°C to remove his6-TEV protease and any uncleaved his10-TEV-mNG-GGGGG-SHIP1. Unbound protein was then concentrated in a 30 kDa MWCO Amicon concentrator (Sigma Millipore) and then loaded onto a 24 mL Superdex

200 10/300 GL (GE Healthcare, Cat# 17-5174-01) size exclusion column equilibrated in 20 mM Tris pH [8], 200 mM NaCl, 10% glycerol, and 1 mM TCEP buffer. Peak fractions were concentrated in a 30 kDa MWCO Vivaspin 6 centrifuge tube and flash frozen at a final concentration of 10-30 μ M using liquid nitrogen.

Sortase mediated peptide ligation

All lipid sensors were labeled on a N-terminal (Gly)₅ motif using sortase mediated peptide ligation (Ton-That et al. 1999; Guimaraes et al. 2013). Hansen et al. devised a novel approach for chemically modifying an LPETGG peptide with fluorescent dyes, which we then conjugated to our protein of interest. The LPETGG peptide was synthesized to >95% purity by ELIM Biopharmaceutical (Hayward, CA) and labeled on the N-terminal amine with N-Hydroxysuccinimide (NHS) fluorescent dye derivatives (e.g. NHS-Alexa488). This was achieved by combining 10 mM LPETGG peptide, 15 mM NHS-Alexa488 (or other fluorescent derivatives), and 30 mM Triethylamine (Sigma, Cat# 471283) in anhydrous DMSO (Sigma, Cat# 276855). This reaction was incubated overnight in the dark at 23°C before being stored in a -20°C freezer. Prior to labeling (Gly)₅ containing proteins, unreacted NHS-Alexa488 remaining in the LPETGG labeling reaction was quenched with 50 mM *Tris*(hydroxymethyl)aminomethane (Tris) [pH 8.0] buffer for at least 6 hours. Complete quenching of unreacted NHS-Alexa488 was verified by the inability to label (Gly)₅ containing proteins in the absence of a Sortase. When labeling (Gly)₅ containing proteins with the fluorescently labeled LPETGG peptide we typically combined the following reagents: 50 mM Tris [pH 8.0], 150 mM NaCl, 50 μ M (Gly)₅-protein, 500 μ M Alexa488-LPETGG, and 10-15 μ M His₆-Sortase (Δ 1-57aa).

This reaction mixture was incubated at 16-18°C for 16-20 hours, before buffer exchange with a G25 Sephadex column (e.g. PD10 or NAP5) to remove majority of dye and dye-peptide. The his₆-Sortase was then captured on NiNTA agarose resin (Qiagen) and unbound, labeled protein was separated from remaining fluorescent dye and peptide using a Superdex 75 or Superdex 200 size exclusion chromatography column (24 mL bed volume).

Preparation of small unilamellar vesicles

The following lipids were used to generate small unilamellar vesicles (SUVs): 1,2-dioleoyl-*sn*-glycero-3-phosphocholine (18:1 DOPC, Avanti # 850375C), 1,2-dioleoyl-*sn*-glycero-3-phospho-L-serine (18:1 DOPS, Avanti # 840035C), 1,2-dioleoyl-*sn*-glycero-3-phosphoethanolamine-N-[4-(*p*-maleimidomethyl)cyclohexane-carboxamide] (18:1 MCC-PE, Avanti # 780201C), D-*myo*-Phosphatidylinositol 3,4,5-trisphosphate (PI(3,4,5)P₃ diC16, Echelon P-3916-100ug). Lipids from Avanti were purchased as single use ampules containing between 0.1-5 mg of lipids dissolved in chloroform. PI(3,4,5)P₃ lipids from Echelon were purchased as salts and solubilized in 263 μL CHCl₃, 526 μL MeOH, and 211 μL H₂O.

To make liposomes, 2 μmoles total lipids are combined in a 35 mL glass round bottom flask containing 2 mL of chloroform. Lipids are dried to a thin film using rotary evaporation with the glass round-bottom flask submerged in a 42°C water bath. After evaporating all the chloroform, the round bottom flask was placed under a vacuum for 15 minutes. The lipid film was then resuspended in 2 mL of PBS [pH 7.4], making a final concentration of 1 mM total lipids. All lipid mixtures expressed as percentages (e.g. 98%

DOPC, 2% PI(3,4,5)P₃) are equivalent to molar fractions. For example, a 1 mM lipid mixture containing 98% DOPC and 2% PI(3,4,5)P₃ is equivalent to 0.98 mM DOPC and 0.02 mM PI(3,4,5)P₃. To generate 30-50 nm SUVs, 1 mM total lipid mixtures were extruded through a 0.05 μm pore size 19 mm polycarbonate membrane (Avanti #610002) with filter supports (Avanti #610014) on both sides of the PC membrane. Hydrated lipids at a concentration of 1 mM were extruded through the PC membrane 11 times.

Preparation of supported lipid bilayers

Supported lipid bilayers are formed on 25x75 mm coverglass (IBIDI, #10812). Coverglass was first cleaned with 2% Hellmanex III (Fisher, Cat#14-385-864) heated to 60-70°C in a glass coplin jar for at least 30 minutes. Coverglass is then washed extensively with MilliQ water and then etched with Piranha solution (1:3, hydrogen peroxide:sulfuric acid) for 5-10 minutes the same day SLBs were formed. Etched coverglass, washed extensively with MilliQ water again, is rapidly dried with nitrogen gas before adhering to a 6-well sticky-side chamber (IBIDI, Cat# 80608). SLBs are formed by flowing 30 nm SUVs diluted in 1x PBS pH [7.2] to a total lipid concentration of 0.25 mM into the assembled chamber. After 30 minutes, IBIDI chambers are washed with 4 mL of PBS [pH 7.4] to remove non-absorbed SUVs. Membrane defects are blocked for 10 minutes with a 1 mg/mL beta casein (Thermo FisherSci, Cat# 37528) diluted in 1x PBS [pH 7.4]. Before it was used as a blocking protein, frozen 10 mg/mL beta casein stocks were thawed, centrifuged for 30 minutes at 21370 x g, and 0.22 μm syringe filtered. After blocking SLBs with beta casein, membranes were washed again with 1mL of 1x PBS, followed by 1 mL of kinase buffer (20 mM HEPES [pH 7.0], 150

mM NaCl, 1 mM ATP, 5 mM MgCl₂, 0.5 mM EGTA, 200 µg/mL beta casein, 20 mM BME, and 20 mM glucose) before TIRF-M.

Conjugation of pY peptide to supported membranes

SLBs with MCC-PE lipids were used to covalently couple phosphorylated peptides to the maleimide lipid headgroups. Phosphorylated peptides (CKTEAENTIT(**pY**)SLIK, Elim Biopharmaceuticals) correspond to the ITIM sequence of the FcγRIIB C-terminus (Mukherjee et al. 2012). A cysteine (**bold**) was added to the N-terminus of the peptide to form a covalent interaction with the maleimide lipid headgroup of the MCC-PE lipids. We refer to this peptide as pY-ITIM throughout the manuscript. For these SLBs, 100 µL of 10 µM pY-ITIM peptides diluted in a 1x PBS [pH 7.4] and 0.1 mM TCEP buffer was added to the IBIDI chamber and incubated for 2 hours. The addition of TCEP significantly increases the coupling efficiency. SLBs with MCC-PE lipids were then washed with 2 mL of 5mM BME diluted in 1x PBS [pH 7.4] and incubated for 15 minutes to destroy the unreacted maleimide headgroups. SLBs were washed with 1mL of 1x PBS, followed by 1 mL of kinase buffer before TIRF-M.

Oxygen scavenging system

Glucose oxidase (32 mg/mL, 100x stock) and catalase (5 mg/mL, 100x stock) were solubilized in 20 mM HEPES [pH 7.0], 150 mM NaCl, 10% glycerol, and 1 mM TCEP buffer, and then flash frozen in liquid nitrogen and stored at -80°C. Trolox (200mM, 100x stock) is UV treated and stored at -20°C. Approximately 10 minutes before imaging, thawed 100x oxygen scavenger stocks were diluted in kinase buffer

containing 20 mM glucose to achieve a final concentration of 320 $\mu\text{g}/\text{mL}$ glucose oxidase (Serva, #22780.01 *Aspergillus niger*), 50 $\mu\text{g}/\text{mL}$ catalase (Sigma, #C40-100MG Bovine Liver), and 2 mM Trolox (UV treated, see description above).

Kinetics measurements of phosphatidylinositol lipid dephosphorylation

The kinetics of PI(3,4,5)P₃ dephosphorylation via SHIP1 was measured on SLBs formed in IBIDI chambers and visualized using TIRF microscopy. The reaction buffer contains 20 mM HEPES [pH 7.0], 150 mM NaCl, 1 mM ATP, 5 mM MgCl₂, 0.5 mM EGTA, 200 $\mu\text{g}/\text{mL}$ beta casein, 20 mM BME, and 20 mM glucose. Most kinetics assays used initial membrane compositions of 96% DOPC, 2% PI(3,4,5)P₃, and 2% MCC-PE, or 86% DOPC, 10% DOPS, 2% PI(3,4,5)P₃, 2% MCC-PE. Membrane compositions that varied from the above conditions are described in figure legends. For all experiments, we measured the conversion PI(3,4,5)P₃ to PI(3,4)P₂ by measuring the membrane dissociation of 20nM Alexa647-Grp1 (PH domain; PI(3,4,5)P₃ sensor) with TIRF-M. By convention, enzyme kinetics are plotted in terms of product formation rather than substrate depletion. Therefore, normalized kinetic traces were inverted to reflect PI(3,4)P₂ production. Assuming a footprint of 0.72 nm² as reported for DOPC lipids (Vacklin et al. 2005), we calculated a density of 27778 lipids/ μm^2 for 2% PI(3,4)P₂. Apparent rate constants (k_{app}) were calculated using the half-time relationship for first-order reactions: $t_{1/2} = 0.693/k_{\text{app}}$.

Microscope hardware and imaging acquisition

Membrane binding and lipid phosphorylation reactions reconstituted on supported lipid bilayers (SLBs) were visualized using an inverted Nikon Eclipse Ti2 microscope using a 100x Nikon (1.49 NA) oil immersion TIRF objective. TIRF-M images of SLBs were acquired using an iXion Life 897 EMCCD camera (Andor Technology Ltd., UK). Fluorescently labeled proteins were excited with either a 488 nm, 561 nm, or 637 nm diode laser (OBIS laser diode, Coherent Inc. Santa Clara, CA) controlled with a Vortran laser drive with acousto-optic tunable filters (AOTF) control. The power output measured through the objective for single particle imaging was 1-2 mW. Excitation light was passed through the following dichroic filter cubes before illuminating the sample: (1) ZT488/647rpc and (2) ZT561rdc (ET575LP) (Semrock). Fluorescence emission was detected on the iXion Life 897 EMCCD camera position after a Nikon emission filter wheel housing the following emission filters: ET525/50M, ET600/50M, ET700/75M (Semrock). All experiments were performed at room temperature (23°C). Microscope hardware was controlled by Nikon NIS elements.

Single particle tracking algorithm

After the 16-bit .tif images were cropped down to 400x400 to minimize differences in field illumination. Upon starting the TrackMate plugin (Jaqaman et al. 2008) on ImageJ/Fiji, the initial calibration settings were default and enter 'YES' for allow swapping of Z or T (depth or time). Select the LoG detector and enter the appropriate protein-related dimensions. Check the boxes applying median filter and sub-pixel localization. Apply default settings for initial thresholding, run hyperstack display,

and then filter particles based on mean intensity. Choose a tracker (simple LAP tracker was used in this paper, but LAP tracker also works). Set the following filters on the tracks: Track Start (remove particles at start of movie); Track End (remove particles at end of movie); Track displacement; X - Y location (above and below totaling 4 filters). Continue running program and display options according to one's preference. From the generated files, the dwell times and step sizes were extracted manually. A histogram and then a cumulative distribution was generated for each data set. Dwell times were fitted with a one or two species exponential function. Step sizes were fitted to the Stokes-Einstein equation for one or two species.

Calculation of single molecule dwell times

To calculate the dwell times for membrane bound molecules, we sorted into a cumulative distribution frequency (CDF) plot with the frame interval as the bin (e.g. 50 ms). The $\log_{10}(1-\text{CDF})$ is then plotted against the dwell time and fit to a single or double exponential.

Single exponential model: $f(t) = e^{(-x/\tau)}$

Two exponential model: $f(t) = \alpha * e^{(-x/\tau_1)} + (1 - \alpha) * e^{(-x/\tau_2)}$

Fitting procedure initiated with a single exponential. In cases of a low-quality single exponential fit, a maximum of two populations were used. For double exponential fit, alpha represents the percentage of the fast-dissociating molecules characterized by τ_1 .

Bridge to Chapter III

In this Chapter, I demonstrated that SHIP1 is autoinhibited by both its N-terminal SH2 domain and intrinsically disordered C-terminus. Contrary to previous reports, I show that SHIP1 displays little to no lipid binding both *in vitro* and *in vivo*. This result challenges the current model and suggests that SHIP1 relies on protein interactions to localize to intracellular membranes. I supported this by reconstituting the activation and membrane localization of SHIP1 with receptor derived phosphorylated peptides that bind the SH2 domain. This work validates a new model of SHIP1 autoregulation and identifies a novel activation mechanism. In Chapter III, I characterize SHIP1 membrane recruitment mechanisms in human neutrophils. I found that the C-terminal 110 amino acids of SHIP1 is required for localization to the excitable signaling network in resting cells and to the leading edge of migrating cells. Understanding the key motifs recruiting SHIP1 in neutrophils is important for clarifying the role of autoinhibition in this cellular context, discerning between protein scaffold and lipid phosphatase functions, and identifying critical interaction partners in the future.

CHAPTER III

MOLECULAR DISSECTION OF SHIP1 RECRUITMENT INTO THE EXCITABLE SIGNALING NETWORK IN HUMAN NEUTROPHILS

This chapter includes unpublished and co-authored material. Experiments were performed by me, Henry Rupp, and Emma Drew. This chapter was written by me with editorial assistance from Scott D. Hansen.

Introduction

The innate immune system relies on neutrophils to recognize and destroy invading pathogens, such as viruses, bacteria, and even cancer cells. This process requires neutrophils to properly sense chemicals released by pathogens, orient, polarize, and directionally migrate (chemotaxis). Critical for this cellular response is the relay of signals between cell surface receptors, small GTPases, and phosphatidylinositol phosphate (PIP) lipids at the plasma membrane. Deciphering the spatiotemporal organization of these signaling networks is critical for understanding how cell polarity is established, maintained, and modulated during immune cell signaling.

In neutrophils, activation of the formyl peptide receptor by chemoattractant peptides such as N-formyl-methionine-leucine-phenylalanine (fMLF) results in G β G γ and Rho family GTPase dependent activation of phosphoinositide 3-kinase (PI3K) (Z. Li et al., n.d.; Weiner et al. 2002; Rickert 2000). Once active, PI3K rapidly produces PI(3,4,5)P₃ at the leading edge resulting in polarized F-actin polymerization, pseudopod

extension, and cell migration in the direction of the chemoattractant gradient (Servant 2000; Yoo et al. 2010; Pollard and Borisy 2003). Directed cell migration relies on tight spatial and temporal regulation of PI(3,4,5)P₃ levels. Through the activity of two negative regulators: the 3'-phosphatase PTEN and the 5'-phosphatase SHIP1, cells limit the concentration of PI(3,4,5)P₃ at the plasma membrane (L. Stephens, Ellson, and Hawkins 2002; Weiner 2002). PTEN converts PI(3,4,5)P₃ to PI(4,5)P₂, localizes to the rear of migrating *Dictyostelium*. Cells lacking PTEN are unable to polarize and directionally migrate (Iijima and Devreotes 2002). It is, therefore, surprising that neutrophils lacking PTEN display only subtle changes in cell migration speed (Nishio et al. 2007). Src homology 2 containing inositol 5'-phosphatase 1 (SHIP1) dephosphorylates PI(3,4,5)P₃ to generate PI(3,4)P₂ (Damen et al. 1996; Pauls and Marshall 2017). In contrast to PTEN, neutrophils lacking SHIP1 display an accumulation of PI(3,4,5)P₃, atypical F-actin polymerization across the membrane, and defects in cell migration (Nishio et al. 2007; Mondal et al. 2012; Lam et al. 2012; Collins et al. 2015). Neutrophils lacking SHIP1 exhibit a large, flattened, and hyperprotrusive cell polarity phenotype due to increased adhesion to extracellular matrix proteins (Nishio et al. 2007). Studies using neutrophil cell lysate show that 5'-phosphatases contribute the largest amount (>90%) of the total PI(3,4,5)P₃ phosphatase activity (L. R. Stephens, Hughes, and Irvine 1991), suggesting SHIP1 represents the major pathway for PI(3,4,5)P₃ degradation in neutrophils. It is, therefore, critical to understand key functional details regarding how SHIP1 is regulated, activated, and recruited to the plasma membrane to fully understand the mechanisms of cell polarity and migration in leukocytes.

SHIP1 is a multidomain protein that contains several proposed lipid binding domains and multiple protein interaction motifs proposed to regulate membrane localization and catalytic activity (Pauls and Marshall 2017). SHIP1 contains a N-terminal Src homology 2 domain (SH2), a pleckstrin-homology related (PH-R) domain, a phosphatase domain, a C2 domain, two C-terminal NPXY motifs that can be tyrosine phosphorylated, and several C-terminal polyproline regions (Pauls and Marshall 2017). Research in immune cells has shown that SHIP1 is recruited from the cytoplasm to the plasma membrane following immune receptor activation (Pauls et al. 2016; Manno et al. 2016). In many cases, membrane recruitment of SHIP1 has been attributed to interactions with phosphorylated tyrosine-based inhibitory motifs (ITIM) or tyrosine-based activating motifs (ITAMs), which are present in many classes of immunoreceptors (Ono, Bolland, and Tempst 1996; Ono et al. 1997; Isnardi et al. 2006; Mukherjee et al. 2012; Nakamura, Malykhin, and Coggeshall 2002).

In mast cells, SHIP1 and the F-BAR (Bin/Amphiphysin/Rvs) domain-containing protein denoted FBP17 (or FNBP1), display cortical oscillations that are regulated by phosphoinositide turnover (D. Xiong et al. 2016; M. Wu, Wu, and De Camilli 2013). The product of SHIP1 phosphatase activity, PI(3,4)P₂, specifically regulates the frequency of cortical oscillations (D. Xiong et al. 2016; Y. Yang et al. 2017). Cortical oscillations are a hallmark of excitability and involve repetitive cycles of enzyme recruitment, activation, and inactivation at the plasma membrane to regulate cell polarity and migration (Y. Xiong et al. 2010; P. N. Devreotes et al. 2017). Excitability has been observed in neutrophils in the form of a self-organized propagating wave (Weiner et al. 2007; H. W. Yang, Collins, and Meyer 2016), and a critically important GTPase for cell navigation,

Cdc42, exhibits local excitability in neutrophils (H. W. Yang, Collins, and Meyer 2016). Research in *Dictyostelium*, fibroblasts, and immune cells has revealed that regulators of the actin cytoskeleton (Weiner et al. 2007), PIP lipids (Arai et al. 2010), small GTPases (M. Wu, Wu, and De Camilli 2013; H. W. Yang, Collins, and Meyer 2016), and membrane curvature sensing proteins (Z. Wu et al. 2018) also display features of excitability, such as all-or-nothing responsiveness and wave propagation (P. N. Devreotes et al. 2017; Y. Yang and Wu 2018). Together, these molecules make up the excitable signaling network.

Using human neutrophils as a model system for examining SHIP1, we performed a molecular dissection to determine which motifs control plasma membrane localization of SHIP1. In the absence of chemoattractant, SHIP1 forms cortical oscillations that sweep across the plasma membrane with a period length of 20-35 seconds/cycle. These oscillations are spatially and temporally coupled to Cdc42(GTP) and FBP17 in the excitable signaling network. Following the activation of the formyl peptide receptor, we observed the translocation of mNG-SHIP1 to actin-based membrane protrusions at leading edge membranes. Truncation mutants of SHIP1 revealed that polarized and oscillatory membrane localization both require proline rich motifs in the C-terminal domain. Sequence homology analysis of SHIP1 and SHIP2 identified a conserved proline rich motif suggested to indicate with a Src homology 3 (SH3) domain containing protein. These results indicate that SHIP1 and Cdc42 function in the same pathway to regulate the excitable signaling network, and that protein interaction motifs in the C-terminus are required for SHIP1 localization to the excitable signaling network in neutrophils.

RESULTS

SHIP1 exhibits polarized leading edge membrane localization and excitability in neutrophils

A major limitation in understanding the role SHIP1 plays in chemotaxis is our gap in knowledge concerning how SHIP1 localization is spatially regulated during cell polarity and migration. Previous research visualizing the localization of SHIP1 during neutrophil migration in zebrafish larva lacked the resolution to define the mechanisms that control SHIP1 membrane recruitment and dynamics (Lam et al. 2012). Similarly, SHIP1 localization studies in B-cells and mast cells have revealed localization patterns that exist in chemically fixed and non-motile cells, respectively (Pauls, Hou, and Marshall 2020; D. Xiong et al. 2016). To decipher the mechanisms that regulate SHIP1 localization during chemotaxis, we established methods for visualizing SHIP1 in both resting and motile PLB-985 neutrophil-like cells using TIRF microscopy.

In the presence of fibronectin coated glass slide, differentiated PLB-985 neutrophil-like cells adhere through integrin receptors. Under these conditions, cells expressing mNeonGreen-SHIP1 (mNG-SHIP1) polarized and randomly migrated when exposed to a uniform concentration of formyl-methionine-leucine-phenylalanine (fMLF). Localization of mNG-SHIP1 was polarized to leading-edge actin-based membrane protrusions (**Figure 3.1A**). This localization pattern was also observed when mNG-SHIP1 expressing cells were imaged under an agarose gel matrix in the absence of fibronectin. Under these conditions, mNG-SHIP1 localized to the leading-edge membrane of randomly migrating cells. To characterize mNG-SHIP1 localization and

dynamics in the presence of a chemoattractant gradient, we added photocaged N-nitroveratryl derivatized fMLF (nv-fMLF) (Collins et al. 2015; Pirrung et al. 2000) to the agarose matrix. Using a pulse of UV light, we photo-uncaged nv-fMLF and stimulated the polarization and persistent migrations of mNG-SHIP1 expressing cells (**Figure 3.1B**).

In the absence of chemoattractant, non-motile cells displayed cortical oscillations of mNG-SHIP1 that traveled across the plasma membrane with a period length of 20-35 seconds/cycle (**Figure 3.1C**). This behavior was similar to the localization pattern previously observed for SHIP1 in mast cells (D. Xiong et al. 2016). Interestingly, cortical oscillations of SHIP1 were not observed in undifferentiated PLB-985 cells (**Supplemental Figure 1**), indicating that this behavior requires the expression profile of a neutrophil-like cell type. Also of note, expressing mNG-SHIP1 at low levels revealed that it also localizes to small diffraction-limited puncta in resting cells. It's unlikely that these puncta are SHIP1 accumulating at focal adhesions because spots were observed in cells in the absence and presence of fibronectin (**Supplemental Figure 2**). When visualized with high spatiotemporal dynamics, we can observe the puncta become internalized (**Supplemental Figure 2**), which suggests that SHIP1 is localizing to endocytic pits in addition to cortical oscillations.

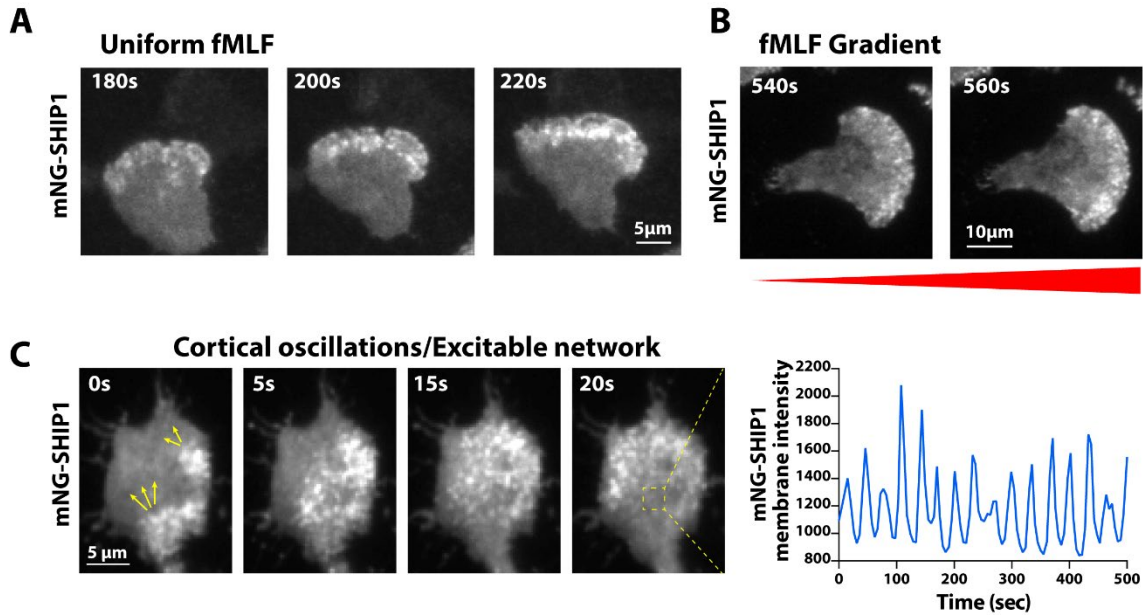


Figure 3.1: SHIP1 localizes to both actin-based membrane protrusions and cortical oscillations in differentiated neutrophil-like cells. A) Stimulation of differentiated PLB-985 cells with a uniform concentration of 20 nM fMLF promotes polarized leading edge membrane localization of mNG-SHIP1. Cells were adhered to fibronectin coated coverslips and imaged with TIRF microscopy. B) Cells were plated under agarose matrix containing caged fMLF. Light-triggered photorelease of fMLF generates a chemoattractant gradient and drives polarized membrane localization of mNG-SHIP1 during chemotaxis. Red bar indicates direction of gradient. C) In the absence of fMLF, mNG-SHIP1 localizes to cortical oscillations in differentiated PLB-985 cells adhered to fibronectin. Graph shows the fluctuations in mNG-SHIP1 plasma membrane localization with respect to time.

Role of PIP lipids in regulating SHIP1 membrane localization in neutrophils

A direct implication of SHIP1's involvement in cortical waves is the reported role of PI(3,4)P₂ in setting oscillation frequency in mast cells (D. Xiong et al. 2016). However, the lack of a high specificity biosensor in previous studies has limited our understanding of when and where PI(3,4)P₂ is generated during chemotaxis. In order to visualize the spatial distribution of PI(3,4)P₂ lipids, we stably integrated TAPP1-GFP with a nuclear export signal into PLB-985 cells. When exposed to a uniform concentration of fMLF, we observe a spike in PI(3,4)P₂ levels across the plasma membrane. Within minutes, signal

adaptation returns PI(3,4)P₂ levels to the original resting state (Hoeller, Gong, and Weiner 2014) (**Figure 3.2A**). In some cells, however, we can see polarization of the sensor at the leading edge (**Figure 3.2B**). The high TAPP1 signal suggests that SHIP1 is catalytically active downstream of activated formyl peptide receptors.

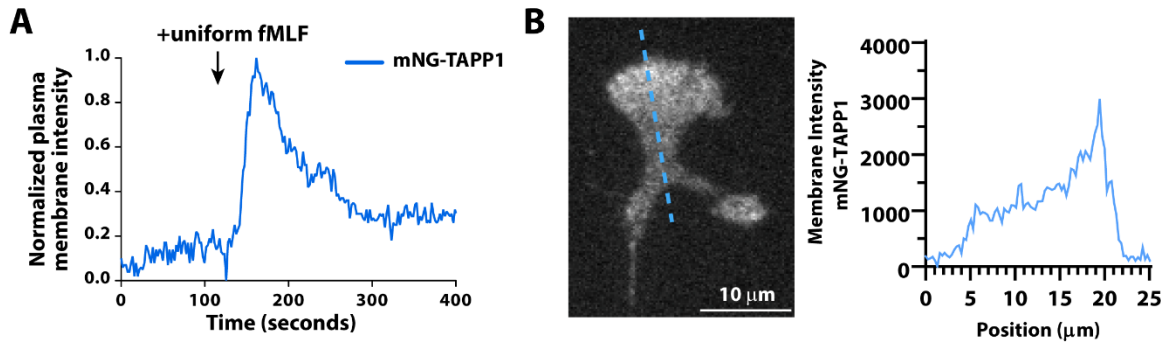


Figure 3.2: Dynamics of SHIP1 product in stimulated neutrophil-like cells. A) fMLF induced spike in PI(3,4)P₂ production followed by signal adaptation in a single differentiated PLB-985 cell. B) mNG-TAPP1 can be observed localizing to the leading edge of differentiated PLB-985 cell following stimulation with fMLF. Line scan on the right corresponds to the blue dashed line. Bottom of the line is position zero, indicating that the leading edge has the highest mNG-TAPP1 intensity.

Molecular dissection of SHIP1 membrane localization

SHIP1 is a multidomain protein that has several different protein interaction motifs and domains (**Figure 3.3A**); therefore, it is unclear which region(s) are required for cortical oscillations and localization at the leading edge. We performed a molecular dissection of SHIP1 by truncating or mutating various parts of the protein and then visualizing SHIP1 oscillations and membrane polarization. Our results revealed that polarized and oscillatory membrane localization requires the C-terminal domain. SHIP1 mutants lacking the C-terminus display uniform plasma membrane localization in neutrophils (**Figure 3.3B**). We

also discovered that the SHIP1 C-terminal domain alone lacking the phosphatase activity was sufficient for localization to the excitable network (**Figure 3.3B**).

The C-terminus of SHIP1 contains numerous proline-rich motifs and phosphotyrosine residues that can facilitate protein-protein interactions to recruit SHIP1 to the membrane. We made a phospho-tyrosine mutant (Y1022A) to determine if this interaction in the C-terminus is required for SHIP1 oscillations. Mutating one of the reportedly important phosphorylated tyrosine (Y1022) did not impact SHIP1's membrane localization pattern (**Figure 3.3B**); therefore, we hypothesize that SHIP1 membrane localization requires proline-rich motifs that interact with Src homology 3 (SH3) domain containing proteins (Teyra et al. 2017).

The last 322 amino acid of the SHIP1 C-terminus is predicted to be a random coil. This region contains several poly-proline motifs predicted to interact with SH3 domain containing proteins (Teyra et al. 2017). Mutating the previously characterized and uncharacterized poly proline-rich regions did not disrupt SHIP1 cortical oscillations (**Figure 3.3B**). To identify the minimal motif required for SHIP1's polarized membrane localization pattern, we created two SHIP1 mutants with truncated C-terminal domains. These experiments revealed that the last 110 amino acids of the SHIP1 C-terminus are required for polarized and oscillatory membrane localization in neutrophils. A SHIP1 mutant lacking this region (Δ miniCT) uniformly localized across the plasma membrane in the absence and presence of chemoattractant. In addition, expression of the C-terminal 110 amino acids fused mNG (miniCT) was capable of localizing to cortical oscillations and to the leading edge of polarized neutrophils (**Figure 3.3B**).

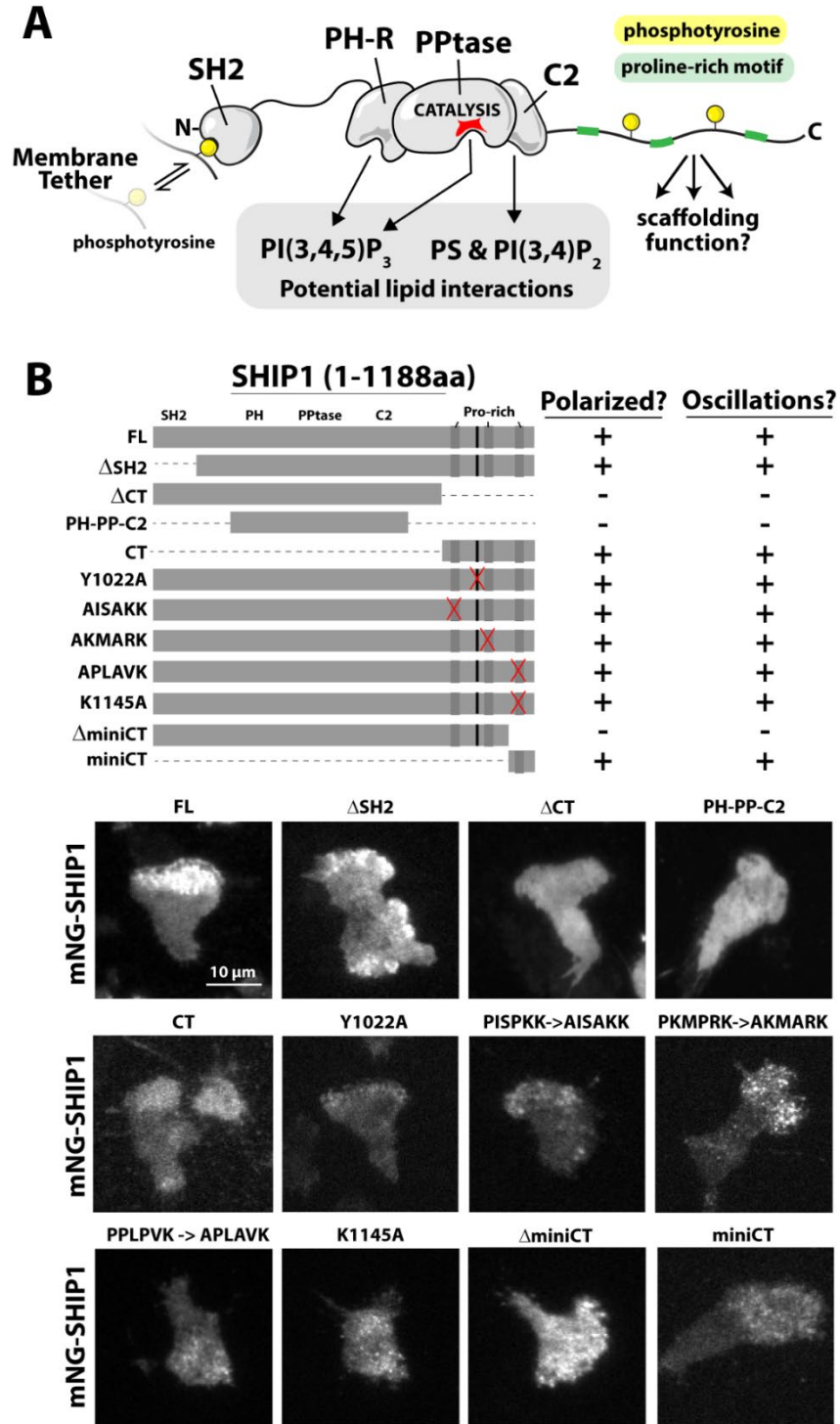


Figure 3.3: Molecular dissection of SHIP1 membrane localization. A) Domain organization of SHIP1 and proposed molecular interactions. B) (Top) Table summarizing the localization and oscillatory behavior of SHIP1 mutants. (Bottom) Select images showing the localization of mNG-SHIP1 mutants in differentiated PLB-985 cells stimulated with 20nM fMLF.

SHIP1 and SHIP2 share a high degree of homology, but the C-terminus of SHIP2 diverges from that of SHIP1 considerably. It was, therefore, surprising that SHIP2 localization patterns were indistinguishable from SHIP1 (**Figure 3.4A**). Like SHIP1, unstimulated non-motile cells expressing mNG-SHIP2 displayed cortical oscillations (**Figure 3.4A**). Sequence alignment revealed that SHIP1 and SHIP2 have one highly conserved C-terminal proline rich motif (**Figure 3.4B**). This motif is within the last 110 amino acids of SHIP1, which is the region required for SHIP1 to localize to cortical oscillations and leading-edge membranes. SH3 domains recognize proline rich motifs (Teyra et al. 2017); therefore it seems likely that a SH3 domain containing protein regulates SHIP1 and SHIP2 localization to cortical oscillations via this specific proline rich motif.

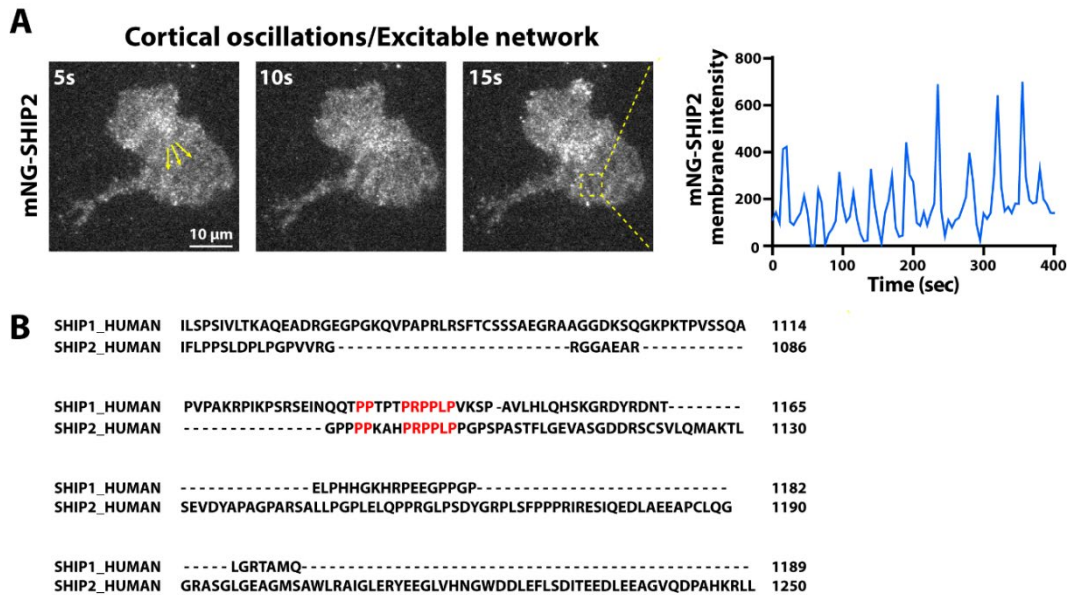


Figure 3.4: SHIP2 localizes to cortical oscillations in differentiated neutrophil-like cells. A) In the absence of fMLF, mNG-SHIP2 localizes to cortical oscillations in differentiated PLB-985 cells adhered to fibronectin. Graph shows the fluctuations in mNG-SHIP2 plasma membrane localization with respect to time. B) Clustal O (1.2.4) multiple sequence alignment of SHIP1 (Q92835) and SHIP2 (O15357-1) C-terminal regions. Red text indicates conserved proline rich motif.

SHIP1 and FBP17 colocalize and display synchronized oscillations in PLB-985 cells

Previous research in mast cells revealed that an SH3 domain containing protein, FBP17, also localizes to the plasma membrane in the form of cortical oscillations (D. Xiong et al. 2016). FBP17 also reportedly interacts with Cdc42, PIP lipids, and SHIP1 (D. Xiong et al. 2016; Chan Wah Hak et al. 2018; M. Wu, Wu, and De Camilli 2013). Co-expression of GFP-FBP17 and mCherry-SHIP1 in human neutrophils revealed that the two proteins can colocalize to actin-based membrane protrusions at leading edge membranes (**Figure 3.5A**) and cortical oscillations are spatially and temporally synchronized (**Figure 3.5B**).

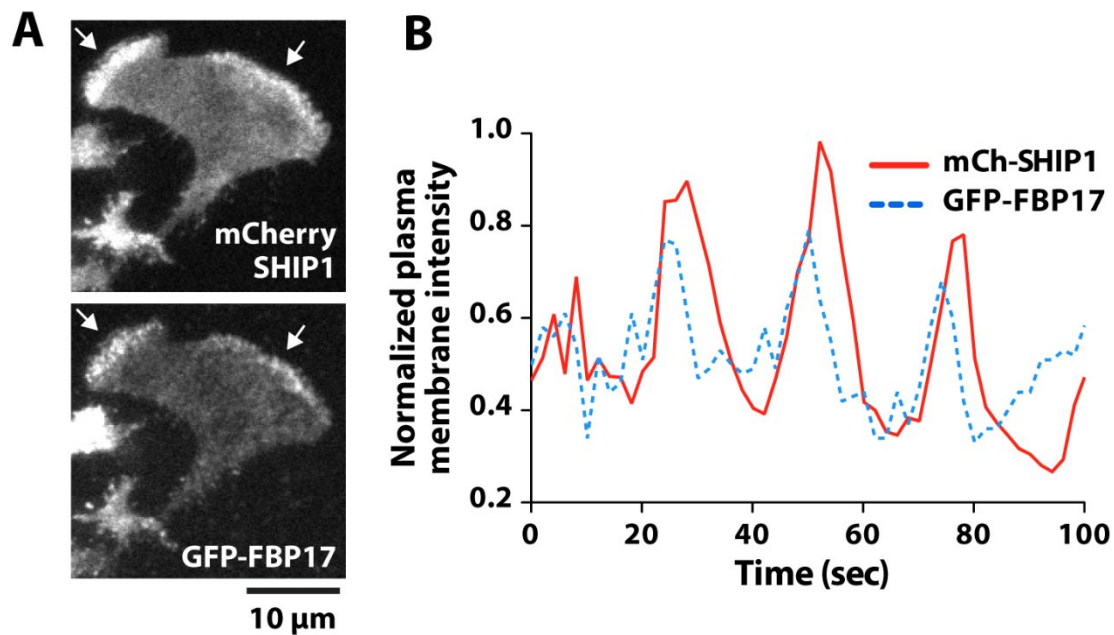


Figure 3.5: SHIP1 and FBP17 colocalize to leading-edge membranes and cortical oscillations. A) Differentiated PLB-985 cells expressing mCherry-SHIP1 and GFP-FBP17 adhered to fibronectin coated coverslips were stimulated with a uniform concentration of 20 nM fMLF. Arrows indicate colocalization of SHIP1 and FBP17 at leading-edge membranes. B) Unstimulated (resting) neutrophil-like cells expressing mCherry-SHIP1 and GFP-FBP17 display synchronized cortical oscillations. Graph shows the fluctuations in mCherry-SHIP1 and GFP-FBP17 plasma membrane localization with respect to time. Cells were imaged with TIRF microscopy.

Cdc42 functions upstream of SHIP1 and FBP17

SHIP1 and FBP17 localizes to the plasma membrane in the form of cortical oscillations, which phenocopies the spatial and temporal dynamics previously observed for active Cdc42 in PLB-985 cells (H. W. Yang, Collins, and Meyer 2016). The small GTPase, Cdc42, also plays critical roles in cell navigation and reportedly interacts with FBP17 (Collins et al. 2015; Chan Wah Hak et al. 2018; H. W. Yang, Collins, and Meyer 2016; M. Wu, Wu, and De Camilli 2013). Therefore, we hypothesized that SHIP1, FBP17, and Cdc42 in the same signaling pathway. Cdc42 is a membrane anchored small GTPase that can switch between a GDP bound or OFF state and a GTP bound or ON state. Expression of an iRFP tagged CRIB domain that specifically binds to Cdc42(GTP) showed that Cdc42 oscillates between its two different nucleotide states (**Figure 3.6A**). Coexpression of SHIP1 and iRFP-CRIB in PLB-985 cells showed that the cortical oscillations of SHIP1 and Cdc42(GTP) are spatially and temporally coupled in the excitable signaling network (**Figure 3.6B**). Similarly, GFP-FBP17 and iRFP-CRIB displayed spatially and temporally coupled cortical oscillations (**Figure 3.6C**). Treatment of neutrophils with an allosteric inhibitor that blocks GEF dependent activation of Cdc42 perturbed the localization of both SHIP1 and FBP17 cortical oscillations (**Figure 3.6D & E**). These results indicate that Cdc42 functions in the same pathway as SHIP1 and FBP17 to regulate the excitable signaling network. The domain architecture of SHIP1 suggests that the interaction with Cdc42 is indirect.

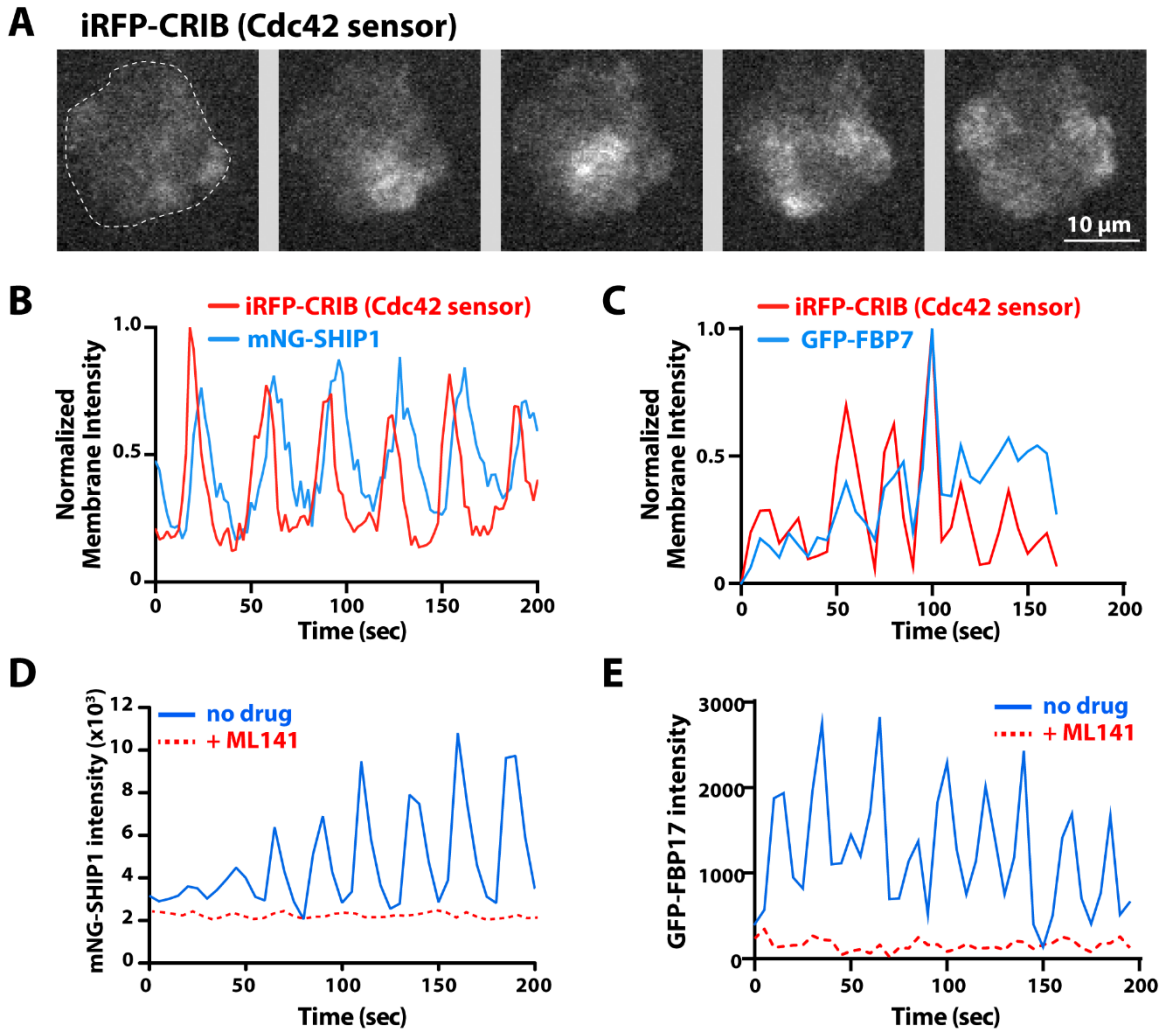


Figure 3.6: Cdc42 inhibition disrupts SHIP1 and FBP17 cortical oscillations A) In the absence of fMLF, neutrophil-like cells expressing iRFP-CRIB (Cdc42(GTP) sensor) display cortical oscillations. Images were taken 5 seconds apart. B) Normalized membrane intensity of resting neutrophil-like cell expressing iRFP-CRIB and mNG-SHIP1. C) Normalized membrane intensity of resting neutrophil-like cell expressing iRFP-CRIB and GFP-FBP17. D-E) Membrane intensity of neutrophil-like cells expressing mNG-SHIP1 (D) or GFP-FBP17 (E) that were exposed to 50 μ M ML141 (red line) or untreated (blue line). A-E) Cells were adhered to fibronectin coated glass and imaged with TIRF microscopy.

Discussion

Localized accumulation of PI(3,4,5)P₃ at leading edge membranes plays an important role in the establishment and maintenance of cell polarity pathways necessary for proper cell migration (Servant 2000; P. Devreotes and Horwitz 2015). Following the activation of the formyl peptide receptor with fMLF, we observed the translocation of mNG-SHIP1 and mNG-TAPP1 (PI(3,4)P₂ sensor) to leading edge membranes (**Figure 3.1 and 3.2**). This is consistent with SHIP1 actively dephosphorylating PI(3,4,5)P₃ at the plasma membrane and corroborates previous reports that SHIP1 regulates neutrophil chemotaxis by limiting PI(3,4,5)P₃ levels (Lam et al. 2012; Mondal et al. 2012; Nishio et al. 2007). In resting cells (no chemoattractant), we find that SHIP1 localizes to periodic traveling waves that propagate across the plasma membrane (**Figure 3.1C**). This is the first time SHIP1 cortical waves have been visualized in human neutrophils, but SHIP1 excitability has been previously observed in mast cells (D. Xiong et al. 2016). It is interesting to note that PTEN, another important PI(3,4,5)P₃ phosphatase that is essential for *Dictyostelium* migration (Iijima and Devreotes 2002), wasn't found to display cortical oscillations in mast cells in the above-mentioned study. Knockdown of PTEN was also found to have little to no impact on neutrophil chemotaxis (Nishio et al. 2007; Mondal et al. 2012). Given that SHIP1 seems to be the primary PI(3,4,5)P₃ phosphatase regulating neutrophil cell migration, these observations regarding PTEN could imply some biological significance to SHIP1 cortical waves.

Identifying the domain or motif used to recruit SHIP1 to intracellular membranes is the first step to understanding how SHIP1 contributes to the numerous feedback circuits that control neutrophil cell polarity and migration. Our molecular dissection

revealed that SHIP1's polarized and oscillatory membrane localization requires proline-rich motifs in the C-terminal domain. Proline rich motifs are known to bind to SH3 domains, and several SH3 domain containing proteins have been implicated in regulating the actin cytoskeleton (Teyra et al. 2017). Consistent with this, we found that SHIP1 colocalizes with FBP17 and Cdc42, two proteins that are heavily implicated in regulating actin dynamics and cell polarity processes (H. W. Yang, Collins, and Meyer 2016; Y. Yang et al. 2017; Chan Wah Hak et al. 2018, 17). In our human neutrophil-like cells, SHIP1, FBP17, and Cdc42 cortical waves are synchronized and have nearly identical periodicities. This is a somewhat surprising result because while SHIP1 was previously shown to interact with FBP17, SHIP1 cortical oscillations trailed behind an oscillating FBP17/Cdc42 module by 5.6 seconds in rat mast cells (D. Xiong et al. 2016). It's unclear if these different dynamics are a result of differentiation (mast cell versus neutrophil) or evolution (rat versus human). Using human neutrophils, we demonstrated that inhibiting Cdc42 disrupted both SHIP1 and FBP17 oscillations suggesting these proteins are functioning in the same pathway and supports the presence of a FBP17/Cdc42 module in human neutrophils.

More recently, it was shown that the assembly of clathrin mediates the onset and direction of cortical waves and requires feedback from downstream endocytic factors such as FBP17, Cdc42, and N-WASP (Y. Yang et al. 2017). A direct implication of SHIP1's involvement in cortical oscillations is the role of PI(3,4)P₂ in defining the refractory period and, therefore, setting oscillation frequency, and the finding that knocking down SHIP1 inhibited clathrin waves (D. Xiong et al. 2016; Y. Yang et al. 2017). In neutrophils, we observed SHIP1 localizing to puncta across the cell cortex,

resembling localization patterns of endocytic proteins. SHIP2, a closely related homolog of SHIP1, has been previously shown to localize to clathrin coated pits and enhance the rate of pit maturation (Nakatsu et al. 2010), suggesting that SHIP1/2 and lipid product, PI(3,4)P₂, could contribute to the feedback mechanism that is crucial for regulating clathrin assembly and cortical waves in immune cells.

Cortical oscillations are powerful readouts for understanding the components and design principles regulating dynamic biological systems (Kruse and Jülicher 2005). We found that in addition to localizing to leading edge membranes, SHIP1, FBP17, and Cdc42 display cortical oscillations that are spatially and temporally synchronized. Inhibition of Cdc42 disrupted both FBP17 and SHIP1 cortical waves, suggesting that these molecules are functioning in the same pathway. Decreasing the expression of SHIP1 revealed that SHIP1 also localizes to puncta across the cell membrane that become internalized and resemble endocytosis. Emerging research is beginning to suggest that CME plays pivotal roles regulating cell polarity processes, like cell migration (Tan, Luo, and Liu 2018). This is further supported by the importance of SHIP1 for proper neutrophil chemotaxis and the critical role of SHIP1's lipid product, PI(3,4)P₂, in setting the oscillation frequency of endocytic machinery in mast cells (Nishio et al. 2007; Mondal et al. 2012; Lam et al. 2012; Y. Yang et al. 2017). Identifying the factor(s) that recruit SHIP1 to leading edge membranes and cortical waves would further increase our understanding of both these processes and how they are connected.

Materials and Methods

Molecular Biology

Genes encoding INPP5D (SHIP1), INPPL1 (SHIP2), FNBP1 (FBP17), TAPP1 PH domain (PI(3,4)P₂ sensor), and N-WASP CRIB domain (Cdc42(GTP) sensor) were PCR amplified with *Pfx* Accuprime mastermix in a T100 Bio-Rad thermal cycler.

Following gel extraction and purification, DNA fragments were combined with the appropriate restriction enzyme digested plasmids and Gibson assembly was performed. The complete open reading frame of all vectors used in this study were sequenced to ensure the plasmids lacked deleterious mutations.

Lentivirus production

Lentivirus was generated by transfecting 60-70% confluent HEK293 Lenti-X cells in a 6 well plate. Each well in the 6-well dish should contain ~2-3 mL of media at the time of transfection. 1.34 µg of pCMVdR8.91 (2nd generation packing vector), 0.17 µg of pMD2.G (2nd generation VSV-G pseudotype viral package), 1.5 µg of transfer lentiviral vector, and 6 µL of 1 mg/mL PEI were added to 200 µl of Opti-Mem (ThermoFisher Scientific cat#31985070) and incubated for 10 minutes at room temperature before being added dropwise to each well. Media was harvested 48 hours after the transfection and clarified by centrifugation. 333 µL of Lenti-X concentrator was added for every 1 mL of supernatant, incubated overnight at 4°C, and then centrifuged at 1500 x g for 45 minutes producing a small white pellet containing the virus. The white viral containing pellet was resuspended in 0.4 mL of complete RPMI media (9% FBS) and stored at -80°C. To infect PLB-985 cells, add 0.2 mL of concentrated lentivirus plus 8 µg/mL final concentration of polybrene (Millipore, Cat# TR-1003-G, 10 mg/mL stock,

1250x) to 5 mL of undifferentiated cells at a density of 0.2×10^6 cells/mL. The cells were passaged at least one time before differentiating.

Cell culture

PLB-985 cells are an established model cell line for human neutrophils and were obtained as a gift from the laboratory of Dr. Sean Collins (University of California at Davis). PLB-985 cells were grown in suspension in RPMI 1640 + GlutaMAX media containing 25 mM HEPES (Life Technologies, catalog #72400047), 9% fetal bovine serum (FBS), penicillin (100 units/ml) (Life Technologies, catalog #15140122), streptomycin (100 μ g/ml) (Life Technologies, catalog #15140122). Cell lines were grown in humidified incubators at 37°C in the presence of 5% CO₂ and split three times per week, keeping densities between $0.1-2 \times 10^6$ cells/mL. PLB-985 cells were differentiated into a neutrophil-like state by culturing 0.2×10^6 cells/mL for 6 to 7 days in RPMI media supplemented with 2% FBS, penicillin (100 units/ml), streptomycin (100 μ g/ml), 1.3% DMSO, and 2% Nutridoma-CS (Sigma #11363743001). Nutridoma-CS was added to increase the chemotactic response of the cells, but this supplement is optional (Rincón, Rocha-Gregg, and Collins 2018).

HEK293T Lenti-X cells were cultured in DMEM + GlutMAX + High Glucose (4.5 g/L) + sodium pyruvate (110 mg/L) (Life Technologies, catalog #10569010) supplemented with 10% FBS, penicillin (100 units/ml), and streptomycin (100 μ g/ml). Cells were grown in 10 cm dishes in humidified incubators at 37°C in the presence of 5% CO₂ and split at a confluency of 80-90% every 2-3 days. HEK293T Lenti-X cells were split using using 1.5mL of 0.25% Trypsin. Trypsin was that quenched with 8.5 mL complete DMEM media containing 10% FBS. Cells were diluted 1:10 and seeded on a

new 10cm dish containing a total volume of 10 mL complete DMEM media warmed to 37°C.

Live cell imaging of PLB-985 cells

Extracellular Buffer (ECB: 5mM KCl, 125 mM NaCl, 1.5 mM CaCl₂, 1.5 mM MgCl₂, 10 mM glucose, 20 mM HEPES pH 7.4) and Leibovitz-15 (Life Technologies, catalog #21083027) complete media (10% FBS, 100 U/mL Pen/Strep) were warmed to 37°C and combined 1:4 to make the Imaging Media. Differentiated PLB-985 cells were prepared for imaging by centrifuging 0.5 mL of cells at 100 xg for 10 minutes, aspirating off the medium, and resuspending the cells in warm imaging media (L-15 complete media to ECB (1:4)). Differentiated PLB-985 cells were then imaged using one of two different live cell imaging methods: a method using fibronectin coated glass attached to an IBIDI flow cell chamber or a previously described 96-well format under-agarose method (Bell, Natwick, and Collins 2018).

To image cells on fibronectin coated glass, 25 x 75 mm coverslips were cleaned with 2% Hellmanex (Fisher Scientific, catalog #14-385-864), washed with MilliQ water, dried with N₂ gas, and attached to an IBIDI flow cell chamber (IBIDI sticky-Slide VI 0.4, catalog #80608). A 0.2 mg/mL fibronectin (Sigma, F1141, stock concentration=1 mg/mL) solution diluted in 1x PBS was added to each well of the IBIDI chamber, incubated for 30-60 minutes, and unbound fibronectin was washed out with 1x PBS. 100 µL of differentiated PLB-985 cells were flowed into the IBIDI chamber. Cells would adhere within 5-10 minutes. Cells were imaged in the presence of uniform chemoattract by flowing in 100 µL of 20 nM fMLF.

To image cells under agarose, 5 μL of differentiated PLB-985 cells were spotted in the center of a well in a glass-bottom 96 well plate (Cellvis, catalog #P96-1.5H-N) and allowed to settle by gravity onto the bottom of the glass for 5 minutes. A 3% wt/vol low melting agarose (Gold-Bio, Cat # 204-100) solution (3% LMA) was prepared in ECB, heated to 70°C to ensure the agarose was fully dissolved, and combined 1:1 with warmed imaging media so that the final concentration of the LMA is 1.5% wt/vol. 195 μL of this warm 1.5% LMA mixture is then gently pipetted above the 5 μL of differentiated PLB-985 cells. Slowly pipetting down the side of the well is the best way to avoid disturbing the 5 μL of settled cells. The plate was covered with aluminum foil to protect it from light and left at room temperature for 10 minutes to allow the agarose to solidify. After 10 minutes the cells could be immediately imaged or allowed to incubate for another 10 minutes in a 37°C incubator before starting the imaging experiment. This method can also be used to image cells in the presence of a chemoattractant gradient. We prepared 2x solutions of caged fluorescein (CMNB-F (2x = 2 μM), Life Technologies, Cat# F-7103) or caged chemoattractant (nv-fMLF (2x = 300 nM), Collins lab) in imaging media. These solutions can then be combined 1:1 with the warm 3% LMA mixture and gently plated above the cells as described above. During an imaging experiment, a UV laser can be used to uncage nv-fMLF to create a chemoattractant gradient.

Microscope hardware and imaging acquisition

Live cell TIRF microscopy experiments were performed using an inverted Nikon Ti2 microscope. All images were acquired using an iXon Life 897 EMCCD camera (Andor Technology Ltd., UK). Nikon 60x and 100x oil immersion objectives, sometimes in combination with a 1.49 NA, were used for all live cell imaging experiments.

Fluorescently labeled proteins were excited with either a 405, 488, 561, or 647 nm diode lasers (Coherent Inc. Santa Clara, CA) controlled with a Vortran (Sacramento, CA) laser driver digital modulation. The following the laser powers measured through the objective were used to excite mNG-SHIP1 (1 mW 488 nm), iRFP-CRIB (1 mW 647 nm), mCherry-SHIP1 (1 mW 561 nm). Excitation light was passed through the following dichroic filter cubes before illuminating the sample: (1) ZT488/647rpc and (2) ZT561rdc (ET575LP) (Semrock) and Nikon emission filter wheel housing 25mm ET525/50M, ET600/50M, and ET700/75M filters (Semrock). Unless otherwise noted, live cell imaging experiments were performed at room temperature (i.e. 23°C). All microscope hardware was controlled with NIS elements.

Image processing and data analysis

Image analysis was performed with ImageJ and Prism 8 (GraphPad).

CHAPTER IV

CONCLUDING REMARKS

Signal transduction downstream of most receptors on immune cells relies on the activation of phosphoinositide 3-kinase (PI3K) and the subsequent generation of PI(3,4,5)P₃ (Deane and Fruman 2004). PI(3,4,5)P₃ has been shown to initiate numerous cell processes including cell survival, cell proliferation, cell migration, and cell activation (Cantley 2002; Balla 2013). SHIP1 is highly expressed in immune cells and is thought to be a major regulator of PI(3,4,5)P₃ signaling events in these cell types (Qiurong Liu et al. 1998; Geier et al. 1997; Rohrschneider et al. 2000). Given the overall importance of SHIP1 for balanced immune cell activation and its emerging role in various hematopoietic diseases, it's important to have a full understanding of its regulatory mechanisms (Kerr 2011; Pauls and Marshall 2017).

Since the discovery of SHIP1 over 25 years ago, significant strides have been made characterizing its function and regulation in various types of immune cells, but there are few biochemical studies to date. This is in part due to the challenging nature of purifying SHIP1 and biochemically characterizing an enzyme that acts on a lipid substrate. The work presented in chapter II demonstrates the power of reductionist biochemistry approaches and revealed molecular details that would have been difficult to realize with cell biology approaches alone. For the first time, we provide evidence that SHIP1 is autoinhibited by its N- and C-terminus. We found that SHIP1 is predominantly autoinhibited by its N-terminal SH2 domain and partially by its disordered C-terminal

tail. Consistent with this mode of regulation, we reconstituted the membrane localization and activation of SHIP1 using receptor derived phosphopeptides that bind to the SH2 domain. This work validates a new model of SHIP1 autoregulation and demonstrates the effect of phosphotyrosine peptide engagement in controlling enzymatic activity.

SHIP1 was previously shown to interact with PI(3,4,5)P₃ and PI(3,4)P₂ (Ming-Lum et al. 2012; Ong et al. 2007; Nelson et al. 2021). Despite rigorously testing these interactions *in vitro* and *in vivo*, we were unable to measure any membrane binding dynamics that were consistent with the nanomolar affinities reported in the aforementioned studies. Instead, we show that interactions between SHIP1 and various lipid species are extremely transient in nature and unable to localize SHIP1 to membrane surfaces. These inconsistencies can likely be attributed to differences in methodology. Contrary to previous reports, we used supported lipid bilayers, which mimic the plasma membrane, and directly visualized the membrane association and dissociation dynamics of SHIP1 with single molecule TIRF microscopy. Overall, these experiments highlight the importance of high-resolution assays and suggests that SHIP1 membrane recruitment is mediated by protein-protein interactions.

Another critical finding of this work is that SHIP1 requires its C-terminal domain to localize to leading-edge membranes and cortical oscillations in human neutrophils. The C-terminus of SHIP1 has an abundance of proline rich regions. Therefore, it seems likely that SHIP1 is being membrane recruited by an SH3 domain-containing protein. We showed that SHIP1 colocalizes with FBP17 at leading edge membranes and that both proteins display synchronized cortical oscillations. FBP17 is curvature sensing molecule that has an SH3 domain that has previously been shown to interact with SHIP1 (D. Xiong

et al. 2016), making it a potential candidate for recruiting SHIP1 to cortical waves and leading edge membranes in human neutrophils. We also show that treatment of neutrophils with an allosteric inhibitor that blocks Cdc42 activation perturbs SHIP1 and FBP17 cortical oscillations. FBP17 has been previously reported to interact with Cdc42(GTP), which is prenylated and anchored in the plasma membrane (Chan Wah Hak et al. 2018). Therefore, it is possible that FBP17 binds to Cdc42(GTP) and localizes SHIP1 to the plasma membrane. It is also possible that these molecules oscillate at the same frequency but participate in separate feedback loops. To address these possibilities, it will be important to use a combination of *in vitro* biochemistry, genetics, and cell biology approaches to account for genetic redundancy or oversimplified reconstituted systems (i.e. loss of membrane curvature).

Taken together, this work further supports a membrane recruitment mechanism that is dependent on protein interactions instead of lipids. Using a peptide derived from the FcγRIIb receptor, we were able to activate and recruit SHIP1 via its N-terminal SH2 domain. FcγRIIB is a B cell specific receptor, and SHIP1 recruitment via its SH2 domain is critical for its inhibitory effect on B cell activation (Isnardi et al. 2006; Pauls et al. 2016). In the context of neutrophils, we found that the C-terminus of SHIP1 is required to localize to leading-edge membranes in cells stimulated with fMLF, which activates G protein coupled receptors (GPCR). These results suggests that SHIP1 regulatory mechanisms are context dependent and multifaceted.

The requirement of SHIP1's C-terminus for plasma localization in neutrophils is interesting given the predominant inhibitory role of SHIP1's N-terminal SH2 domain. This suggests that while SHIP1 is recruited to the membrane by its C-terminus, it's not

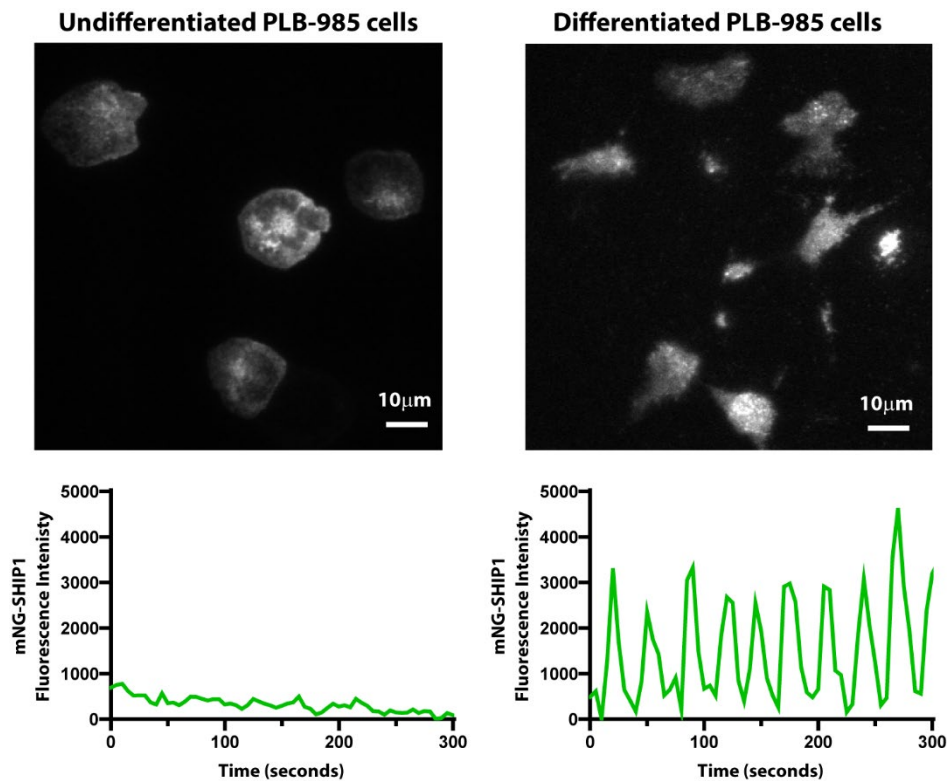
necessarily active. SHIP1 may require additional receptor signaling events (integrins, immune receptors, or receptor tyrosine kinases) that promote phosphorylation of receptor tyrosine residues to achieve full activation. In resting neutrophils, we demonstrate that SHIP1 localizes to cortical oscillations via its C-terminal domain. The significance of these oscillations could be that SHIP1 is constantly surveying the membrane in an autoinhibited state in order to immediately localize and become active during a receptor signaling event. This would ensure tight regulation of PI(3,4,5)P₃ because it is likely that these receptor signaling events are activating PI3K at the same time, especially in the case of GPCR activation. This potential mechanism would be consistent with the reported transient life-time of PI(3,4,5)P₃ (Goulden et al. 2019; Balla 2013).

In conclusion, the work presented in this thesis greatly enhanced our understanding of SHIP1 autoinhibition and membrane recruitment mechanisms. This work also laid the foundation for several ongoing projects in the Hansen lab. Future work aims to determine the precise intramolecular contacts that inhibit SHIP1 activity and identify critical interaction partners for SHIP1 localization to the excitable signaling network. Ultimately, a detailed understanding of these mechanisms through basic research will lead to better therapeutics for the multitude of physical ailments that result from imbalances in PI(3,4,5)P₃.

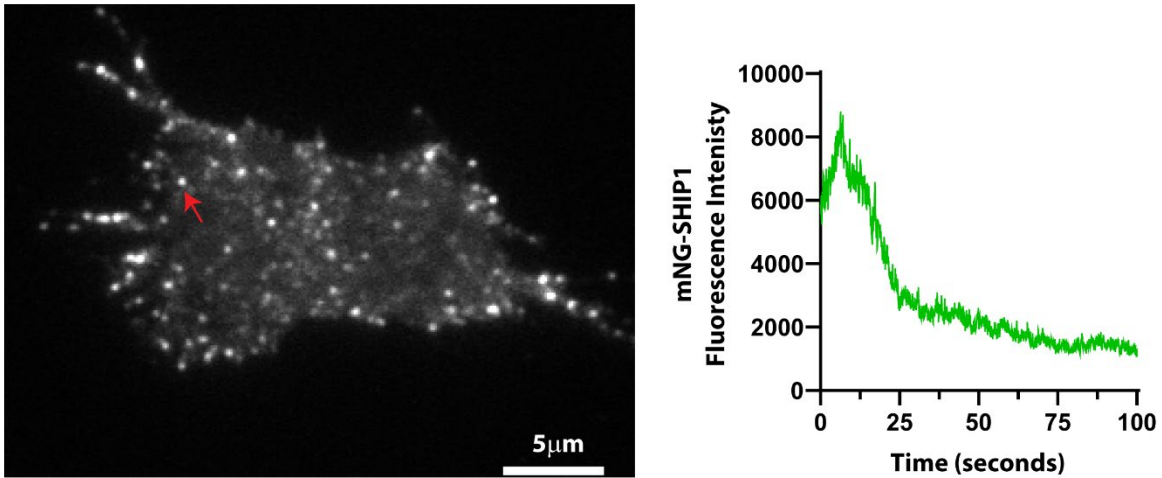
APPENDIX A

SUPPLEMENTARY INFORMATION FOR CHAPTER III

Appendix A is the supplementary information for Chapter III of this dissertation. It includes data relevant to the content of Chapter III.



Supplemental Figure 1: Cortical oscillations are specific to differentiated PLB-985 cells. Left) Undifferentiated PLB-985 cells are morphologically larger and rounder. Plotting the fluorescence intensity of mNG-SHIP1 with respect to time shows a lack of oscillations. Right) Differentiated PLB-985 cells have polarized bodies and SHIP1 dynamically localizes to the plasma membrane. Plotting the fluorescence intensity of mNG-SHIP1 with respect to time shows oscillations.



Supplemental Figure 2: SHIP1 localizes to puncta on neutrophil membranes. Left) Differentiated PLB-985 cell expressing mNG-SHIP1 under the ubiquitin promoter to lower overexpression levels reveals SHIP1 puncta across the membrane. Visualizing these puncta with high spatiotemporal dynamics shows them become internalized and leave the evanescent TIRF field. Arrow indicates puncta plot on the right. Right) Plotting the fluorescence intensity of single mNG-SHIP1 puncta with respect to time shows fluorescence intensity decrease as it becomes internalized within the cell.

REFERENCES CITED

- Aman, M. Javad, Thomas D. Lamkin, Hidetaka Okada, Tomohiro Kurosaki, and Kodimangalam S. Ravichandran. 1998. "The Inositol Phosphatase SHIP Inhibits Akt/PKB Activation in B Cells." *Journal of Biological Chemistry* 273 (51): 33922–28. <https://doi.org/10.1074/jbc.273.51.33922>.
- Aman, M Javad, Scott F Walk, Michael E March, Hua-Poo Su, D Jeannean Carver, and Kodimangalam S Ravichandran. 2000. "Essential Role for the C-Terminal Noncatalytic Region of SHIP in Fc γ RIIB1-Mediated Inhibitory Signaling." *MOL. CELL. BIOL.* 20: 14.
- Arai, Y., T. Shibata, S. Matsuoka, M. J. Sato, T. Yanagida, and M. Ueda. 2010. "Self-Organization of the Phosphatidylinositol Lipids Signaling System for Random Cell Migration." *Proceedings of the National Academy of Sciences* 107 (27): 12399–404. <https://doi.org/10.1073/pnas.0908278107>.
- Backers, Katrien, Daniel Blero, Nathalie Paternotte, Jing Zhang, and Christophe Erneux. 2003. "The Termination of PI3K Signalling by SHIP1 and SHIP2 Inositol 5-Phosphatases." *Advances in Enzyme Regulation* 43 (1): 15–28. [https://doi.org/10.1016/S0065-2571\(02\)00043-2](https://doi.org/10.1016/S0065-2571(02)00043-2).
- Balla, Tamas. 2013. "Phosphoinositides: Tiny Lipids With Giant Impact on Cell Regulation." *Physiological Reviews* 93 (3): 1019–1137. <https://doi.org/10.1152/physrev.00028.2012>.
- Baumann, Martina K., Marcus J. Swann, Marcus Textor, and Erik Reimhult. 2011. "Pleckstrin Homology-Phospholipase C- δ 1 Interaction with Phosphatidylinositol 4,5-Bisphosphate Containing Supported Lipid Bilayers Monitored *in Situ* with Dual Polarization Interferometry." *Analytical Chemistry* 83 (16): 6267–74. <https://doi.org/10.1021/ac2009178>.
- Bell, George R. R., Dean E. Natwick, and Sean R. Collins. 2018. "Parallel High-Resolution Imaging of Leukocyte Chemotaxis Under Agarose with Rho-Family GTPase Biosensors." In *Rho GTPases*, edited by Francisco Rivero, 1821:71–85. *Methods in Molecular Biology*. New York, NY: Springer New York. https://doi.org/10.1007/978-1-4939-8612-5_6.
- Brooks, Robert, Gwenny M. Fuhler, Sonia Iyer, Michelle J. Smith, Mi-Young Park, Kim H. T. Paraiso, Robert W. Engelman, and William G. Kerr. 2010. "SHIP1 Inhibition Increases Immunoregulatory Capacity and Triggers Apoptosis of Hematopoietic Cancer Cells." *The Journal of Immunology* 184 (7): 3582–89. <https://doi.org/10.4049/jimmunol.0902844>.
- Burke, John E. 2018. "Structural Basis for Regulation of Phosphoinositide Kinases and Their Involvement in Human Disease." *Molecular Cell* 71 (5): 653–73. <https://doi.org/10.1016/j.molcel.2018.08.005>.

- Cantley, Lewis C. 2002. "The Phosphoinositide 3-Kinase Pathway." *Science* 296 (5573): 1655–57. <https://doi.org/10.1126/science.296.5573.1655>.
- Chan Wah Hak, Laura, Shaheen Khan, Ilaria Di Meglio, Ah-Lai Law, Safa Lucken-Ardjomande Häslér, Leonor M. Quintaneiro, Antonio P. A. Ferreira, Matthias Krause, Harvey T. McMahon, and Emmanuel Boucrot. 2018. "FBP17 and CIP4 Recruit SHIP2 and Lamellipodin to Prime the Plasma Membrane for Fast Endophilin-Mediated Endocytosis." *Nature Cell Biology* 20 (9): 1023–31. <https://doi.org/10.1038/s41556-018-0146-8>.
- Chen, Zhengshan, Seyedmehdi Shojaee, Maike Buchner, Huimin Geng, Jae Woong Lee, Lars Klemm, Björn Titz, et al. 2015. "Signalling Thresholds and Negative B-Cell Selection in Acute Lymphoblastic Leukaemia." *Nature* 521 (7552): 357–61. <https://doi.org/10.1038/nature14231>.
- Collins, Sean R, Hee Won Yang, Kimberly M Bongér, Emmanuel G Guignet, Thomas J Wandless, and Tobias Meyer. 2015. "Using Light to Shape Chemical Gradients for Parallel and Automated Analysis of Chemotaxis." *Molecular Systems Biology* 11 (4): 804. <https://doi.org/10.15252/msb.20156027>.
- Condé, Claude, Xavier Rambout, Marielle Lebrun, Aurore Lecat, Emmanuel Di Valentin, Franck Dequiedt, Jacques Piette, Geoffrey Gloire, and Sylvie Legrand. 2012. "The Inositol Phosphatase SHIP-1 Inhibits NOD2-Induced NF-KB Activation by Disturbing the Interaction of XIAP with RIP2." Edited by Jörg Hermann Fritz. *PLoS ONE* 7 (7): e41005. <https://doi.org/10.1371/journal.pone.0041005>.
- Corbin, John A., Ronald A. Dirkx, and Joseph J. Falke. 2004. "GRP1 Pleckstrin Homology Domain: Activation Parameters and Novel Search Mechanism for Rare Target Lipid." *Biochemistry* 43 (51): 16161–73. <https://doi.org/10.1021/bi049017a>.
- Damen, J. E., L. Liu, P. Rosten, R. K. Humphries, A. B. Jefferson, P. W. Majerus, and G. Krystal. 1996. "The 145-KDa Protein Induced to Associate with Shc by Multiple Cytokines Is an Inositol Tetrphosphate and Phosphatidylinositol 3,4,5-Triphosphate 5-Phosphatase." *Proceedings of the National Academy of Sciences* 93 (4): 1689–93. <https://doi.org/10.1073/pnas.93.4.1689>.
- Deane, Jonathan A., and David A. Fruman. 2004. "PHOSPHOINOSITIDE 3-KINASE : Diverse Roles in Immune Cell Activation." *Annual Review of Immunology* 22 (1): 563–98. <https://doi.org/10.1146/annurev.immunol.22.012703.104721>.
- Devreotes, Peter, and Alan Rick Horwitz. 2015. "Signaling Networks That Regulate Cell Migration." *Cold Spring Harbor Perspectives in Biology* 7 (8): a005959. <https://doi.org/10.1101/cshperspect.a005959>.

- Devreotes, Peter N., Sayak Bhattacharya, Marc Edwards, Pablo A. Iglesias, Thomas Lampert, and Yuchuan Miao. 2017. "Excitable Signal Transduction Networks in Directed Cell Migration." *Annual Review of Cell and Developmental Biology* 33 (1): 103–25. <https://doi.org/10.1146/annurev-cellbio-100616-060739>.
- Di Paolo, Gilbert, and Pietro De Camilli. 2006. "Phosphoinositides in Cell Regulation and Membrane Dynamics." *Nature* 443 (7112): 651–57. <https://doi.org/10.1038/nature05185>.
- Drubin, David G, and W. James Nelson. 1996. "Origins of Cell Polarity." *Cell* 84 (3): 335–44. [https://doi.org/10.1016/S0092-8674\(00\)81278-7](https://doi.org/10.1016/S0092-8674(00)81278-7).
- Fruman, David A., Honyin Chiu, Benjamin D. Hopkins, Shubha Bagrodia, Lewis C. Cantley, and Robert T. Abraham. 2017. "The PI3K Pathway in Human Disease." *Cell* 170 (4): 605–35. <https://doi.org/10.1016/j.cell.2017.07.029>.
- Fu, Qiaofen, Yuhui Huang, Chunlei Ge, Zhen Li, Hui Tian, Qiaolin Li, Hongshuai Li, et al. 2019. "SHIP1 Inhibits Cell Growth, Migration, and Invasion in Non-small Cell Lung Cancer through the PI3K/AKT Pathway." *Oncology Reports* 41 (4): 2337–50. <https://doi.org/10.3892/or.2019.6990>.
- Geier, Susan J., Paul A. Algate, Kristen Carlberg, Dave Flowers, Cynthia Friedman, Barbara Trask, and Larry R. Rohrschneider. 1997. "The Human SHIP Gene Is Differentially Expressed in Cell Lineages of the Bone Marrow and Blood." *Blood* 89 (6): 1876–85. <https://doi.org/10.1182/blood.V89.6.1876>.
- Goulden, Brady D., Jonathan Pacheco, Allyson Dull, James P. Zewe, Alexander Deiters, and Gerald R.V. Hammond. 2019. "A High-Avidity Biosensor Reveals Plasma Membrane PI(3,4)P2 Is Predominantly a Class I PI3K Signaling Product." *Journal of Cell Biology* 218 (3): 1066–79. <https://doi.org/10.1083/jcb.201809026>.
- Harlan, John E., Philip J. Hajduk, Ho Sup Yoon, and Stephen W. Fesik. 1994. "Pleckstrin Homology Domains Bind to Phosphatidylinositol-4,5-Bisphosphate." *Nature* 371 (6493): 168–70. <https://doi.org/10.1038/371168a0>.
- He, Ju, Rachel M. Haney, Mohsin Vora, Vladislav V. Verkhusha, Robert V. Stahelin, and Tatiana G. Kutateladze. 2008. "Molecular Mechanism of Membrane Targeting by the GRP1 PH Domain*." *Journal of Lipid Research* 49 (8): 1807–15. <https://doi.org/10.1194/jlr.M800150-JLR200>.
- Helgason, Cheryl D., Damen Jacqueline E., Rosten Patty, Grewal Rewa, Sorensen Poul, Chappel Suzanne M., Borowski Anita, Jirik Frank, Krystal Gerald, and Humphries R. Keith. 1998. "Targeted Disruption of SHIP Leads to Hemopoietic Perturbations, Lung Pathology, and a Shortened Lifespan." *Genes & Development* 12 (1): 1610–20.

- Hoeller, Oliver, Delquin Gong, and Orion D. Weiner. 2014. "How to Understand and Outwit Adaptation." *Developmental Cell* 28 (6): 607–16. <https://doi.org/10.1016/j.devcel.2014.03.009>.
- Iijima, Miho, and Peter Devreotes. 2002. "Tumor Suppressor PTEN Mediates Sensing of Chemoattractant Gradients." *Cell* 109 (5): 599–610. [https://doi.org/10.1016/S0092-8674\(02\)00745-6](https://doi.org/10.1016/S0092-8674(02)00745-6).
- Isnardi, Isabelle, Pierre Bruhns, Georges Bismuth, Wolf H. Fridman, and Marc Daëron. 2006. "The SH2 Domain-Containing Inositol 5-Phosphatase SHIP1 Is Recruited to the Intracytoplasmic Domain of Human FcγRIIB and Is Mandatory for Negative Regulation of B Cell Activation." *Immunology Letters* 104 (1–2): 156–65. <https://doi.org/10.1016/j.imlet.2005.11.027>.
- Kavanaugh, W.M., D.A. Pot, S.M. Chin, M. Deuter-Reinhard, A.B. Jefferson, F.A. Norris, F.R. Masiarz, L.S. Cousens, P.W. Majerus, and Lewis T. Williams. 1996. "Multiple Forms of an Inositol Polyphosphate 5-Phosphatase Form Signaling Complexes with Shc and Grb2." *Current Biology* 6 (4): 438–45. [https://doi.org/10.1016/S0960-9822\(02\)00511-0](https://doi.org/10.1016/S0960-9822(02)00511-0).
- Kerr, William G. 2011. "Inhibitor and Activator: Dual Functions for SHIP in Immunity and Cancer: Divergent Roles for SHIP in Immune Signaling." *Annals of the New York Academy of Sciences* 1217 (1): 1–17. <https://doi.org/10.1111/j.1749-6632.2010.05869.x>.
- Kruse, Karsten, and Frank Jülicher. 2005. "Oscillations in Cell Biology." *Current Opinion in Cell Biology* 17 (1): 20–26. <https://doi.org/10.1016/j.ceb.2004.12.007>.
- Kutateladze, Tatiana G. 2010. "Translation of the Phosphoinositide Code by PI Effectors." *Nature Chemical Biology* 6 (7): 507–13. <https://doi.org/10.1038/nchembio.390>.
- Lam, P.-y., S. K. Yoo, J. M. Green, and A. Huttenlocher. 2012. "The SH2-Domain-Containing Inositol 5-Phosphatase (SHIP) Limits the Motility of Neutrophils and Their Recruitment to Wounds in Zebrafish." *Journal of Cell Science* 125 (21): 4973–78. <https://doi.org/10.1242/jcs.106625>.
- Lamkin, Thomas D., Scott F. Walk, Ling Liu, Jacqueline E. Damen, Gerald Krystal, and Kodimangalam S. Ravichandran. 1997. "Shc Interaction with Src Homology 2 Domain Containing Inositol Phosphatase (SHIP) in Vivo Requires the Shc-Phosphotyrosine Binding Domain and Two Specific Phosphotyrosines on SHIP." *Journal of Biological Chemistry* 272 (16): 10396–401. <https://doi.org/10.1074/jbc.272.16.10396>.

- Le Coq, Johanne, Marta Camacho-Artacho, José Vicente Velázquez, Clara M Santiveri, Luis Heredia Gallego, Ramón Campos-Olivas, Nicole Dölker, and Daniel Lietha. 2017. “Structural Basis for Interdomain Communication in SHIP2 Providing High Phosphatase Activity.” *ELife* 6 (August): e26640. <https://doi.org/10.7554/eLife.26640>.
- Lee, Young Kwang, Shalini T. Low-Nam, Jean K. Chung, Scott D. Hansen, Hiu Yue Monatrice Lam, Steven Alvarez, and Jay T. Groves. 2017. “Mechanism of SOS PR-Domain Autoinhibition Revealed by Single-Molecule Assays on Native Protein from Lysate.” *Nature Communications* 8 (1): 15061. <https://doi.org/10.1038/ncomms15061>.
- Li, Fan, Lisha Li, Meijuan Cheng, Xiumin Wang, Jun Hao, Shuxia Liu, and Huijun Duan. 2017. “SHIP, a Novel Factor to Ameliorate Extracellular Matrix Accumulation via Suppressing PI3K/Akt/CTGF Signaling in Diabetic Kidney Disease.” *Biochemical and Biophysical Research Communications* 482 (4): 1477–83. <https://doi.org/10.1016/j.bbrc.2016.12.060>.
- Li, Zhong, Michael Hannigan, Zhicheng Mo, Bo Liu, Wei Lu, Yue Wu, Alan V Smrcka, et al. n.d. “Directional Sensing Requires G_{NLQ}-Mediated PAK1 and PIX_Q-Dependent Activation of Cdc42,” 13.
- Lioubin, Mario N, and Larry R Rohrschneider’. 1994. “Shc, Grb2, Sos1, and a 150-Kilodalton Tyrosine-Phosphorylated Protein Form Complexes with Fms in Hematopoietic Cells.” *MOL. CELL. BIOL.* 14: 10.
- Liu, Q., T. Sasaki, I. Kozieradzki, A. Wakeham, A. Itie, D. J. Dumont, and J. M. Penninger. 1999. “SHIP Is a Negative Regulator of Growth Factor Receptor-Mediated PKB/Akt Activation and Myeloid Cell Survival.” *Genes & Development* 13 (7): 786–91. <https://doi.org/10.1101/gad.13.7.786>.
- Liu, Qiurong, Takehiko Sasaki, Ivona Kozieradzki, Andrew Wakeham, Annick Itie, Daniel J. Dumont, and Josef M. Penninger. 1999. “SHIP Is a Negative Regulator of Growth Factor Receptor-Mediated PKB/Akt Activation and Myeloid Cell Survival.” *Genes and Development* 13 (7): 786–91. <https://doi.org/10.1101/gad.13.7.786>.
- Liu, Qiurong, Fouad Shalaby, Jamie Jones, Denis Bouchard, and Daniel J. Dumont. 1998. “The SH2-Containing Inositol Polyphosphate 5-Phosphatase, Ship, Is Expressed During Hematopoiesis and Spermatogenesis.” *Blood* 91 (8): 2753–59. https://doi.org/10.1182/blood.V91.8.2753.2753_2753_2759.
- Luo, Hongbo R, and Subhanjan Mondal. 2015. “Molecular Control of PtdIns(3,4,5)P3 Signaling in Neutrophils.” *EMBO Reports* 16 (2): 149–63. <https://doi.org/10.15252/embr.201439466>.

- Maehama, Tomohiko, Gregory S. Taylor, and Jack E. Dixon. 2001. "PTEN and Myotubularin: Novel Phosphoinositide Phosphatases." *Annual Review of Biochemistry* 70 (1): 247–79. <https://doi.org/10.1146/annurev.biochem.70.1.247>.
- Majerus, Philip W., and John D. York. 2009. "Phosphoinositide Phosphatases and Disease." *Journal of Lipid Research* 50 (April): S249–54. <https://doi.org/10.1194/jlr.R800072-JLR200>.
- Manno, Birgit, Thomas Oellerich, Tim Schnyder, Jasmin Corso, Marion Lösing, Konstantin Neumann, Henning Urlaub, Facundo D. Batista, Michael Engelke, and Jürgen Wienands. 2016. "The Dok-3/Grb2 Adaptor Module Promotes Inducible Association of the Lipid Phosphatase SHIP with the BCR in a Coreceptor-Independent Manner." *European Journal of Immunology* 46 (11): 2520–30. <https://doi.org/10.1002/eji.201646431>.
- McKeever, Paul M., Tae Hyung Kim, Andrew R. Hesketh, Laura MacNair, Denise Miletic, Giorgio Favrin, Stephen G. Oliver, Zhaolei Zhang, Peter St George-Hyslop, and Janice Robertson. 2017. "Cholinergic Neuron Gene Expression Differences Captured by Translational Profiling in a Mouse Model of Alzheimer's Disease." *Neurobiology of Aging* 57: 104–19. <https://doi.org/10.1016/j.neurobiolaging.2017.05.014>.
- Ming-Lum, Andrew, Shaheen Shojania, Eva So, Erin McCarrell, Eileen Shaw, David Vu, Ida Wang, Lawrence P. McIntosh, and Alice L.-F. Mui. 2012. "A Pleckstrin Homology-related Domain in SHIP1 Mediates Membrane Localization during Fcγ Receptor-induced Phagocytosis." *The FASEB Journal* 26 (8): 3163–77. <https://doi.org/10.1096/fj.11-201475>.
- Mondal, Subhanjan, Kulandayan K. Subramanian, Jiro Sakai, Besnik Bajrami, and Hongbo R. Luo. 2012. "Phosphoinositide Lipid Phosphatase SHIP1 and PTEN Coordinate to Regulate Cell Migration and Adhesion." *Molecular Biology of the Cell* 23 (7): 1219–30. <https://doi.org/10.1091/mbc.E11-10-0889>.
- Mukherjee, Oindrilla, Lars Weingarten, Inken Padberg, Catrin Pracht, Rileen Sinha, Thomas Hochdörfer, Stephan Kuppig, Rolf Backofen, Michael Reth, and Michael Huber. 2012. "The SH2-Domain of SHIP1 Interacts with the SHIP1 C-Terminus: Impact on SHIP1/Ig-α Interaction." *Biochimica et Biophysica Acta (BBA) - Molecular Cell Research* 1823 (2): 206–14. <https://doi.org/10.1016/j.bbamcr.2011.11.019>.
- Nakamura, Koji, Alexander Malykhin, and K. Mark Coggeshall. 2002. "The Src Homology 2 Domain-Containing Inositol 5-Phosphatase Negatively Regulates Fcγ Receptor-Mediated Phagocytosis through Immunoreceptor Tyrosine-Based Activation Motif-Bearing Phagocytic Receptors." *Blood* 100 (9): 3374–82. <https://doi.org/10.1182/blood-2002-03-0787>.

- Nakatsu, Fubito, Rushika M. Perera, Louise Lucast, Roberto Zoncu, Jan Domin, Frank B. Gertler, Derek Toomre, and Pietro De Camilli. 2010. "The Inositol 5-Phosphatase SHIP2 Regulates Endocytic Clathrin-Coated Pit Dynamics." *Journal of Cell Biology* 190 (3): 307–15. <https://doi.org/10.1083/jcb.201005018>.
- Nalaskowski, Marcus M., Patrick Ehm, Christoph Rehbach, Nina Nelson, Maike Täger, Kathrin Modest, and Manfred Jücker. 2018. "Nuclear Accumulation of SHIP1 Mutants Derived from AML Patients Leads to Increased Proliferation of Leukemic Cells." *Cellular Signalling* 49 (May): 87–94. <https://doi.org/10.1016/j.cellsig.2018.05.006>.
- Nasuhoglu, Cem, Siyi Feng, Janping Mao, Masaya Yamamoto, Helen L. Yin, Svetlana Earnest, Barbara Barylko, Joseph P. Albanesi, and Donald W. Hilgemann. 2002. "Nonradioactive Analysis of Phosphatidylinositides and Other Anionic Phospholipids by Anion-Exchange High-Performance Liquid Chromatography with Suppressed Conductivity Detection." *Analytical Biochemistry* 301 (2): 243–54. <https://doi.org/10.1006/abio.2001.5489>.
- Nelson, Nina, Adelia Razeto, Alessia Gilardi, Mira Grättinger, Johannes Kirchmair, and Manfred Jücker. 2021. "AKT1 and PTEN Show the Highest Affinities among Phosphoinositide Binding Proteins for the Second Messengers PtdIns(3,4,5)P3 and PtdIns(3,4)P2." *Biochemical and Biophysical Research Communications* 568 (September): 110–15. <https://doi.org/10.1016/j.bbrc.2021.06.027>.
- Newton, Alexandra C., Martin D. Bootman, and John D. Scott. 2016. "Second Messengers." *Cold Spring Harbor Perspectives in Biology* 8 (8): a005926. <https://doi.org/10.1101/cshperspect.a005926>.
- Ngoh, Eyler N., Shelley B. Weisser, Young Lo, Lisa K. Kozicky, Roger Jen, Hayley K. Brugger, Susan C. Menzies, et al. 2016. "Activity of SHIP, Which Prevents Expression of Interleukin 1 β , Is Reduced in Patients with Crohn's Disease." *Gastroenterology* 150 (2): 465–76. <https://doi.org/10.1053/j.gastro.2015.09.049>.
- Nishio, Miki, Ken-ichi Watanabe, Junko Sasaki, Choji Taya, Shunsuke Takasuga, Ryota Iizuka, Tamas Balla, et al. 2007. "Control of Cell Polarity and Motility by the PtdIns(3,4,5)P3 Phosphatase SHIP1." *Nature Cell Biology* 9 (1): 36–44. <https://doi.org/10.1038/ncb1515>.
- Ong, Christopher J., Andrew Ming-Lum, Matt Nodwell, Ali Ghanipour, Lu Yang, David E. Williams, Joseph Kim, et al. 2007. "Small-Molecule Agonists of SHIP1 Inhibit the Phosphoinositide 3-Kinase Pathway in Hematopoietic Cells." *Blood* 110 (6): 1942–49. <https://doi.org/10.1182/blood-2007-03-079699>.

- Ono, Masao, Silvia Bolland, and Paul Tempst. 1996. "Role Ofthe Inositol Phosphatase SHIP in Negative Regulation of the Immune System by the Receptor FcyRIIB" 383: 4.
- Ono, Masao, Hidetaka Okada, Silvia Bolland, Shigeru Yanagi, Tomohiro Kurosaki, and Jeffrey V Ravetch. 1997. "Deletion of SHIP or SHP-1 Reveals Two Distinct Pathways for Inhibitory Signaling." *Cell* 90 (2): 293–301.
[https://doi.org/10.1016/S0092-8674\(00\)80337-2](https://doi.org/10.1016/S0092-8674(00)80337-2).
- Pauls, Samantha D., Sen Hou, and Aaron J. Marshall. 2020. "SHIP Interacts with Adaptor Protein Nck and Restricts Actin Turnover in B Cells." *Biochemical and Biophysical Research Communications* 527 (1): 207–12.
<https://doi.org/10.1016/j.bbrc.2020.04.101>.
- Pauls, Samantha D., and Aaron J. Marshall. 2017. "Regulation of Immune Cell Signaling by SHIP1: A Phosphatase, Scaffold Protein, and Potential Therapeutic Target." *European Journal of Immunology* 47 (6): 932–45.
<https://doi.org/10.1002/eji.201646795>.
- Pauls, Samantha D., Arnab Ray, Sen Hou, Andrew T. Vaughan, Mark S. Cragg, and Aaron J. Marshall. 2016. "FcyRIIB-Independent Mechanisms Controlling Membrane Localization of the Inhibitory Phosphatase SHIP in Human B Cells." *The Journal of Immunology* 197 (5): 1587–96.
<https://doi.org/10.4049/jimmunol.1600105>.
- Pawson, Tony. 2004. "Specificity in Signal Transduction: From Phosphotyrosine-SH2 Domain Interactions to Complex Cellular Systems." *Cell* 116 (2): 191–203.
[https://doi.org/10.1016/S0092-8674\(03\)01077-8](https://doi.org/10.1016/S0092-8674(03)01077-8).
- Pirrung, Michael C., Sandra J. Drabik, Jasimuddin Ahamed, and Hydar Ali. 2000. "Caged Chemotactic Peptides." *Bioconjugate Chemistry* 11 (5): 679–81.
<https://doi.org/10.1021/bc000001g>.
- Pollard, Thomas, and Gary Borisy. 2003. "Cellular Motility Driven by Assembly and Disassembly of Actin Filaments." *Cell* 112 (4): 453–65.
[https://doi.org/10.1016/S0092-8674\(03\)00120-X](https://doi.org/10.1016/S0092-8674(03)00120-X).
- Prasad, Nagendra K., Michael E. Werner, and Stuart J. Decker. 2009. "Specific Tyrosine Phosphorylations Mediate Signal-Dependent Stimulation of SHIP2 Inositol Phosphatase Activity, While the SH2 Domain Confers an Inhibitory Effect To Maintain the Basal Activity." *Biochemistry* 48 (27): 6285–87.
<https://doi.org/10.1021/bi900492d>.
- Rickert, P. 2000. "Leukocytes Navigate by Compass: Roles of PI3K γ and Its Lipid Products." *Trends in Cell Biology* 10 (11): 466–73.
[https://doi.org/10.1016/S0962-8924\(00\)01841-9](https://doi.org/10.1016/S0962-8924(00)01841-9).

- Rincón, Esther, Briana L. Rocha-Gregg, and Sean R. Collins. 2018. “A Map of Gene Expression in Neutrophil-like Cell Lines.” *BMC Genomics* 19 (1): 573. <https://doi.org/10.1186/s12864-018-4957-6>.
- Rohrschneider, Larry R, John F Fuller, Ingrid Wolf, Yan Liu, and David M Lucas. 2000. “Structure, Function, and Biology of SHIP Proteins.” *Genes & Development*, 17.
- Sattler, Martin, Shalini Verma, Yuri B. Pride, Ravi Salgia, Larry R. Rohrschneider, and James D. Griffin. 2001. “SHIP1, an SH2 Domain Containing Polyinositol-5-Phosphatase, Regulates Migration through Two Critical Tyrosine Residues and Forms a Novel Signaling Complex with DOK1 and CRKL.” *Journal of Biological Chemistry* 276 (4): 2451–58. <https://doi.org/10.1074/jbc.M006250200>.
- Servant, G. 2000. “Polarization of Chemoattractant Receptor Signaling During Neutrophil Chemotaxis.” *Science* 287 (5455): 1037–40. <https://doi.org/10.1126/science.287.5455.1037>.
- Séverin, Sonia, Marie Pierre Gratacap, Nadège Lenain, Laetitia Alvarez, Etienne Hollande, Josef M. Penninger, Christian Gachet, Monique Plantavid, and Bernard Payrastre. 2007. “Deficiency of Src Homology 2 Domain-Containing Inositol 5-Phosphatase 1 Affects Platelet Responses and Thrombus Growth.” *Journal of Clinical Investigation* 117 (4): 944–52. <https://doi.org/10.1172/JCI29967>.
- Sicheri, Frank, Ismail Moarefi, and John Kuriyan. 1997. “Crystal Structure of the Src Family Tyrosine Kinase Hck.” *Nature* 385 (6617): 602–9. <https://doi.org/10.1038/385602a0>.
- Stephens, L. R., K. T. Hughes, and R. F. Irvine. 1991. “Pathway of Phosphatidylinositol(3,4,5)-Trisphosphate Synthesis in Activated Neutrophils.” *Nature* 351 (6321): 33–39. <https://doi.org/10.1038/351033a0>.
- Stephens, Len, Chris Ellson, and Phillip Hawkins. 2002. “Roles of PI3Ks in Leukocyte Chemotaxis and Phagocytosis.” *Current Opinion in Cell Biology* 14 (2): 203–13. [https://doi.org/10.1016/S0955-0674\(02\)00311-3](https://doi.org/10.1016/S0955-0674(02)00311-3).
- Sunao, Takeshita, Namba Noriyuki, Zhao Jenny J., Jiang Yebin, Genant Harry K., Silva Matthew J., Brodt Michael D., et al. 2002. “SHIP-Deficient Mice Are Severely Osteoporotic Due to Increased Numbers of Hyper-Resorptive Osteoclasts.” *Nature Medicine* 8 (9): 943–49. <https://doi.org/10.1038/nm>.
- Tan, Xinyu, Mingzhi Luo, and Allen P. Liu. 2018. “Clathrin-Mediated Endocytosis Regulates FMLP-Mediated Neutrophil Polarization.” *Heliyon* 4 (9): e00819. <https://doi.org/10.1016/j.heliyon.2018.e00819>.
- Teyra, Joan, Haiming Huang, Shobhit Jain, Xinyu Guan, Aiping Dong, Yanli Liu, Wolfram Tempel, et al. 2017. “Comprehensive Analysis of the Human SH3 Domain Family Reveals a Wide Variety of Non-Canonical Specificities.” *Structure* 25 (10): 1598-1610.e3. <https://doi.org/10.1016/j.str.2017.07.017>.

- Vacklin, Hanna P., Fredrik Tiberg, Giovanna Fragneto, and R. K. Thomas. 2005. "Phospholipase A₂ Hydrolysis of Supported Phospholipid Bilayers: A Neutron Reflectivity and Ellipsometry Study." *Biochemistry* 44 (8): 2811–21. <https://doi.org/10.1021/bi047727a>.
- Vadas, Oscar, John E. Burke, Xuxiao Zhang, Alex Berndt, and Roger L. Williams. 2011. "Structural Basis for Activation and Inhibition of Class I Phosphoinositide 3-Kinases." *Science Signaling* 4 (195). <https://doi.org/10.1126/scisignal.2002165>.
- Vance, J, and R Steenbergen. 2005. "Metabolism and Functions of Phosphatidylserine." *Progress in Lipid Research* 44 (4): 207–34. <https://doi.org/10.1016/j.plipres.2005.05.001>.
- Weiner, Orion D. 2002. "Regulation of Cell Polarity during Eukaryotic Chemotaxis: The Chemotactic Compass." *Current Opinion in Cell Biology* 14 (2): 196–202. [https://doi.org/doi.org/10.1016/S0955-0674\(02\)00310-1](https://doi.org/doi.org/10.1016/S0955-0674(02)00310-1).
- Weiner, Orion D, William A Marganski, Lani F Wu, Steven J Altschuler, and Marc W Kirschner. 2007. "An Actin-Based Wave Generator Organizes Cell Motility." Edited by Manfred Schliwa. *PLoS Biology* 5 (9): e221. <https://doi.org/10.1371/journal.pbio.0050221>.
- Weiner, Orion D., Paul O. Neilsen, Glenn D. Prestwich, Marc W. Kirschner, Lewis C. Cantley, and Henry R. Bourne. 2002. "A PtdInsP₃- and Rho GTPase-Mediated Positive Feedback Loop Regulates Neutrophil Polarity." *Nature Cell Biology* 4 (7): 509–13. <https://doi.org/10.1038/ncb811>.
- Wenk, Markus R, Louise Lucast, Gilbert Di Paolo, Anthony J Romanelli, Sharon F Suchy, Robert L Nussbaum, Gary W Cline, Gerald I Shulman, Walter McMurray, and Pietro De Camilli. 2003. "Phosphoinositide Profiling in Complex Lipid Mixtures Using Electrospray Ionization Mass Spectrometry." *Nature Biotechnology* 21 (7): 813–17. <https://doi.org/10.1038/nbt837>.
- Wu, Min, Xudong Wu, and Pietro De Camilli. 2013. "Calcium Oscillations-Coupled Conversion of Actin Travelling Waves to Standing Oscillations." *Proceedings of the National Academy of Sciences* 110 (4): 1339–44. <https://doi.org/10.1073/pnas.1221538110>.
- Wu, Zhanghan, Maohan Su, Cheesan Tong, Min Wu, and Jian Liu. 2018. "Membrane Shape-Mediated Wave Propagation of Cortical Protein Dynamics." *Nature Communications* 9 (1): 136. <https://doi.org/10.1038/s41467-017-02469-1>.
- Xiong, Ding, Shengping Xiao, Su Guo, Qingsong Lin, Fubito Nakatsu, and Min Wu. 2016. "Frequency and Amplitude Control of Cortical Oscillations by Phosphoinositide Waves." *Nature Chemical Biology* 12 (3): 159–66. <https://doi.org/10.1038/nchembio.2000>.

- Xiong, Y., C.-H. Huang, P. A. Iglesias, and P. N. Devreotes. 2010. "Cells Navigate with a Local-Excitation, Global-Inhibition-Biased Excitable Network." *Proceedings of the National Academy of Sciences* 107 (40): 17079–86.
<https://doi.org/10.1073/pnas.1011271107>.
- Xu, Wenqing, Stephen C. Harrison, and Michael J. Eck. 1997. "Three-Dimensional Structure of the Tyrosine Kinase c-Src." *Nature* 385 (6617): 595–602.
<https://doi.org/10.1038/385595a0>.
- Yang, Hee Won, Sean R. Collins, and Tobias Meyer. 2016. "Locally Excitable Cdc42 Signals Steer Cells during Chemotaxis." *Nature Cell Biology* 18 (2): 191–201.
<https://doi.org/10.1038/ncb3292>.
- Yang, Yang, and Min Wu. 2018. "Rhythmicity and Waves in the Cortex of Single Cells." *Philosophical Transactions of the Royal Society B: Biological Sciences* 373 (1747): 20170116. <https://doi.org/10.1098/rstb.2017.0116>.
- Yang, Yang, Ding Xiong, Anne Pipathsouk, Orion D. Weiner, and Min Wu. 2017. "Clathrin Assembly Defines the Onset and Geometry of Cortical Patterning." *Developmental Cell* 43 (4): 507–521.e4.
<https://doi.org/10.1016/j.devcel.2017.10.028>.
- Yeung, Tony, Gary E. Gilbert, Jialan Shi, John Silvius, Andras Kapus, and Sergio Grinstein. 2008. "Membrane Phosphatidylserine Regulates Surface Charge and Protein Localization." *Science* 319 (5860): 210–13.
<https://doi.org/10.1126/science.1152066>.
- Yoo, Sa Kan, Qing Deng, Peter J. Cavnar, Yi I. Wu, Klaus M. Hahn, and Anna Huttenlocher. 2010. "Differential Regulation of Protrusion and Polarity by PI(3)K during Neutrophil Motility in Live Zebrafish." *Developmental Cell* 18 (2): 226–36. <https://doi.org/10.1016/j.devcel.2009.11.015>.
- Zhang, Jun, Kodi S. Ravichandran, and James C. Garrison. 2010. "A Key Role for the Phosphorylation of Ser440 by the Cyclic AMP-Dependent Protein Kinase in Regulating the Activity of the Src Homology 2 Domain-Containing Inositol 5'-Phosphatase (SHIP1)." *Journal of Biological Chemistry* 285 (45): 34839–49.
<https://doi.org/10.1074/jbc.M110.128827>.
- Zhang, Z.Y., J.C. Clemens, H.L. Schubert, J.A. Stuckey, M.W. Fischer, D.M. Hume, M.A. Saper, and J.E. Dixon. 1992. "Expression, Purification, and Physicochemical Characterization of a Recombinant Yersinia Protein Tyrosine Phosphatase." *Journal of Biological Chemistry* 267 (33): 23759–66.
[https://doi.org/10.1016/S0021-9258\(18\)35903-9](https://doi.org/10.1016/S0021-9258(18)35903-9).